Asian Journal of Tropical Biotechnology

| Asian J Trop Biotechnol | vol. 22 | no. 1 | June 2025 |
| ISSN 2775-300X | E-ISSN 2775-4715 |

Beta lactams, photo by Larry Psolis

Asian Journal of Tropical Biotechnology

| Asian J Trop Biotechnol | vol. 22 | no. 1 | June 2025 |

Published semiannually **PRINTED IN INDONESIA**

P-ISSN 2775-300X
E-ISSN 2775-4715

9 772775 471439

Asian Journal of Tropical Biotechnology

| Asian J Trop Biotechnol | vol. 22 | no. 1 | June 2025 |

ONLINE
http://smujo.id/bbs

p-ISSN
2775-300X

e-ISSN
2775-4715

PUBLISHER
Smujo International

ASSOCIATION
Society for Indonesian Biodiversity

INSTITUTION
Universitas Sebelas Maret, Surakarta, Indonesia

OFFICE ADDRESS
Jl. Ir. Sutami 36A Surakarta 57126, Central Java, Indonesia. Tel./Fax.: +62-271-663375, email: editors@smujo.id

PERIOD OF ISSUANCE
June, December

Society for Indonesian Biodiversity

Universitas Sebelas Maret Surakarta, Indonesia

Published by Smujo International for The Society for Indonesian Biodiversity and Sebelas Maret University, Surakarta, Indonesia

GUIDANCE FOR AUTHORS

Aims and Scope ***Asian Journal of Tropical Biotechnology*** (**Asian J Trop Biotechnol**)(*formerly Bioteknologi, Biotechnological Studies*) encourages submission of manuscripts dealing with all aspects of biotechnology, especially from tropical regions, that emphasize issues germane to improve human life, includes cell biochemistry, enzymes and proteins, applied genetics and molecular biotechnology, genomics and proteomics, applied microbiology and cell physiology, environmental biotechnology, improvement of crop productivity, public health and waste management, as as well as product formation and manipulation of biological processes for use in the agricultural, pharmaceutical biotechnology and allied industries.

Article types The journal seeks original full-length: (i) **Research papers**, (ii) **Reviews**, and (iii) **Short communications**. Original research manuscripts are limited to 8,000 words (including tables and figures) or proportional to articles in this publication number. Review articles are also limited to 8,000 words, while Short communications should be less than 2,500 words, except for pre-study.

Submission: The journal only accepts online submissions through the open journal system **(https://smujo.id/bbs/about/submissions)** or, for login problems, email the editors at unsjournals@gmail.com (or editors@smujo.id). Submitted manuscripts should be the original works of the author(s). Please ensure that the manuscript is submitted using the template, which can be found at (https://biodiversitas.mipa.uns.ac.id/D/template.doc). The manuscript must be accompanied by a cover letter containing the article title, the first name and last name of all the authors, and a paragraph describing the claimed novelty of the findings versus current knowledge. Please also provide a list of five potential reviewers in your cover letter. They should come from outside your institution and better from three different countries. Submission of a manuscript implies the submitted work has not been published (except as part of a thesis or report, or abstract) and is not being considered for publication elsewhere. When a group writes a manuscript, all authors should read and approve the final version of the submitted manuscript and its revision; and agree on the submission of manuscripts for this journal. All authors should have made substantial contributions to the concept and design of the research, acquisition of the data and its analysis, drafting the manuscript, and correcting the revision. All authors must be responsible for the work's quality, accuracy, and ethics.

Ethics Author(s) must be obedient to the law and/or ethics in treating the object of research and pay attention to the legality of material sources and intellectual property rights.

Copyright If the manuscript is accepted for publication, the author(s) still hold the copyright and retain publishing rights without restrictions. For the new invention, authors must manage its patent before publication.

Open Access The journal is committed to free-open access that does not charge readers or their institutions for access. Readers are entitled to read, download, copy, distribute, print, search, or link to the full texts of articles, as long as not for commercial purposes. The license type is CC-BY-NC-SA.

Acceptance Only articles written in US English are accepted for publication. Manuscripts will be reviewed by editors and invited reviewers (double-blind review) according to their disciplines. Authors will generally be notified of acceptance, rejection, or need for revision within 1 to 2 months of receipt. Manuscripts will be rejected if the content does not align with the journal scope, does not meet the standard quality, is in an inappropriate format, or contains complicated grammar, dishonesty (i.e., plagiarism, duplicate publications, fabrication of data, citations manipulation, etc.), or ignoring correspondence in three months. The primary criteria for publication are scientific quality and significance. **Uncorrected proofs** will be sent to the corresponding author by system or email as .doc or .docx files for checking and correcting typographical errors. The corrected proofs should be returned in 7 days to avoid publication delays. The accepted papers will be published online in chronological order at any time but printed at the end of each month.

Free of charge This publication is dedicated entirely to the advancement of science and technology, therefore author(s), or author institution(s) are not subject to publication fees. **Reprints** The sample journal reprint is only available by special request. Additional copies may be purchased when ordering by email and sending back the uncorrected proofs.

Manuscript preparation Manuscript is typed on A4 (210x297 mm^2) paper size, in a single column, single space, 10-point (10 pt) Times New Roman font. The margin text is 3 cm from the top, 2 cm from the bottom, and 1.8 cm from the left and right. Smaller lettering sizes can be applied in presenting tables and figures (9 pt). Word processing program or additional software can be used; however, it must be PC compatible, use the template, and be Microsoft Word based (.doc or .rtf; not .docx). **Scientific names** of species (incl. subspecies, variety, etc.) should be written in italics, except in italicized sentences. Scientific names (genus, species, author) and cultivar or strain should be mentioned completely for the first time mentioning it in the body text, especially for taxonomic manuscripts. The genus name can be shortened after the first mention, except in early sentences, or where this may generate confusion; name of the author can be eliminated after the first mention. For example, *Rhizopus oryzae* L. UICC 524 can be written hereinafter as *R. oryzae* UICC 524. Using trivial names should be avoided. **Biochemical and chemical nomenclature** should follow the order of the IUPAC-IUB. For DNA sequences, it is better to use Courier New font. Standard chemical abbreviations can be applied for common and clear used, for example, completely written butilic hydroxyl toluene (BHT) to be BHT hereinafter. **Metric measurements** should use IS denominations, and other systems should use equivalent values with the denomination of IS mentioned first. A dot should not follow abbreviations like g, mg, mL, etc. Minus index (m^{-2}, L^{-1}, h^{-1}) suggested being used, except in things like "per-plant" or "per-plot." **Mathematical equations** can be written down in one column with text; in that case, they can be written separately. **Numbers** one to ten are written in words, except if it relates to measurement, while values above them are written in number, except in early sentences. The fraction should be expressed in decimal. In the text, it should be used "%" rather than "percent." Avoid expressing ideas with complicated sentences and verbiage/phrasing, and use efficient and effective sentences.

The title of the article should be written in compact, clear, and informative sentence, preferably not more than 20 words. Name of author(s) should be completely written, especially for the first and the last name. **Name and institution** address should also be completely written with street name and number (location), postal code, telephone number, facsimile number, and email address. We choose local names in Bahasa Indonesia for universities in Indonesia. The mention of "strata" program, should be avoided. Manuscript written by a group, author for correspondence along with address is required (marked with "♥"). **The title page** (first page) should include title of the article, full name(s), institution(s) and address(es) of the author(s); the corresponding authors detailed postage and e-mail addresses (P), and phone (O) and fax numbers (O).

Abstract A concise abstract is required (about 200 words). The abstract should be informative and state briefly the aim of the research, the principal results and major conclusions. An abstract is often presented separately from the article, thus it must be able to stand alone (completely self-explanatory). References should not be cited, but if essential, then cite the author(s) and year(s). Abbreviations should be avoided, but if essential, they must be defined at their first mention. **Keywords** are about five words, covering scientific and local name (if any), research themes, and special methods used; and sorted from A to Z. **Abbreviations** (if any): All important abbreviations must be defined at their first mention there. **Running title** is about five words.

Introduction is about 600 words, covering the aims of the research and provide an adequate background, avoiding a detailed literature survey or a summary of the results. **Materials and Methods** should emphasize on the procedures and data analysis. **Results and Discussion** should be written as a series of connecting sentences, however, for a manuscript with long discussion should be divided into subtitles. Thorough discussion represents the causal effect mainly explains why and how the results of the research were taken place, and do not only re-express the mentioned results in the form of sentences. **Concluding** sentence should be given at the end of the discussion. **Acknowledgements** are expressed in a brief; all sources of institutional, private and corporate financial support for the work must be fully acknowledged, and any potential conflicts of interest are noted.

Figures and Tables of a maximum of three pages should be clearly presented. The title of a picture is written down below the picture, while the title of a table is written above the table. Colored figures can only be accepted if the information in the manuscript can lose without those images; the chart is preferred to use black and white images. The author could consign any picture or photo for the front cover, although it does not print in the manuscript. All images property of others should be mentioned the source. Author is suggested referring to Wikipedia for international boundaries and Google Earth for satellite imagery. If not specifically mentioned, it is assumed to refer to these sources. **There is no appendix**, all data or data analysis is incorporated into Results and Discussions. For broad data, it can be displayed on the website as a supplement.

References Preferably 80% of it comes from scientific journals published in the last 10 years. In the text, give the author names followed by the year of publication and arrange from oldest to newest and from A to Z; in citing an article written by two authors, both of them should be mentioned; however, for three and more authors only the first author is mentioned followed by et al. For example, Saharjo and Nurhayati (2006) or (Boonkerd 2003a, b, c; Sugiyarto 2004; El-Bana and Nijs 2005; Balagadde et al. 2008; Webb et al. 2008). Extent citation should be avoided, as shown with the word "cit." Reference to unpublished data and personal communication should not appear in the list but should be cited in the text only (e.g., Rifai MA 2007, pers. com. (personal communication); Setyawan AD 2007, unpublished data). In the reference list, the references should be listed in alphabetical order. Names of journals should be abbreviated. Always use the standard abbreviation of a journal's name according to the **ISSN List of Title Word Abbreviations** (www.issn.org/2-22661-LTWA-online.php). Please include DOI links for journal papers. The following examples are for guidance.

Journal:

Saharjo BH, Nurhayati AD. 2006. Domination and composition structure change at hemic peat natural regeneration following burning; a case study in Pelalawan, Riau Province. Biodiversitas 7: 154-158. DOI: 10.13057/biodiv/d070213.

The usage of "et al." in long author lists will also be accepted:

Smith J, Jones M Jr, Houghton L et al. 1999. Future of health insurance. N Engl J Med 965: 325-329. DOI: 10.10007/s002149800025.

Book:

Rai MK, Carpinella C. 2006. Naturally Occurring Bioactive Compounds. Elsevier, Amsterdam.

Chapter in the book:

Webb CO, Cannon CH, Davies SJ. 2008. Ecological organization, biogeography, and the phylogenetic structure of rainforest tree communities. In: Carson W, Schnitzer S (eds.). Tropical Forest Community Ecology. Wiley-Blackwell, New York.

Abstract:

Assaeed AM. 2007. Seed production and dispersal of *Rhazya stricta*. 50th annual symposium of the International Association for Vegetation Science, Swansea, UK, 23-27 July 2007.

Proceeding:

Alikodra HS. 2000. Biodiversity for development of local autonomous government. In: Setyawan AD, Sutarno (eds.). Toward Mount Lawu National Park; Proceeding of National Seminary and Workshop on Biodiversity Conservation to Protect and Save Germplasm in Java Island. Universitas Sebelas Maret, Surakarta, 17-20 July 2000. [Indonesian]

Thesis, Dissertation:

Sugiyarto. 2004. Soil Macro-invertebrates Diversity and Inter-Cropping Plants Productivity in Agroforestry System based on Sengon. [Dissertation]. Universitas Brawijaya, Malang. [Indonesian]

Information from the internet:

Balagadde FK, Song H, Ozaki J, Collins CH, Barnet M, Arnold FH, Quake SR, You L. 2008. A synthetic *Escherichia coli* predator-prey ecosystem. Mol Syst Biol 4: 187. DOI: 10.1038/msb.2008.24. www.molecularsystembiology.com.

THIS PAGE INTENTIONALLY LEFT BLANK

ASIAN J TROP BIOTECHNOL
Volume 22, Number 1, June 2025
Pages: 1-6

ISSN: 0216-6887
E-ISSN: 2301-8658
DOI: 10.13057/biotek/c220101

Beta hemolytic and beta-lactam antibiotic-resistant strain of *Lysinibacillus sphaericus* isolated from a tea growing region of West Bengal, India

SUDESHNA NANDI, MALAY BHATTACHARYA♥
Laboratory of Molecular Biology and Tissue Culture, Department of Tea Science, University of North Bengal. Raja Rammohunpur, Siliguri, Darjeeling, West Bengal, India. Tel.: +91-983-2094875, ♥email: malaytsnbu@gmail.com

Manuscript received: 2 December 2024. Revision accepted: 10 February 2025.

Abstract. *Nandi S, Bhattacharya M. 2025. Beta hemolytic and beta-lactam antibiotic-resistant strain of* Lysinibacillus sphaericus *isolated from a tea growing region of West Bengal, India. Asian J Trop Biotechnol 22: 1-6.* River water and soil are primary sources of bacteria. Some of them often acquire pathogenicity under stressful environmental conditions. Regarding the pathogenicity of a bacterium, hemolysin is the most virulence factor. In this study, 16 isolates possess beta-hemolytic abilities out of 32 isolated copper tolerant bacteria. One of the strains was identified as *Lysinibacillus sphaericus* (NJCT1) using 16S rRNA sequencing. *Lysinibacillus sphaericus* is rarely pathogenic in humans but is known for its larvicidal and antagonistic activity in bacteremia-associated infections in immunocompromised patients. Kaljani River basin, the lifeline for the rapidly growing population in the tea-producing region of West Bengal, India, is the source of Gram-positive bacteria used in this study. Due to its pathogenic character, it can create a health problem for the locals if they use the river water frequently. The antibiotic susceptibility study, which involved testing the bacterial strain against a panel of commonly used antibiotics, showed that *L. sphaericus* (NJCT1) is resistant to 7 antibiotics (colistin, penicillin-g, amoxicillin, ceftazidime, cefuroxime, rifampin, and methicillin). This bacterial strain exhibited resistance against the β-lactam drug class, whereas complete susceptibility was recorded against drug classes like fluoroquinolones. As the most sensitive drug, fluoroquinolones could solve the problem caused by *L. sphaericus* isolated from the Kaljani River.

Keywords: Antibiotic sensitivity, bacteremia, *Lysinibacillus sphaericus*, pathogenicity, tea garden

INTRODUCTION

Under stressful conditions, microorganisms might become pathogenic. Bacteria often secrete extracellular proteins like coagulases, cytolysins, and enterotoxins to minimize competition, harm their adjacent cells, and exploit the nutrients (Tomita and Kamino 1997). Hemolysins have received the most attention among these toxins because their activity could be easily detected in mammalian erythrocytes. Red Blood Cells (RBC) could be lysed in the presence of hemolysins. Hemolysins can destroy cellular membranes, damage nearby tissues, cause cell lysis, and thus can be regarded as a crucial determinant of virulence in infection models of laboratory animals (Bhakdi et al. 1994; Tomita and Kamio 1997).

Alpha (α), beta (β), and gamma (γ) are three distinct types of hemolysin enzymes produced by bacteria. In some studies, distinctiveness between α and β hemolysis is essential to evaluate probiotics safety (Jeon et al. 2017). Still, other phenotypes are not crucial as they only indicate the virulence potential of those phenotypes (Ramachandran 2013). Bacterial isolates from environmental samples have rarely been tested for hemolysins (Albarral et al. 2016). However, in medical sectors, beta hemolysis is one of the important phenotypic features for identifying any bacteremia or septicemia-causing pathogenic bacteria, especially for group A and group B *Streptococcus* spp. (Nizet 2022).

Viable bacteria inside the blood are called 'bacteremia'. Bacteremia could originate from daily activities like oral hygiene or after undergoing some medical procedures. Asymptomatic bacteremia can enter the human bloodstream and lead to infections with symptoms of fever, hypotension, and chills. This disease can be life-threatening for those suffering from immune system disorders (Smith and Nehring 2017). Bacteremia is now one of the most common causes of death in non-coronary Intensive Care Units (ICU). It could be treated using antibiotics for patients with such infections. People with organ transplants, last-stage renal disease, diabetics, rheumatoid arthritis, and chemotherapy receivers are more likely to develop bacteremia-associated deadly infections, and antibiotics are effective in alleviating these infections. However, the efficacy of antibiotics seems to be in jeopardy since many bacteria have developed partial or total resistance against them. Excessive and misuse of antibiotics are the causes of bacterial resistance. Research policies and development efforts are required to find an effective solution to this problem of bacterial resistance (Larsson and Flach 2022).

River water is a significant reservoir of pathogenic bacteria. Previous studies have been done mainly on the enteric bacteria. Investigations on enteric bacteria are focused on their prevalence and antimicrobial assessment (Langendorf et al. 2015; Getie et al. 2019; Denku et al. 2022). Previous reports showed that patients who had undergone splenectomy, long-term intravenous drug users,

and people living with HIV commonly reported coping with bacteremia-based issues caused by these bacteria (Wenzler et al. 2015; Kinoshita et al. 2023; Meng et al. 2023). Rivers and its tributaries serve as water sources for the inhabitants of tea garden-dominated districts in the northern part of West Bengal. The river's water is used for drinking, other domestic purposes, and irrigation. The river also is a source of livelihood for fishermen living on both sides of the river. Several deaths have been reported in this region due to diseases caused by poor water quality (Sarkar 2012). Not only that, bacteremia-related diseases are now becoming a headache for the people living in this area. Therefore, the current study is critical, as people living in tea gardens adjoining the Kaljani River basin may unknowingly interact with beta-hemolytic bacteria regularly. Immuno-compromised individuals and people with external dermal wounds would be more susceptible to beta-hemolytic bacteria, resulting in bacteremia-associated disorders. Hence, the present investigation highlights the antibiotic susceptibility and resistance attributes of a beta-hemolytic strain, *Lysinibacillus sphaericus* (NJCT1), persisting in the Kaljani River basin.

MATERIALS AND METHODS

Study area and sample collection

Soil samples were collected from 14 tea gardens and 14 river beds near West Bengal, India's Indo-Bhutan border, covering Jalpaiguri, Alipurduar, and Kalimpong Districts. All collections were carried out from February 2022 to September 2023 in the early morning. In this research, the studied strain was isolated from the Kaljani River basin (26°34'30″N & 89°25'29″E to 26°34'27″N & 89°25'22″E), located in the Kalchini Sub-division under Alipurduar District of West Bengal, India. Nimtijhora tea garden is situated in the Kaljani River basin and is one of the primary water sources for tea garden workers (Figure 1). This collection was done in the early morning of September 2022. Top soil samples were collected in a zigzag pattern, and about 10 samples were collected from this site and the distance of each sampling was about 100 meters. The collections were kept in sterile vials and instantly preserved inside an ice box during transportation to the laboratory, ensuring their integrity. The samples were mixed uniformly before laboratory experiments.

Isolation of pure bacteria

500 mg of each sample was taken into a sterile eppendorf containing 1 mL of distilled water to make soil suspensions. 500 µL of suspension was inoculated into 20 mL of nutrient broth, followed by 24 hours of incubation at 35°C (Saha et al. 2021). As the collection area is contaminated with dolomite debris and mining effluents, and copper is one of the predominant metals present in dolomite, the primary goal was to isolate copper-tolerant bacteria. The copper-tolerant bacteria were isolated by spread plate method on nutrient agar plates with different copper salt solutions ranging between 0.05 and 0.20 mg/mL and then incubated at 35°C. After 24 hours of incubation, distinct colonies were isolated and were streaked repeatedly to get the pure isolates. Morphological characters were done using a microscope.

Pathogenicity test

All the obtained isolates were assessed for pathogenicity through a blood agar test. 5% goat blood was added to 50% cooled blood agar base media, and the plates were prepared carefully without bubble formation. Isolates were individually streaked on the plates, followed by twenty-four hours of incubation at 35°C (Rosa-Fraile and Spellerberg 2017).

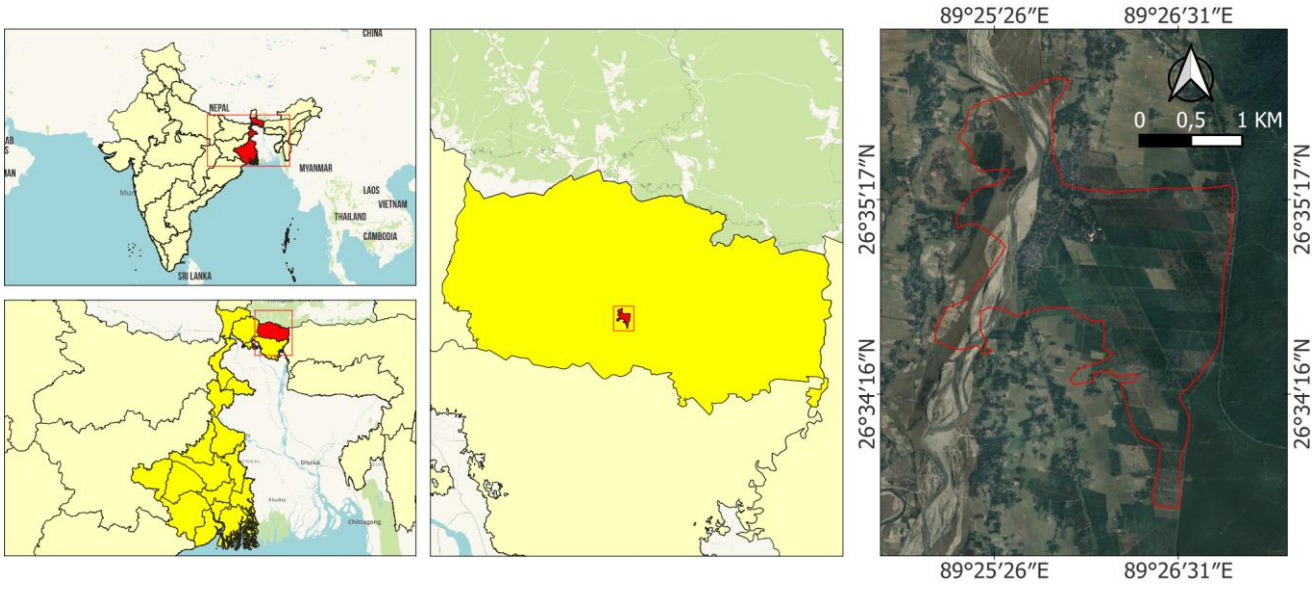

Figure 1. Map of the study area in Nimtijhora Tea Garden, Alipurduar, West Bengal, India

Molecular characterization

The isolated beta-hemolytic strain was characterized by 16S rRNA gene sequencing. For this purpose, the 16S rDNA region was isolated from 24-hour-old cultures. The isolated region of the studied strain was further amplified and purified through column purification. The purified product sequence was analyzed using Snager's method by Eddison Life Science (India). The sequencing data result was then compared using BLAST analysis against the available sequence data in the NCBI database.

Antibiotic susceptibility test of studied strain

Antibiotic susceptibility profiling against selected strains was done using the Kirby Bauer disc diffusion procedure by Robert et al. (2009), according to the National Committee for Clinical Laboratory Standards (NCCLS). Then, 24 hours of the culture of strain was spread on Muller Hinton agar media using a sterile spreader. Natural, semi-synthetic, and synthetic antibiotics were selected to assess the sensitivity of the bacterial strain. Natural antibiotics include streptomycin, bacitracin, penicillin–g, colistin, pristinamycin, vancomycin, kanamycin, polymixin-b, spectinomycin; semi-synthetic antibiotics include amoxicillin, ceftazidime, cefoxitin, cefuroxime, imipenem, and azithromycin. synthetic antibiotics include teicoplanin, nitrofurantoin, tetracycline, tigecycline, rifampin, methicillin, linezolid, erythromycin, ofloxacin, fusidic acid, gemifloxacin, ciprofloxacin, enoxacin, co-trimoxazole, fosfomycin, clindamycin, gentamycin and novobiocin. The diameter of inhibition zones was measured in 'mm' and tabulated. They were further classified as susceptible, resistant, and intermediate towards antibiotics to determine their sensitivity.

RESULTS AND DISCUSSION

Bacteria isolation

After 24 hours of incubation on nutrient agar plates containing different ranges of copper salt concentrations, distinct colonies were observed on the plates made with 0.20 mg/mL copper salts. About 32 pure isolates with various morphological characters were obtained. Gram staining analysis showed that 28 isolates were Gram-positive bacilli and 4 were Gram-negative cocci.

Pathogenicity test

A blood agar test was conducted to determine the hemolytic capabilities of the isolates. A clear halo zone around the streaked lines of isolates depicted beta hemolysis (Figure 2). Green or brown color formation around the streaked line in the media depicted alpha hemolysis, whereas no halo zone or color formation confirmed gamma hemolysis. After 24 hours of incubation, 16 isolates showed clear zones around the streaked lines and exhibited beta-hemolytic capabilities, whereas the rest were gamma-hemolytic.

Molecular characterization

Through 16S rDNA identification, analyzed sequenced data showed a 1204 base pair and 99.24% homology with *L. sphaericus*, thus confirming the identity of one of the isolated beta-hemolytic strains. Further, the obtained sequence data was deposited in GenBank, and an accession number OP810683 was procured (Nandi et al. 2024). The previous case studies related to *L. sphaericus* showed that this isolate is a potential threat.

Antibiotic susceptibility test of studied strain

Among all the beta-hemolytic strains, *L. sphaericus* (NJCT1) was selected to evaluate its antibiotic susceptibility profiling. In this study, the antibiotic sensitivity of *L. sphaericus* (NJCT1) was assessed against 33 standard antibiotics (Figure 3; Table 1).

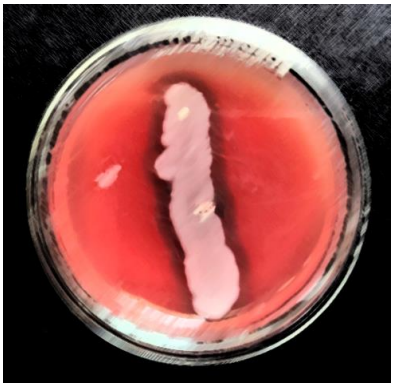

Figure 2. Clear halo zone around streak line of studied strain (NJCT1) on blood agar plate depicting beta hemolysis

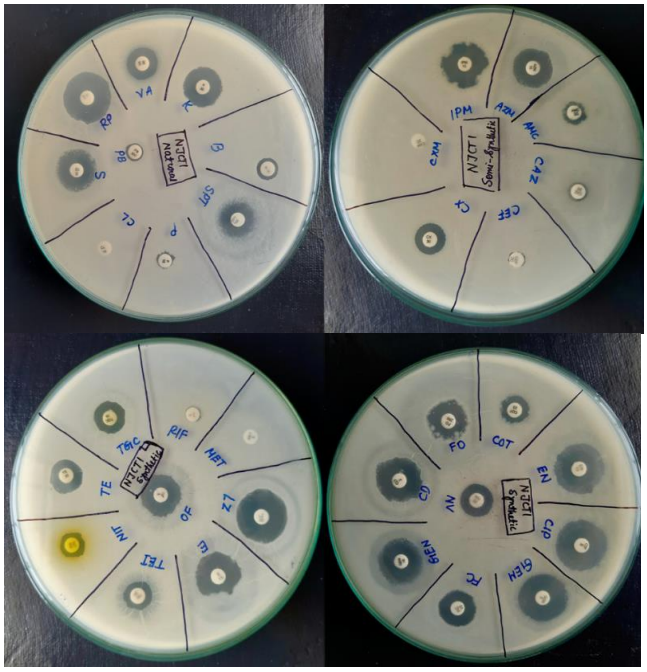

Figure 3. Antibiotic susceptibility of *Lysinibacillus sphaericus* (NJCT1) against several antibiotics

Table 1. Antibiotic susceptibility profile of *Lysinibacillus sphaericus* (NJCT1)

Drug class	Antibiotic	S/R/I
β lactam/ cephalosporin	Penicillin- G	R
	Methicillin	R
	Amoxicillin	R
	Cefuroxime	R
	Ceftazidime	R
	Cefoxitin	S
Sulfonamide	Co-trimoxazole	S
Fluoroquinolones	Ofloxacin	S
	Ciprofloxacin	S
	Enoxacin	S
	Gemifloxacin	S
Aminocoumarin	Novobiocin	S
Anti-mycobacterial	Rifampin	R
Aminoglycoside	Gentamycin	S
Glycylcycline	Tigecycline	S
Macrolide	Erythromycin	S
	Azithromycin	S
	Pristinamycin	S
Fosfomycin	Fosfomycin	S
Glycopeptide	Teicoplanin	S
	Vancomycin	S
Lincomycin	Clindamycin	S
Tetracycline	Tetracycline	S
Oxazolidinones	Linezolid	S
Nitrofurantoin	Nitrofurantoin	S
Fusidane	Fusidic acid	S
Polypeptide	Polymixin-B	I
	Colistin (Polymixin-E)	R
	Bacitracin	I
Carbapenems	Imipenem	S
Aminoglycosides	Streptomycin	S
	Spectinomycin	S
	Kanamycin	S

Note: 0.0-4.9 mm = Resistant (R); 5.0-9.9 mm = Intermediate (I); 10mm< = Susceptible (S)

Based on the National Committee for Clinical Laboratory Standards (NCCLS), the results showed *L. sphaericus* (NJCT1) had complete resistance against 7 antibiotics, namely 2 natural (colistin, penicillin-g); 3 semi-synthetic (amoxicillin, ceftazidime and cefuroxime); and 2 synthetic antibiotics (rifampin and methicillin). Based on the inhibition, *L. sphaericus* (NJCT1) showed intermediate resistance against 2 natural antibiotics (bacitracin and polymixin-b), and the rest were susceptible. Ciprofloxacin, gemifloxacin, ofloxacin, and enoxacin, belonging to the fluoroquinolones class, showed a 21 mm inhibition zone, the most sensitive antibiotic for *L. sphaericus*.

Discussion

In this study, 32 copper-tolerant bacteria have been isolated from river beds and tea gardens near the Indo-Bhutan border of West Bengal, India. Several bacteria possess beta-hemolytic abilities. Bacteria mainly possess three different types of hemolytic activities. Beta (β) hemolysis is indicated by total lysis of red blood cells, and hence, it is called "true lysis," visible as a clear and transparent area in blood agar culture. Alpha (α) hemolysis caused the increase of methemoglobin, indicated by a brown or green area in the blood agar culture, suggesting that there is no lysis of hemoglobin but just a reduction of hemoglobin to methemoglobin. Gamma (γ) hemolysis or non-hemolysis indicates no cell damage or transformation in the agar plates. One of the isolates, *L. sphaericus*, with beta-hemolytic activity, was found in the Kaljani River basin. This isolate, which exhibits the highest activity, is an antagonist in rare cases of infection caused by bacteremia in patients with weakened immune systems. However, it is rarely pathogenic in humans. These findings could have significant implications for understanding and potentially treating such infections.

Lysinibacillus sphaericus (NJCT1), a Gram-positive bacillus spore-forming bacteria, might produce cytolytic toxin, a common toxin produced by Gram-positive bacteria (Masignani et al. 2006; Ramachandran 2013). Under extreme environmental conditions, *Bacillus* spp. also produces some toxins as a survival strategy. Bacteria mainly produce cytotoxin to access nutrients or eliminate competition from their surroundings (Harding et al. 2011). *L. sphaericus* was previously called *Bacillus sphaericus*, which is known for its insecticidal activity and hemolysin encoding genes, which include *hylA*, *hylC*, *hylD*, and *xhlA* are the crucial factors for this activity (Gómez-Garzón et al. 2017). *Bacillus* is not known for its pathogenicity. However, some *Bacillus*, such as *L. sphaericus*, could be an opportunistic pathogen due to its ubiquity and ability to cause severe human infections. The most commonly observed systematic infection due to *Bacillus* spp. is 'bacteremia", which is generally associated with intravascular catheterization. Neutropenic patients, neonates, and intravenous drug users suffer the most from disseminated *Bacillus* spp infection. Various antibiotics were prescribed to treat *L. sphaericus*, as the obtained bacteria mixed with different blood cultures from different patients revealed susceptibility to various antibiotics (Wenzler et al. 2015).

Bacteremia can be life-threatening to immunocompromised people and is now a common problem with people dealing with some serious health issues. The water from the Kaljani River supports the livelihood of people and animals residing in the tea gardens. Infection of *L. sphaericus* originating from the Kaljani River could be dangerous. A detailed antibiotic study was conducted to understand the potential treatment of infection. The findings showed that *L. sphaericus* in this study is resistant to 5 out of 6 antibiotics belonging to the β-lactam drug class.

β-lactams (penicillin, cephalosporins, and monobactams) have been at the top of the antibiotic market since the beginning due to their efficiency against bacterial infections linked to other species that look like losing their edge, as bacteria have seemingly grown resistance against them in recent days. β-lactamase is the enzyme secreted by bacteria to attack the ring of β-lactam antibiotic, thus aiding in developing resistance in bacteria against this drug class (Pandey and Cascella 2019). Complete resistance was obtained against polymixin-e (colistin), and polymixin-b has an intermediate resistance, which can be a concern to clinical approaches as nowadays polymixins are regarded

as a gateway in multidrug resistance conditions (Poirel et al. 2017). Complete resistance of rifampin expressed that it might not inhibit the DNA-dependent RNA polymerase of the isolate, which generally aids in bactericidal activity (Campbell et al. 2001).

Resistance capability in bacteria is often associated with an isolate's heavy metal resistance pattern, as several studies stated the existence of both heavy metal and Antibiotic Resistance Genes (ARGs) in a bacterium, specifically with the occurrence of genes imparting heavy metal tolerance in the chromosome and antibiotic resistance in the plasmid. Further, the co-existence of heavy metal and antibiotic tolerance genes in plasmid conferring resistance to both stress factors has also been reported (Murray et al. 2024). A plasmid harboring heavy metal tolerance genes is more likely to possess ARGs than plasmids lacking heavy metal resistance genes. In this regard, *L. sphaericus* isolated from the Kaljani River grew at 0.20 mg/mL copper stress, illustrating its copper resistance capability. Wu et al. (2022) stated that isolates capable of tolerating copper up to 0.12 mg/mL are considered resistant and have copper detoxifying abilities. The resistance potential of *L. sphaericus* may contribute to its various antibiotics. Li et al. (2017) reported that resistance genes against multiple antibiotics, i.e., beta-lactam and polymyxin, are associated with heavy metal tolerant genes.

The result showed that fluoroquinolones were the most susceptible against *L. sphaericus* (NJCT1). This outcome is identical to the well-known occurrence of 12 *L. sphaericus* bacteremia infection cases in a Children's Cancer Hospital in Italy, reported in 10 years. Verification of 12 out of 469 cases (around 2%) of bacteremia infections, who were also cancer patients or were in the process of bone-marrow transplant were successfully treated with ciprofloxacin, which belongs to the fluoroquinolone drug class (Castagnola et al. 2001). This 2% success rate is significant as it demonstrates the potential of ciprofloxacin in treating *L. sphaericus* infections. Amoxicillin was recommended and had positive outcomes for two other immunosuppressed patients suffering from acute sepsis and dialysis-associated peritonitis (Wenzler et al. 2015; Kinoshita et al. 2023). However, *L. sphaericus* (NJCT1) in this study showed unusual in-vitro resistance against amoxicillin. Meng et al. (2023) reported that an HIV patient infected by the *L. sphaericus* (FY22) strain was treated with levofloxacin and vancomycin had an effective result. This study also observed the susceptibility of *L. sphaericus* (NJCT1) towards vancomycin.

In conclusion, bacteremia-associated infections are becoming a threat nowadays. Even though some significant infections associated with *L. sphaericus* have been reported, a detailed antibiotic study is essential to reduce the bacterial pool and, consequently, infections. Evaluating potential threats is greatly assisted by determining pathogenic phenotypes of environmental strains, identifying potential adaptations, and initiating clinically relevant bacteria. Antibiotic assessment of the *L. sphaericus* strain isolated from the Kaljani River basin can be a future approach to control the possible threat posed by this species through its beta-hemolytic abilities.

ACKNOWLEDGEMENTS

Sudeshna Nandi would like to acknowledge the University Grant Commission (UGC), Govt of India, for providing the SJSGC fellowship (2022-23-UGCES-22-WESF-SJSGC-2360)

REFERENCES

Albarral V, Sanglas A, Palau M, Miñana-Galbis D, Fusté MC. 2016. Potential pathogenicity of *Aeromonas hydrophila* complex strains isolated from clinical, food, and environmental sources. Can J Microbiol 62 (4): 296-306. DOI: 10.1139/cjm-2015-0466.

Bhakdi S, Grimminger F, Suttorp N, Walmrath D, Seeger W. 1994. Proteinaceous bacterial toxins and pathogenesis of sepsis syndrome and septic shock: The unknown connection. Med Microbiol Immunol 183: 119-144. DOI: 10.1007/BF00196684.

Campbell EA, Korzheva N, Mustaev A, Murakami K, Nair S, Goldfarb A, Darst SA. 2001. Structural mechanism for rifampicin inhibition of bacterial RNA polymerase. Cell 104 (6): 901-912. DOI: 10.1016/S0092-8674(01)00286-0.

Castagnola E, Fioredda F, Barretta MA, Pescetto L, Garaventa A, Lanino E, Micalizzi C, Giacchino R, Dini G. 2001. *Bacillus sphaericus* bacteraemia in children with cancer: Case reports and literature review. J Hosp Infet 48 (2): 142-145. DOI: 10.1053/jhin.2001.0995.

Denku CY, Ambelu A, Mitike G. 2022. Enteric bacterial pathogens and their antibiotic-resistant patterns from the environmental sources in different regions of Ethiopia: A laboratory-based cross-sectional study. Health Sci Rep 5 (2): e521. DOI: 10.1002/hsr2.521.

Getie M, Abebe W, Tessema B. 2019. Prevalence of enteric bacteria and their antimicrobial susceptibility patterns among food handlers in Gondar town, Northwest Ethiopia. Antimicrob Resist Infect Control 8: 111. DOI: 10.1186/s13756-019-0566-7.

Gómez-Garzón C, Hernández-Santana A, Dussán J. 2017. A genome-scale metabolic reconstruction of *Lysinibacillus sphaericus* unveils unexploited biotechnological potentials. PLoS One 12 (6): e0179666. DOI: 10.1371/journal.pone.0179666.

Harding T, Jungblut AD, Lovejoy C, Vincent WF. 2011. Microbes in high arctic snow and implications for the cold biosphere. Appl Environ Microbiol 77 (10): 3234-3243. DOI: 10.1128/AEM.02611-10.

Jeon HL, Lee NK, Yang SJ, Kim WS, Paik HD. 2017. Probiotic characterization of *Bacillus subtilis* P223 isolated from kimchi. Food Sci Biotechnol 26 (6): 1641-1648. DOI: 10.1007/s10068-017-0148-5.

Kinoshita T, Sahara S, Amano T, Ito M, Sakakibara T, Takimoto N, Osada Y, Oka K. 2023. First case report of peritoneal dialysis-associated peritonitis caused by *Lysinibacillus sphaericus*. Intern Med 62 (19): 2919-2922. DOI: 10.2169/internalmedicine.1141-22.

Langendorf C, Le Hello S, Moumouni A, Gouali M, Mamaty AA, Grais RF, Weill FX, Page AL. 2015. Enteric bacterial pathogens in children with diarrhea in Niger: Diversity and antimicrobial resistance. PloS One 10 (3): e0120275. DOI: 10.1371/journal.pone.0120275.

Larsson DG, Flach CF. 2022. Antibiotic resistance in the environment. Nat Rev Microbiol 20: 257-269. DOI: 10.1038/s41579-021-00649-x.

Li LG, Xia Y, Zhang T. 2017. Co-occurrence of antibiotic and metal resistance genes revealed in complete genome collection. ISME J 11 (3): 651-662. DOI: 10.1038/ismej.2016.155.

Masignani V, Pizza M, Rappuoli R. 2006. Bacterial Toxins. In: Dworkin M, Falkow S, Rosenberg E, Schleifer KH, Stackebrandt E (eds.). The prokaryotes. Springer, New York, NY. DOI: 10.1007/0-387-30742-7_28.

Meng Z, Duan R, Lv D, Bu G, Gao Y, Zhang P, Sun Y, Guo G, Qin S, Sun L, Zhang D, Liang J, Jing H, Wang X. 2023. Rare case of bacteremia due to *Lysinibacillus sphaericus* in a person living with HIV. Intl J Infect Dis 135: 91-94. DOI: 10.1016/j.ijid.2023.08.013.

Murray LM, Hayes A, Snape J, Kasprzyk-Hordern B, Gaze WH, Murray AK. 2024. Co-selection for antibiotic resistance by environmental

contaminants. NPJ Antimicrob Resist 2 (1): 9. DOI: 10.1038/s44259-024-00026-7.

Nandi S, Subba P, Bhattacharya M. 2024. *Lysinibacillus sphaericus* isolated from dolomite and copper ore contaminated Kaljani River basin exhibits high copper tolerance and plant growth promoting property. Geomicrobiol J 41 (7): 742-754. DOI: 10.1080/01490451.2024.2376104.

Nizet V. 2002. Streptococcal β-hemolysins: Genetics and role in disease pathogenesis. Trends Microbiol 10 (12): 575-580. DOI: 10.1016/s0966-842x(02)02473-3.

Pandey N, Cascella M. 2019. Beta lactam antibiotics. StatPearls Publishing, Treasure Island (FL).

Poirel L, Jayol A, Nordmann P. 2017. Polymyxins: Antibacterial activity, susceptibility testing, and resistance mechanisms encoded by plasmids or chromosomes. Clin Microbiol Rev 30 (2): 557-596. DOI: 10.1128/cmr.00064-16.

Ramachandran G. 2013. Gram-positive and gram-negative bacterial toxins in sepsis: A brief review. Virulence 5 (1): 213-218. DOI: 10.4161/viru.27024.

Robert AP, Lorraine F, Walter M, Ronald MR. 2009. Laboratory exercises in Microbiology 3rd ed. John Wiley and Sons, Inc., Hoboken.

Rosa-Fraile M, Spellerberg B. 2017. Reliable detection of group B *Streptococcus* in the clinical laboratory. J Clin Microbiol 55 (9): 2590-2598. DOI: 10.1128/jcm.00582-17.

Saha S, Acharyya S, Sarkar S, Bhattacharya M. 2021. Study of tolerance ability in phosphate solubilizing microorganisms isolated from tea plantation soil of lower Darjeeling hills. Bull Natl Res Cent 45: 109. DOI: 10.1186/s42269-021-00564-4.

Sarkar D. 2012 Monsoon flow of Dolomite contaminated water from Bhutan hills creates havoc in WB foothills. https://economictimes.indiatimes.com/monsoon-flow-of-dolomite-contaminated-water-from-bhutan-hills-creates-havoc-in-wb-foothills/articleshow/14690093. Accessed 28 April 2024.

Smith DA, Nehring SM. 2017. Bacteremia. StatPearls Publishing, Treasure Island (FL).

Tomita T, Kamio Y. 1997. Molecular biology of the pore-forming cytolysins from *Staphylococcus aureus*, α-and γ-hemolysins and leukocidin. Biosci Biotechnol Biochem 61 (4): 565-572. DOI: 10.1271/bbb.61.565.

Wenzler E, Kamboj K, Balada-Llasat JM. 2015. Severe sepsis secondary to persistent *Lysinibacillus sphaericus*, *Lysinibacillus fusiformis* and *Paenibacillus amylolyticus* bacteremia. Intl J Infect Dis 35: 93-95. DOI: 10.1016/j.ijid.2015.04.016.

Wu B, Luo H, Wang X, Liu H, Peng H, Sheng M, Xu F, Xu H. 2022. Effects of environmental factors on soil bacterial community structure and diversity in different contaminated districts of Southwest China mine tailings. Sci Total Environ 802: 149899. DOI: 10.1016/j.scitotenv.2021.149899.

ASIAN J TROP BIOTECHNOL
Volume 22, Number 1, June 2025
Pages: 7-15

ISSN: 0216-6887
E-ISSN: 2301-8658
DOI: 10.13057/biotek/c220102

Bacterial diversity of *Spheciospongia* spp. from Rancabuaya Beach, West Java, Indonesia, using the NGS approach

YOICE SRIKANDACE[1,2], AISHA WAHHAAB[3], ANWAR FAUZI RAKHMAT[3], KAMARISIMA[3], SASTIA PRAMA PUTRI[3,4,5], PINGKAN ADITIAWATI[3,♥]

[1]School of Life Sciences and Technology, Institut Teknologi Bandung. Jl. Ganesha No.10, Bandung 40132, Indonesia
[2]Research Center for Biomass and Bioproduct, National Research and Innovation Agency. Jl. Raya Jakarta-Bogor km. 46 Cibinong, Bogor 16911, Indonesia
[3]Microbial Biotechnology Research Group, School of Life Sciences and Technology, Institut Teknologi Bandung. Jl. Ganesha No.10, Bandung 40132, Indonesia. Tel.: +62-22-250-3962, ♥email: pingkan@itb.ac.id
[4]Department of Biotechnology, Graduate School of Engineering, Osaka University. 2-1 Yamadaoka, Suita, Osaka 565-0871, Japan
[5]Industrial Biotechnology Initiative Division, Institute for Open and Transdisciplinary Research Initiatives, Osaka University. Osaka 565-0871, Japan

Manuscript received: 30 January 2025. Revision accepted: 16 April 2025.

Abstract. *Srikandace Y, Wahhaab A, Rakhmat AF, Kamarisima, Putri SP, Aditiawati P. 2025. Bacterial diversity of* Spheciospongia *spp. from Rancabuaya Beach, West Java, Indonesia, using the NGS approach. Asian J Trop Biotechnol 22: 7-15*. For the first time, the bacterial community associated with *Spheciospongia* spp. from Rancabuaya Beach in Garut was identified using Next-Generation Sequencing (NGS). The study focused on the bacterial diversity present on the sponge's body surfaces (SEK1, SEK2), within their inner tissues (SEN1, SEN2), and in the surrounding seawater (SW). The results revealed that SW had the highest number of species, with 198 detected, followed by SEN2 and SEN1, with 193 and 165 species, respectively. In contrast, SEK1 and SEK2 contained 32 and 26 bacterial species, respectively. The analysis also showed that SW possessed the highest diversity and evenness indices at the genus level, with values of 2.95 and 0.79, respectively, indicating the absence of a dominant genus. Conversely, SEK1 and SEK2 exhibited low evenness indices (0.33 and 0.24) and low variety indices (0.80 and 0.54), indicating that the community lacks a balance of species. SEN1 and SEN2 demonstrated moderate genus diversity, but their evenness and dominance varied. The dominant phyla across all samples were *Proteobacteria* and Bacteroidota. Notably, the NGS method identified several actinomycete genera for the first time, including *Micrococcus*, *Leucobacter*, *Egibacter*, *Lawsonella*, *Nakamurella*, and *Corynebacterium*. A recent study confirmed that NGS provides a rapid, sensitive, and high-quality method for determining microbial communities.

Keywords: Actinobacteria, diversity, dominance, evenness, indices, next-generation sequencing, *Spheciospongia*

INTRODUCTION

Mangrove sponges play a crucial role in the ecosystem by providing habitats, shelter, and food sources for marine microorganisms. Sponge-associated microbial communities are diverse and exhibit mutualistic relationships with one another, acting as symbionts or pathogens (Bibi et al. 2020). This mutualistic relationship involves the sponge supplying organic particles as nutrition for microorganisms, while microorganisms produce metabolites that inhibit pathogen growth on the sponge (Li et al. 2023; Mehbub et al. 2024). The sponge can also produce bioactive compounds as nutrition for microorganisms and to prevent pathogens (Varijakzhan et al. 2021; Hong et al. 2022). Microorganisms associated with sponges can account for up to 40% of the body weight of particular sponge species, with their population densities being 100 to 10,000 times higher than in surrounding seawater (Sugden et al. 2022). These microbial communities, often located within the sponge's mesohyl, support the sponge's metabolism and produce beneficial molecules, including antimicrobials and other biologically active substances (Dat et al. 2021; Sugden et al. 2022).

The bacterial communities associated with various sponge species have been the subject of numerous studies, employing both culture-dependent and culture-independent methods. Approximately 1% of the bacteria can be effectively cultured in the laboratory, while other bacteria have been discovered through culture-independent approaches based on the 16S rRNA gene (Ito et al. 2019; Ahmad et al. 2024). Actinomycete bacteria are important microorganisms and are still being explored to uncover their potential compounds. Due to the challenges of isolating and culturing actinomycetes in the laboratory, Next-Generation Sequencing (NGS) facilitates the identification of additional actinomycete species and the development of suitable media to isolate them from sponges. NGS has enhanced our understanding of sponge symbiont diversity, revealing that unculturable bacteria can make up 99% of any environment (Bibi et al. 2020; Abbas and Mahmoud 2022).

The NGS approach enables the investigation of microbial communities from various geographical locations, providing deeper insights into the diversity of bacterial populations (Waterworth et al. 2021). Moreover, NGS is a powerful tool for studying bacteria, providing an in-depth, unbiased, and accurate analysis of bacterial communities, revealing complex interactions, diverse species, and functional roles

(Tan et al. 2015). It provides a far more detailed and comprehensive picture of the microbial world than traditional methods, driving discoveries in microbiology and ecology (Satam et al. 2023). NGS enables the exploration of new Actinomycetes or Streptomyces species by allowing researchers to perform comprehensive metagenomic surveys, identify novel genes, and discover previously unknown bacterial strains that may produce bioactive compounds (Alam et al. 2021). Several structural profiles of bacterial communities in sponges have been identified through NGS using the Illumina platform. The bacterial diversity in the freshwater sponges *Eunapius carteri* and *Corvospongilla lapidosa* had 14 phyla, with over 2,900 OTUs for *C. lapidosa* and 980 OTUs for *E. carteri* (Gaikwad et al. 2016). The sponge *Callyspongia* sp., from the Thousand Islands, Indonesia, exhibited a low abundance of Actinomycetes (0.09%) and was dominated by Proteobacteria, which comprised 82% of the community (Retnowati et al. 2021). The bacterial community associated with the sponge *Haliclona oculata* (Linnaeus, 1759) includes 17 phyla, while *Amphius huxleyi* contains 13 phyla. Proteobacteria are the dominant phylum in both sponge species, though other phyla are present in varying abundances (Dat et al. 2021). Therefore, the Illumina platform is chosen for its high throughput, accuracy, and cost-effectiveness, making it ideal for studying the diverse bacterial communities found in sponges and other environments.

The bacteria associated with marine sponges are well-documented, but the symbiotic bacteria found in coastal sponges remain largely unexplored. Rancabuaya Beach in Garut, West Java, has limited human activity, making it an ideal site for study. *Spheciospongia* spp. can be easily found attached to coral rocks. This beach, situated adjacent to the Indian Ocean, boasts coral reefs, powerful waves, a gently sloping seabed, and a pristine white sand shoreline with crystal-clear and blue water. Thus, the current study aimed to investigate the bacterial community of the widespread coastal water and the surface of *Spheciospongia* spp. through the NGS method. This culture-independent and high-throughput method offers an efficient and powerful approach to uncovering the hidden biodiversity of these bacteria.

MATERIALS AND METHODS

Study area

Recent research was conducted at Rancabuaya Beach in the Garut District of West Java, Indonesia (Figure 1).

Procedures

Sponge and water sampling

The samples were taken from the supralittoral to mesolittoral zones using no specialized equipment and were transferred into sterile plastic containers. Beach water was also collected and placed in a 1 L sterile bottle. All samples were stored in a cooler bag, transported to the laboratory, and processed immediately. Collecting sponges did not require permission from the authorities, as it pertained to species that were neither endangered nor protected.

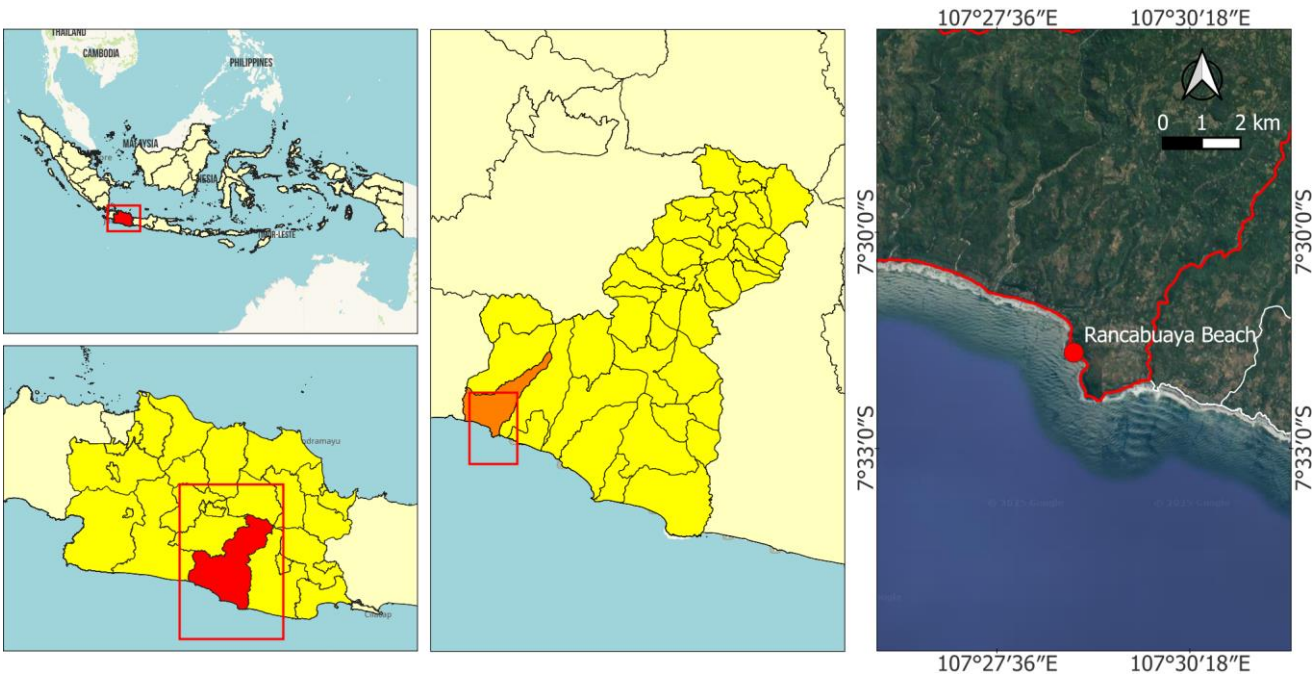

Figure 1. The location of the sampling site is in Rancabuaya Beach, Caringin, West Java, Indonesia

DNA extraction from sponges

Total genomic DNA was extracted from two sponges and seawater samples using a combination of bead-beating and the phenol: chloroform: isoamyl alcohol method (Djurhuus et al. 2017). The surfaces and inside of the sponge bodies were cut, crushed, and dissolved in artificial sterile seawater. The samples were then centrifuged at 8000 rpm for 5 minutes to separate the crushed sponge material from the sterile seawater containing bacteria, resulting in four sponge samples: SEK1, SEK2, SEN1, and SEN2. All samples were concentrated by centrifugation at 8000 rpm for 5 minutes. The pellets from each sample were dissolved in 1 mL of sterile Phosphate-Buffered Saline (PBS). Bacterial DNA was extracted from the pellets using the phenol-chloroform: isoamyl method. The recovered DNA was resuspended in 20 µL of TE buffer (pH 8.0). The integrity of the DNA was assessed by agarose gel electrophoresis. Purity (measured as the λ 260 nm/280 nm ratio) and quantity were evaluated using a NanoDrop 2000 spectrophotometer (Thermo Fisher Scientific, Waltham, MA, USA). The DNA samples were stored at -20°C for PCR amplification. The purification of PCR products was performed using the Promega Wizard PCR Clean-Up Protocol procedure. DNA was visualized using electrophoresis with a 2% agarose gel in 1X TBE buffer and a 1 kbp DNA ladder marker (Promega).

16S rRNA amplification

The 16S rRNA genes were amplified by polymerase chain reaction (PCR) using primers 27F (GAGTTTGATCCTGGCTCAG) and 1492R (GGTTACCTTGTTACGACTT) in the first-stage PCR. The PCR mixture consisted of 12.5 µL GoTaq Green Master Mix (Promega), 1 µL 1492r primer (10 pM), 1 µL 27f primer (10 pM), 1 µL sample DNA, and 25 µL Nuclease-Free Water (NFW) in a final volume of 50 µL. PCR products were purified using the QIAquick PCR kit (Qiagen, Germany) according to the manufacturer's instructions. The cycling conditions are as follows: initial denaturation at 95°C for 5 minutes, followed by 30 cycles of denaturation at 95°C for 1 minute, annealing at 55°C for 1 minute, and extension at 72°C for 1 minute, with a final extension of 5 minutes at 72°C. The gene-specific sequences of 16S V3 and V4 regions were submitted for amplicon sequencing using the Illumina MiSeq platform. The construction of a 16S rRNA library and subsequent Illumina NGS sequencing analysis were conducted by Macrogen Korea, utilizing the purified PCR products as a template. Furthermore, the second-stage PCR reaction utilized the Nextera XT DNA Library Preparation Kit following the two-step cycling standard protocol recommended by the manufacturer.

Data analysis

Sequencing data analysis: OTU clustering and taxon annotation

Based on the unique barcode of each sample, paired-end reads were assigned. The samples were then truncated by removing the barcode and primer sequences, and the reads were merged using FLASH v1.2.7. OTUs were performed with QIIME2 2017.4. Raw sequence data were demultiplexed and quality filtered using the q2-demux plugin, then denoised using DADA2. The sequences were clustered into Operational Taxonomic Units (OTUs) with a similarity of ≥97%. The most frequent sequence within each OTU was selected and screened to obtain the representative sequence. All Amplified Sequence Variants (ASVs) were aligned using MAFFT. Taxonomy assigned to ASVs using feature classifier q2 (Bokulich et al. 2018).

Diversity, evenness, and dominance index calculation

The diversity index (H'), evenness index (E), and dominance index were calculated using the equation formula (Roswell et al. 2021) and classified according to Table 1.

$$H' = \sum_{i=1}^{s} \frac{ni}{N} \ln \frac{ni}{N}$$

$$E = \frac{H'}{lnS}$$

$$D = \Sigma \frac{ni}{N}$$

RESULTS AND DISCUSSION

Sponges collection

The sponges collected belong to *Spheciospongia*, as shown in Figure 2. The condition of the coastal waters was characterized by clear blue water, an odorless quality, a salinity ranging from 2.70 to 3.10 ‰, and a pH of 8.22. *Spheciosponga sp.1* exhibited a light brown underside and a green upper surface, with body surface and internal tissues designated SEK1 and SEN1 samples. *Spheciospongia* sp.2 displayed a bright yellow upper and lower body surface, with its body surface and internal tissues categorized as SEK2 and SEN2 samples. Seawater samples were coded SW.

Table 1. Diversity index value criteria

Index	Value	Criteria
Diversity	H'<1	Low
	1<H'<3	Moderate
	H'>1	High
Evenness	E<1	Low
	1<E<3	Moderate
	E>1	High
Dominance	D<1	Low
	1<D<3	Moderate
	D>1	High
H': Diversity Index	E: Evenness Index	D: Dominance Index
S: No. of species	H': Diversity Index	ni: Individual number
ni: Individual number	ln: Natural logarithm	N: Total individual number
N: Total individual number	S: No. of species	

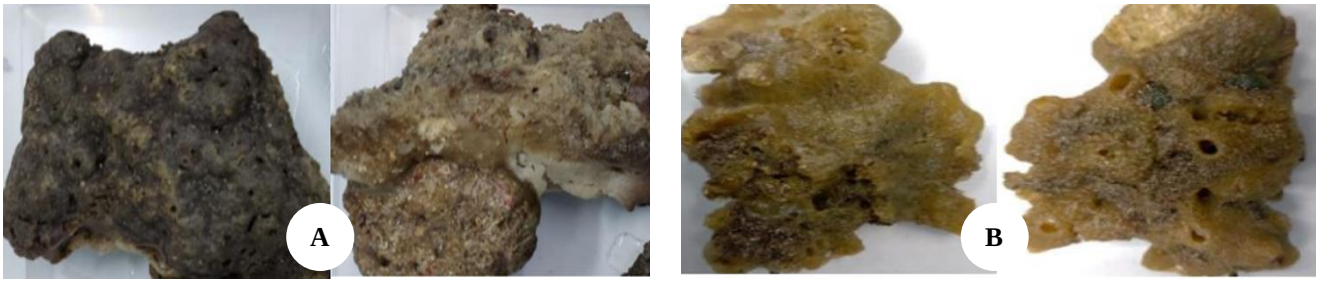

Figure 2. The sponge collection from Rancabuaya beach: A. *Spheciospongia* sp.1; B. *Spheciospongia* sp.2

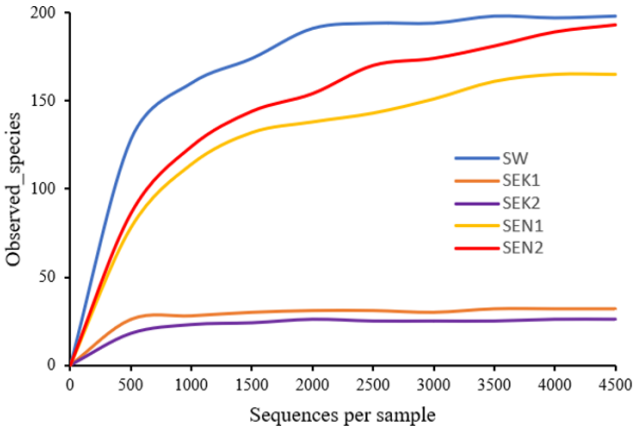

Figure 3. Rarefaction curves showing observed species richness in samples

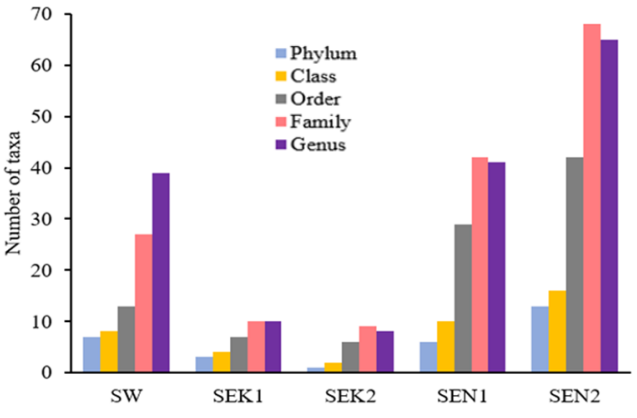

Figure 4. Number of phyla to genera of bacteria observed in samples

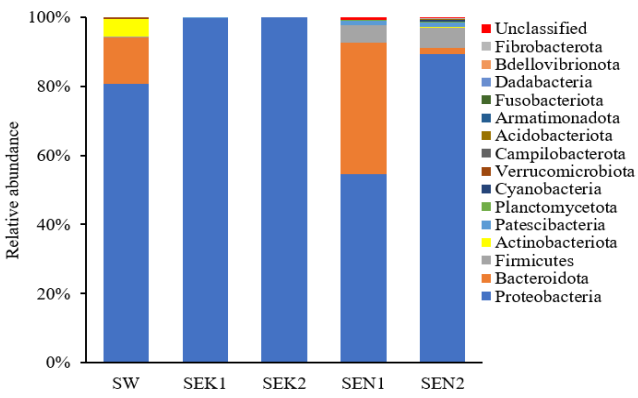

Figure 5. The relative abundances of 15 dominant phyla

Bacterial diversity associated with *Sphesiospongia* spp

The rarefaction curve displayed a horizontal asymptote, indicating that the number of bacterial species (OTUs) detected in each sample had high sequence coverage (Figure 3). In SW, the highest number of bacterial species was detected, totaling 198 species, followed by SEN2 with 193 species and SEN1 with 165 species. Meanwhile, samples SEK1 and SEK2 contained 32 and 26 bacterial species, respectively. The highest abundance of bacteria was found within the sponge, with SEN1 and SEN2 accounting for 83.76 and 88.13% of the total bacterial population, respectively. Bacterial abundance was low on the SEK1 and SEK2, but the highest abundance was observed in SW. Clear saturated plains with adequate coverage and complete sorting (100%) from all samples. According to Willis (2019), A rarefaction curve that approaches a horizontal asymptote, indicating sufficient sampling, can be used to evaluate the observed species richness.

Figure 4 depicts the diversity of microbial communities in different sponge samples. The SW sample contained 7 phyla, 8 classes, 13 orders, 27 families, and 39 genera. The SEK1 and SEK2 samples had 3 and 1 phyla, 4 and 2 classes, 7 and 6 orders, 10 and 9 families, and 10 and 8 genera, respectively. In the SEN1 and SEN2 samples, 6 and 13 phyla, 10 and 16 classes, 29 and 42 orders, 42 and 68 families, and 41 and 65 genera were identified. These findings suggest that sponges create a suitable environment for bacterial growth, resulting in a rich diversity of microbial communities, particularly in the SEN1 and SEN2 samples. These results suggest that sponges serve as a rich organic source in their body tissues, creating a suitable habitat for bacteria. This is evidenced by the higher number of genera identified in the SEN1 and SEN2 samples.

The relative abundance of the top 15 bacterial taxa at the phylum level is shown in Figure 5. Other identified phyla were categorized as Others, while Unclassified was used for unknowns. The predominant phylum found in all samples was Proteobacteria, with the following percentages: SW (80.78%), SEK1 (99.77%), SEK2 (100%), SEN1 (54.49%), and SEN2 (89.27%). In the SW sample, the three dominant phyla were Proteobacteria (80.78%), Bacteroidota (13.47%), and Actinobacteria (5.03%). All SEK samples were also primarily dominated by Proteobacteria. In contrast, the SEN samples were characterized by three dominant phyla: Proteobacteria, Bacteroidota, and Firmicutes. Specifically, SEN1 contained Proteobacteria (54.49%), Bacteroidota (38.19%), and Firmicutes (5.10%), while

SEN2 had Proteobacteria (89.27%), Bacteroidota (1.90%), and Firmicutes (5.90%). No 100% phyla abundance was detected in SEN1 (97.78%) and SEN2 (97.07%), possibly due to insufficient amplification or detection of some fragments of DNA, which could have led to the loss of some sequence information. NGS technology may introduce errors, deletions, insertions, and substitutions. These mistakes may show discrepancies between the actual and observed sequences (Das et al. 2023). Therefore, to detect sequence variants, NGS shows a confidence interval of approximately 98-100% for the identified taxonomy, which may influence the abundance of the detected microorganisms (Rojahn et al. 2022). Proteobacteria is the largest phylum in the bacterial domain, while Firmicutes, Bacteroidetes, and Actinobacteria are the dominant phyla associated with eukaryotes (Taylor et al. 2007).

The dominant class of bacteria across all samples in Figure 6 belonged to the Proteobacteria phylum, specifically Gammaproteobacteria, with the following percentages: SW (71.90%), SEK1 (99.26%), SEK2 (99.85%), SEN1 (54.06%), and SEN2 (84.53%). Alphaproteobacteria were detected only in the SW sample (5.03%), ranking as the fourth most dominant class after Bacteroidia (13.47%) and Actinobacteria (8.88%). In SEK1 and SEK2, small percentages of Actinobacteria were detected (0.51% and 0.15%), making them the second dominant class in those samples. For SEN1, the second and third most common classes were Bacteroidia (38.19%) and Actinobacteria (0.40%). In SEN2, the second and third most prevalent classes were Actinobacteria (4.70%) and Bacteroidia (1.90%).

Gammaproteobacteria emerged as the dominant class compared to Alphaproteobacteria due to their paraphyletic nature, while Alphaproteobacteria are monophyletic (Orata et al. 2018). This makes Gammaproteobacteria the largest and most diverse group within the Proteobacteria phylum (Orata et al. 2018; Nguyen et al. 2023). Furthermore, Bacteroidetes bacteria are often detected in sponges, but their functions in host development remain largely unknown (Li et al. 2021). In marine sponges, Actinobacteria represent a diverse group of microorganisms capable of producing bioactive substances that help protect the sponge from predators (Retnowati et al. 2021).

Figure 7 shows that in the SW sample, three dominant orders were identified: Oceanospirillales (26.92%), Alteromonadales (20.57%)-with the Pseudoalteromonadaceae family making up 11.22%—and Flavobacteriales (13.38%). In the SEK1, SEK2, and SEN2 samples, Alteromonadales was the most prevalent order, with percentages of 84.64, 91.12, and 74.79%, respectively. In contrast, two dominant orders were found in SEN1: Flavobacteriales (37.93%) and Alteromonadales (32.26%). Additionally, several bacterial orders, including Rhodobacterales, Burkholderiales, Nitrosococcales, Rhizobiales, Micrococcales, and Caldalkalibacillales, were not present in SW but were found in SEK and SEN.

Seawater is primarily composed of bacteria from the orders Alteromonadales, Flavobacteriales, Rhodobacterales, Sphingobacteriales, Verrucomicrobiales, and Vibrionales (Rygaard et al. 2017; Rufino and Procópio 2021). These dominant bacterial orders require a variety of mineral sources for their growth. Seawater contains essential minerals such as magnesium (Mg), calcium (Ca), potassium (K), chromium (Cr), selenium (Se), zinc (Zn), and vanadium (V). Additionally, these bacteria play a crucial role in the decomposition of organic matter, contributing to the nutrient availability in seawater. The concentration of these inorganic materials tends to increase with sea depth (Nani et al. 2016).

The Pectobacteriaceae (13.52%), a family of Enterobacterales, is the most prevalent in SW, as shown in Figure 8. The Pseudoalteromonadaceae family is the most abundant in SEK1 and SEK2, accounting for 81.29% and 86.24%, respectively. Flavobacteriaceae is the most prevalent family in SEN1 (38.15%), whereas Pseudoalteromonadaceae again accounts for the highest percentage in SEN2 (70.12%). Only in SEN and SEK were the families Rhodobacteraceae, Alcaligenaceae, and Shewanellaceae present. Pseudoalteromonadaceae and Flavobacteriaceae are commonly found in marine water and sponges (Delgadillo-Ordoñez et al. 2022). Pectobacteriaceae are typically found in brackish water and river systems (Hugouvieux-Cotte-Pattat et al. 2024).

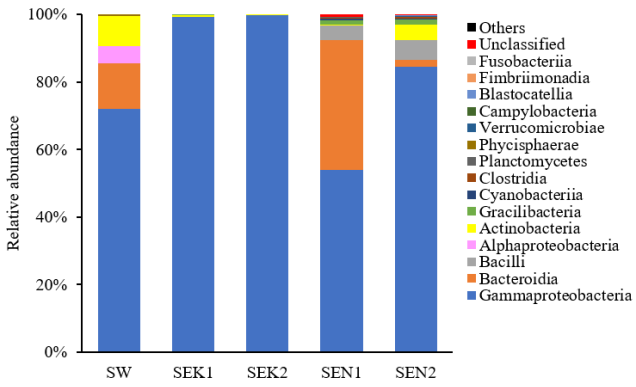

Figure 6. The relative abundances of 15 dominant classes

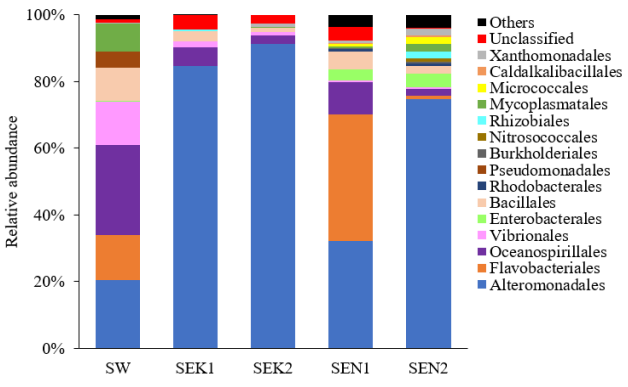

Figure 7. The relative abundances of 15 dominant orders

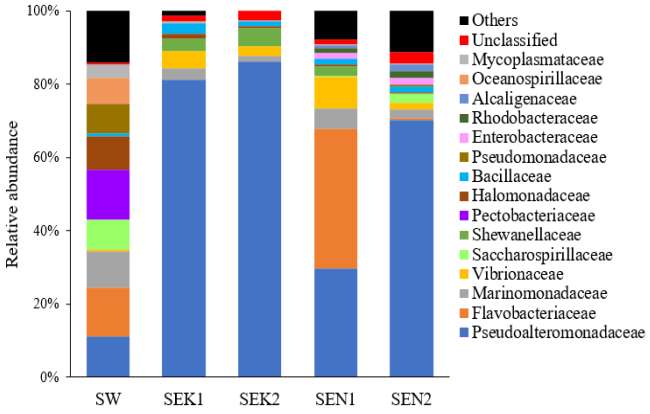

Figure 8. The relative abundances of 15 dominant families

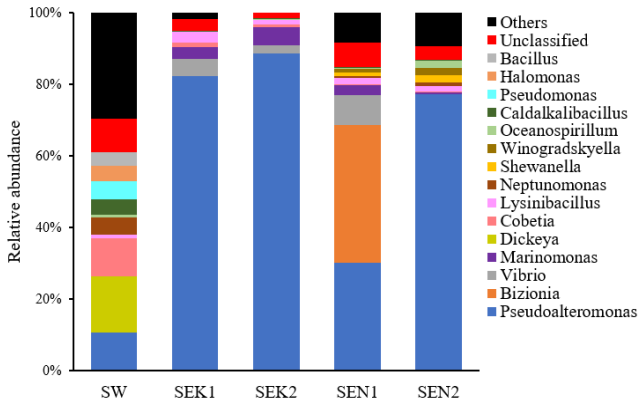

Figure 9. The relative abundances of 15 dominant genera

The abundance of Pectobacteriaceae along river courses is due to the suitability of temperature, nitrate availability, and dissolved organic carbon concentration in the water. Pectobacteriaceae are prevalent in freshwater environments, often causing disease outbreaks in aquatic plants (Ben Moussa et al. 2022). Pseudoalteromonadaceae exhibit versatile metabolic capabilities, making them highly adaptable to various ecological habitats, and play a crucial role in the marine environment. Ecologically, *Pseudoalteromonas* forms a biofilm in ecosystems and engages in predator-like interactions within microbial communities as a defense mechanism (Bowman 2007). Flavobacteriaceae is a group of bacteria found in soil, freshwater, and marine environments. This group is well known for its motility, which is associated with fish diseases. Several species within this family also have the potential for bioremediation of chemical compounds and organic materials, such as hydrocarbons. However, some species are pathogenic to fish (Skovhus et al. 2007).

SW was primarily dominated by *Dickeya*, which makes up 15.69% of the bacterial community in Figure 9. In contrast, SEK1, SEK2, and SEN2 were dominated by *Pseudoalteromonas*, comprising 82.26, 88.55, and 77.27%. *Bizionia* sp., found only in SEN1, accounted for approximately 38.39%. *Dickeya* was exclusively found in SW and was not present in sponges. In addition to beach water, *Dickeya* can be found in river water, as well as in sponges and lake water (Watanabe et al. 2015; Laport et al. 2019; Hugouvieux-Cotte-Pattat et al. 2024). *Pseudoalteromonas* spp. exclusively found in marine environments and are associated with eukaryotic hosts, including shellfish, pufferfish, tunicates, and sponges. The widespread presence of *Pseudoalteromonas* spp. across different habitats demonstrated adaptive strategies and survival capabilities (Holmström and Kjelleberg 1999; Sonnenberg and Haugen 2021). Additionally, *Bizionia argentinensis* sp. nov. and other *Bizionia* spp. have been isolated from Terra Nova Bay in the Ross Sea, and marine bacteria *Cliona* sp. were isolated from the marine sponge *Grantia celata* and Arctic Fjord seawater (Bercovich et al. 2008; Li et al. 2015; Savoca et al. 2019).

Structure the community of bacteria at the genus level

The diversity, evenness, and dominance indices provide insights into community structure. The bacterial diversity index across all samples ranged from low to moderate (Table 2). In SW, there was a high genus population evenness (0.79), with no single genus dominating, indicating a stable community. In contrast, low evenness values were observed in SEK1 (0.33), SEK2 (0.24), and SEN2 (0.31), accompanied by a high dominance index (0.60-0.79). Meanwhile, SEN1 exhibited moderate evenness (0.51) and a low dominance value (0.25). According to Strong (2016), the Shannon-Wiener diversity index (H') is categorized as low diversity ($H'<1$), moderate diversity ($1\leq H'\leq 3$), and high diversity ($H'>3$). The evenness index (E') is classified as low ($E<0.4$), moderate ($0.4\leq E\leq 0.6$), and high ($E>0.6$). The dominance index is categorized as low ($0\leq D\leq 0.3$), moderate ($0.3\leq D\leq 0.6$), and high ($0.6\leq D\leq 1$).

Actinomycetes diversity in sponges and coastal water

The most abundant actinobacteria families in the sponge and coastal waters varied. Actinomycete genera were more prevalent and detected in sponge bodies than in seawater, likely due to differences in nutrient availability. It indicated that the same sponge symbiont bacteria or actinomycetes vary even within the same habitat. Actinomycetes were more prevalent in the Sponge's Inner Tissue (SEN) and seawater (SW). A few actinomycetes were observed on the sponge body's surface (SEK) (Figure 10).

Table 2. Diversity index of the bacteria community associated with sponges at the genus level

Index	SW	SEK1	SEK2	SEN1	SEN2
Diversity	2.95	0.80	0.54	1.92	1.28
Category	Moderate	Low	Low	Moderate	Moderate
Evenness	0.79	0.33	0.24	0.51	0.31
Category	High	Low	Low	Moderate	Low
Dominance	0.07	0.68	0.79	0.25	0.60
Category	Low	Moderate	High	Low	Moderate

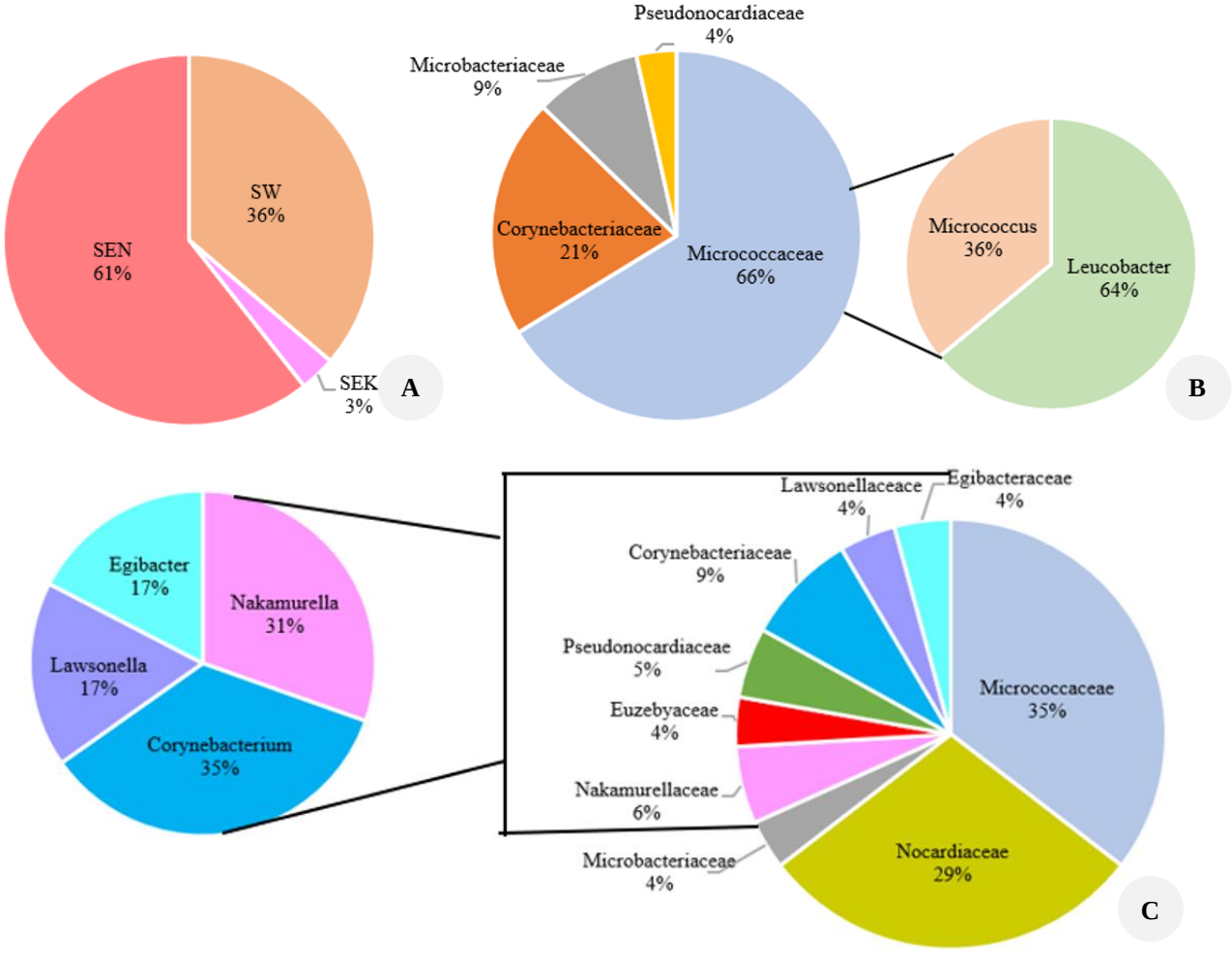

Figure 10. The abundance of the actinobacteria community: A. SW, SEK, SEN; B. two genera belonging to Micrococcaceae in SW; and C. Four genera to certain families in SEN

The SW sample consisted of 4 families, with 2 genera—*Leucobacter* and *Micrococcus*—belonging to the Micrococcaceae family. In SEK, only Micrococcaceae was identified (see Suppl). Nine families were discovered in the SEN sample, with the Micrococaceae and Nocardiaceae families being the most abundant. A recent study reveals that *Micrococcus*, *Leucobacteria*, *Egibacter*, *Lawsonella*, *Nakamurella*, and *Corynebacteria* were discovered using the NGS method. Not all genera could be identified among all the Actinobacteria families identified in this study.

Micrococcaceae are widely recognized as originating from various terrestrial environments, marine sponges, cyanobacterial layers, and marine sediments (Palomo et al. 2013). Additionally, Micrococcaceae have been identified in several sponge species, including *Callyspongia aerizusa*, *Haliclona atra*, *H. fascigera*, *Biemna* sp., *Paratetilla* sp., *Pseudoceratina* sp., *Scopalina hapalia*, *Plakortis kenyensis*, and *Tetrapocillon minor*, all found at a depth of 10 meters in Tanzania (Helber et al. 2018). The abundance of Corynebacteriaceae exceeds 50% in sediments compared to seawater (Sulardiono et al. 2018). A similar study showed approximately 6% Corynebacteriaceae and 1% Nocardiaceae in the sponge *Callyspongia* sp. collected from a depth of 16 meters off Panggang Island in the Thousand Islands, Indonesia (Retnowati et al. 2021). In addition, Nocardiaceae have been reported in various environments and are commonly isolated from freshwater, saltwater, dust, soil, and decaying organic matter (Brown-Elliott et al. 2006). A recent study demonstrates that NGS technology can effectively identify rare actinobacteria groups associated with *Spheciospongia* spp. that use traditional culturing methods. Additionally, utilizing NGS technology to describe bacterial diversity has significantly improved the understanding of the community structure within sponge-associated bacteria, especially actinobacteria.

In conclusion, the highest bacterial abundance was found in the internal tissue of the sponge (SEN), compared to the sponge surface (SEK) and the surrounding seawater (SW). The two main phyla detected were Proteobacteria and Bacteroidota, with the predominant classes being Gammaproteobacteria and Bacteroidia. The dominant families associated with sponges and seawater included Micrococcaceae, Corynebacteriaceae, and Pseudonocardiaceae. The NGS method was the first to

identify genera such as *Corynebacterium*, *Leucobacter*, *Egibacter*, *Lawsonella*, and *Nakamurella*. Many prokaryotes associated with the sponge remain unculturable and previously unknown. However, NGS techniques now enable the determination of bacterial diversity and the development of media for isolating specific bacteria from sponges. This approach also facilitates the exploration of these bacteria, particularly actinomycetes, as potential producers of bioactive compounds.

ACKNOWLEDGEMENTS

The authors thank the School of Life Sciences and Technology, Institut Teknologi Bandung, Indonesia for the NGS analysis data.

REFERENCES

Abbas S, Mahmoud H. 2022. Identification of sponge-associated bacteria from the Coast of Kuwait and their potential biotechnological applications. Front Microbiol 13: 896718. DOI: 10.3389/fmicb.2022.896718.

Ahmad T, Ishaq SE, Liang L, Xie R, Wang Y, Wang F. 2024. A diffusion-based integrative approach for culturing previously uncultured bacteria from marine sediments. Mar Life Sci Technol 2024: 1-12. DOI: 10.1007/s42995-024-00240-2.

Alam K, Abbasi MN, Hao J, Zhang Y, Li A. 2021. Strategies for natural products discovery from uncultured microorganisms. Molecules 26 (10): 2977. DOI: 10.3390/molecules26102977.

Bercovich A, Vazquez SC, Yankilevich P, Coria SH, Foti M, Hernández E, Vidal A, Ruberto L, Melo C, Marenssi S, Criscuolo M, Memoli M, Arguelles M, Mac Cormack WP. 2008. *Bizionia argentinensis* Sp. Nov., isolated from surface marine water in Antarctica. Intl J Syst Evol Microbiol 58 (Pt 10): 2363-2367. DOI: 10.1099/ijs.0.65599-0.

Ben Moussa H, Bertrand C, Rochelle-Newall E, Fiorini S, Pédron J, Barny MA. 2022. The diversity and abundance of soft rot Pectobacteriaceae along the durance river stream in the southeast of France revealed by multiple seasonal surveys. Phytopathology 112 (8): 1676-1685. DOI: 10.1094/PHYTO-12-21-0515-R.

Bibi F, Alvi SA, Al-Sofyani A, Naseer MI, Yasir M, Azhar EI. 2020. Pyrosequencing reveals sponge-specific bacterial communities in marine sponges of Red Sea, Saudi Arabia. Saudi J Biol Sci 27 (1): 67-73. DOI: 10.1016/j.sjbs.2019.05.002.

Bokulich NA, Kaehler BD, Rideout JR, Dillon M, Bolyen E, Knight R, Huttley GA, Gregory Caporaso J. 2018. Optimizing taxonomic classification of marker-gene amplicon sequences with QIIME 2's Q2-Feature-Classifier Plugin. Microbiome 6 (1): 1-17. DOI: 10.1186/s40168-018-0470-z.

Bowman JP. 2007. Bioactive compound synthetic capacity and ecological significance of marine bacterial genus *Pseudoalteromonas*. Mar Drugs 5 (4): 220-241. DOI: 10.3390/md504220.

Brown-Elliott BA, Brown JM, Conville PS, Wallace RJ Jr. 2006. Clinical and laboratory features of the *Nocardia* spp. Based on current molecular taxonomy. Clin Microbiol Rev 19 (2): 259-282. DOI: 10.1128/CMR.19.2.259-282.2006.

Das S, Biswas NK, Basu A. 2023. Mapinsights: Deep exploration of quality issues and error profiles in high-throughput sequence data. Nucleic Acids Res 51 (14): e75. DOI: 10.1093/nar/gkad539.

Dat TTH, Steinert G, Cuc NTK, Smidt H, Sipkema D. 2021. Bacteria cultivated from sponges and bacteria not yet cultivated from sponges-A Review. Front Microbiol 12: 737925. DOI: 10.3389/fmicb.2021.737925.

Delgadillo-Ordoñez N, Raimundo I, Barno AR, Osman EO, Villela H, Bennett-Smith M, Voolstra CR, Benzoni F, Peixoto RS. 2022. Red Sea Atlas of Coral-associated bacteria highlights common microbiome members and their distribution across environmental gradients-A systematic review. Microorganisms 10 (12): 2340. DOI: 10.3390/microorganisms10122340.

Djurhuus A, Port J, Closek CJ, Yamahara KM, Romero-Maraccini O, Walz KR, Goldsmith DB, Michisaki R, Breitbart M, Boehm AB, Chavez FP. 2017. Evaluation of filtration and DNA extraction methods for environmental DNA biodiversity assessments across multiple trophic levels. Front Mar Sci 4: 314. DOI: 10.3389/fmars.2017.00314.

Gaikwad S, Shouche YS, Gade WN. 2016. Microbial community structure of two freshwater sponges using Illumina MiSeq sequencing revealed high microbial diversity. AMB Express 6 (1): 1-9. DOI: 10.1186/s13568-016-0211-2.

Helber SB, Hoeijmakers DJJ, Muhando CA, Rohde S, Schupp PJ. 2018. Sponge chemical defenses are a possible mechanism for increasing sponge abundance on reefs in Zanzibar. PLoS ONE 13 (6): e0197617. DOI: 10.1371/journal.pone.0197617.

Holmström C, Kjelleberg S. 1999. Marine *Pseudoalteromonas* species are associated with higher organisms and produce biologically active extracellular agents. FEMS Microbiol Ecol 30 (4): 285-293. DOI: 10.1016/S0168-6496(99)00063-X.

Hong LL, Ding YF, Zhang W, Lin HW. 2022. Chemical and biological diversity of new natural products from marine sponges: A Review (2009-2018). Mar Life Sci Technol 4 (3): 356-372. DOI: 10.1007/s42995-022-00132-3.

Hugouvieux-Cotte-Pattat N, Flandrois JP, Briolay J, Reverchon S, Brochier-Armanet C. 2024. Description of a new genus of the Pectobacteriaceae family isolated from water in Coastal Brackish wetlands of the French Camargue Region, *Prodigiosinella* gen. nov., including the new species *Prodigiosinella aquatilis* sp. nov. Syst Appl Microbiol 47 (2-3): 126497. DOI: 10.1016/j.syapm.2024.126497.

Ito T, Sekizuka T, Kishi N, Yamashita A, Kuroda M. 2019. Conventional culture methods with commercially available media unveil the presence of novel culturable bacteria. Gut Microbes 10 (1): 77-91. DOI: 10.1080/19490976.2018.1491265.

Laport MS, Pinheiro U, Rachid CTCDC. 2019. Freshwater sponge *Tubella variabilis* presents richer microbiota than marine sponge species. Front Microbiol 10: 2799. DOI: 10.3389/fmicb.2019.02799.

Li H, Zhang XY, Liu C, Liu A, Qin QL, Su HN, Shi M, Zhou BC, Chen XL, Zhang YZ, Xie BB. 2015. *Bizionia arctica* Sp. Nov., isolated from Arctic fjord seawater, and emended description of the genus Bizionia. Intl J Syst Evol Microbiol 65 (9): 2925-2930. DOI: 10.1099/ijs.0.000357.

Li M, Wang K, Jia C, Liu T, Yang S, Ou H, Zhao J. 2021. Bacteroidetes bacteria, important players in the marine sponge larval development process. iScience 24 (6): 102662. DOI: 10.1016/j.isci.2021.102662.

Li P, Lu H, Zhang Y, Zhang X, Liu L, Wang M, Liu L. 2023. The natural products discovered in marine sponge-associated microorganisms: Structures, activities, and mining strategy. Front Mar Sci 10: 1191858. DOI: 10.3389/fmars.2023.1191858.

Mehbub MF, Yang Q, Cheng Y, Franco CM, Zhang W. 2024. Marine sponge-derived natural products: Trends and opportunities for the decade of 2011-2020. Front Mar Sci 11: 1462825. DOI: 10.3389/fmars.2024.1462825.

Nani SZM, Majid FAA, Jaafar AB, Mahdzir A, Musa MN. 2016. Potential Health benefits of deep sea water: A Review. HPC 2016: 1-18. DOI: 10.1155/2016/6520475.

Nguyen VH, Wemheuer B, Song W, Bennett H, Palladino G, Burgsdorf I, Sizikov S, Steindler L, Webster NS, Thomas T. 2023. Functional characterization and taxonomic classification of novel gammaproteobacterial diversity in sponges. Syst Appl Microbiol 46 (2): 126401. DOI: 10.1016/j.syapm.2023.126401.

Orata FD, Meier-Kolthoff JP, Sauvageau D, Stein LY. 2018. Phylogenomic analysis of the gammaproteobacterial methanotrophs (Order Methylococcales) calls for the reclassification of members at the genus and species levels. Front Microbiol 9: 3162. DOI: 10.3389/fmicb.2018.03162.

Palomo S, González I, de la Cruz M, Martín J, Tormo JR, Anderson M, Hill RT, Vicente F, Reyes F, Genilloud O. 2013. Sponge-derived *Kocuria* and *Micrococcus* spp. as sources of the new thiazolyl peptide antibiotic kocurin. Mar Drugs 11 (4): 1071-1086. DOI: 10.3390/md11041071.

Retnowati D, Solihin DD, Ghulamahdi M, Lestari. 2021. Next-generation sequencing-based Actinobacteria community associated with *Callyspongia* Sp. from Kepulauan Seribu Marine National Park, Jakarta, Indonesia. Biodiversitas 22 (9): 3702-3708. DOI: 10.13057/biodiv/d220913.

Rojahn S, Hambuch T, Adrian J, Gafni E, Gileta A, Hatchell H, Johnson B, Kallman B, Karfilis K, Kautzer C, Kennemer M, Kirk L, Kvitek D,

Lettes J, Macrae F, Mendez F, Paul J, Pellegrino M, Preciado R, Risinger J, Schultz M, Spurka L, Swamy S, Truty R, Usem N, Velenich A, Aradhya S. 2022. Scalable detection of technically challenging variants through modified next-generation sequencing. Mol Genet Genomic Med 10 (12): e2072. DOI: 10.1002/mgg3.2072.

Roswell M, Dushoff J, Winfree R. 2021. A conceptual guide to measuring species diversity. Oikos 130 (3): 321-338. DOI: 10.1111/oik.07202.

Rufino BN, Procópio L. 2021. Influence of Salt water flow on structures and diversity of biofilms grown on 316L stainless steel. Curr Microbiol 78 (9): 3394-3402. DOI: 10.1007/s00284-021-02596-5.

Rygaard AM, Thøgersen MS, Nielsen KF, Gram L, Bentzon-Tilia M. 2017. Effects of gelling agent and extracellular signaling molecules on the culturability of marine bacteria. Appl Environ Microbiol 83 (9): e00243-17. DOI: 10.1128/AEM.00243-17.

Satam H, Joshi K, Mangrolia U, Waghoo S, Zaidi G, Rawool S, Thakare RP, Banday S, Mishra AK, Das G, Malonia SK. 2023. Next-Generation sequencing technology: Current trends and advancements. Biology (Basel) 12 (7): 997-1022. DOI: 10.3390/biology12070997.

Savoca S, Lo Giudice A, Papale M, Mangano S, Caruso C, Spanò N, Michaud L, Rizzo C. 2019. Antarctic sponges from the Terra Nova Bay (Ross Sea) host a diversified bacterial community. Sci Rep 9 (1): 16135. DOI: 10.1038/s41598-019-52491-0.

Skovhus TL, Holmstrom C, Kjelleberg S, Dahllof I. 2007. Molecular investigation of the distribution, abundance, and diversity of the genus *Pseudoalteromonas* in marine samples. FEMS Microbiol Ecol 61 (2007): 348-361. DOI: 10.1111/j.1574-6941.2007.00339.x.

Sonnenberg CB, Haugen P. 2021. The *Pseudoalteromonas* multipartite genome: Distribution and expression of pangene categories, and a hypothesis for the origin and evolution of the chromid. G3 (Bethesda) 11 (9): jkab256. DOI: 10.1093/g3journal/jkab256.

Strong WL. 2016. Biased richness and evenness relationships within Shannon-Wiener Index values. Ecol Indic 67: 703-713. DOI: 10.1016/j.ecolind.2016.03.043.

Sugden S, Holert J, Cardenas E, Mohn WW, Stein LY. 2022. The microbiome of the freshwater sponge *Ephydatia muelleri* shares compositional and functional similarities with those of marine sponges. ISME J 16 (11): 2503-2512. DOI: 10.1038/s41396-022-01296-7.

Sulardiono B, A'in Ch, Muskananfola MR. 2018. Profiles of water quality at Menjangan Besar Island, Karimunjawa, Central Java Province, Indonesia. Biodiversitas 19 (6): 2308-2315. DOI: 10.13057/biodiv/d190639.

Tan B, Ng C, Nshimyimana JP, Loh LL, Gin KY, Thompson JR. 2015. Next-Generation Sequencing (NGS) for assessment of microbial water quality: Current progress, challenges, and future opportunities. Front Microbiol 6: 1027. DOI: 10.3389/fmicb.2015.01027.

Taylor MW, Radax R, Steger D, Wagner M. 2007. Sponge-associated microorganisms: Evolution, ecology, and biotechnological potential. Microbiol Mol Biol Rev 71 (2): 295-347. DOI: 10.1128/mmbr.00040-06.

Varijakzhan D, Loh JY, Yap WS, Yusoff K, Seboussi R, Lim SE, Lai KS, Chong CM. 2021. Bioactive compounds from marine sponges: Fundamentals and applications. Mar Drugs 19 (5): 246. DOI: 10.3390/md19050246.

Watanabe T, Kojima H, Fukui M. 2015. Draft genome sequence of a sulfur-oxidizing autotroph, *Sulfuricella* sp. strain T08, isolated from a freshwater lake. Genome Announc 3 (3): e00498-15. DOI: 10.1128/genomeA.00498-15.

Waterworth SC, Parker-Nance S, Kwan JC, Dorrington RA. 2021. Comparative genomics provides insight into the function of broad-host range sponge symbionts. mBio 12 (5): e0157721. DOI: 10.1128/mBio.01577-21.

Willis AD. 2019. Rarefaction, alpha diversity, and statistics. Front Microbiol 10: 1-5. DOI: 10.3389/fmicb.2019.02407.

ASIAN J TROP BIOTECHNOL
Volume 22, Number 1, June 2025
Pages: 16-22

ISSN: 0216-6887
E-ISSN: 2301-8658
DOI: 10.13057/biotek/c220103

Genomic, hormonal, and anthropometric factors as crucial contributors to male infertility in Abeokuta, Southwestern Nigeria

ADEBAYO A. AMBALLI[1,♥], WASIU E. OLOOTO[1], OLAYINKA T. KOSOKO[2], FOLARIN O. OWAGBORIAYE[3]

[1]Department of Chemical Pathology and Immunology, Faculty of Basic Medical Sciences, Olabisi Onabanjo University. Hospital Road, Ogun State, Nigeria. Tel.: +234-803-353-4252, ♥email: amballi.adebayo@oouagoiwoye.edu.ng
[2]Department of Health Services, Federal University of Agriculture Abeokuta, Nigeria. Abeokuta 110111, Ogun State, Nigeria
[3]Department of Plant Science and Applied Zoology, Faculty of Science, Olabisi Onabanjo University. Ogun State, Nigeria

Manuscript received: 12 February 2025. Revision accepted: 2 Mei 2025.

Abstract. *Amballi AA, Olooto WE, Kosoko OT, Owagboriaye FO. 2025. Genomic, hormonal, and anthropometric factors as crucial contributors to male infertility in Abeokuta, Southwestern Nigeria. Asian J Trop Biotechnol 22: 16-22.* The failure to get pregnant despite regular, unprotected sexual intercourse among couples has psychosocial and socioeconomic impacts. This study aims to investigate the contributions of anthropometric, genomic, and hormonal factors to male infertility. Hence, 48 infertile men and 12 men with proven fertility, aged from 26 to 55 years, were selected as cases and controls, respectively. Anthropometric measurements (height and weight) were done, Body Mass Index (BMI) was computed, and serum Follicle-Stimulating Hormones (FSH), Luteinizing Hormones (LH), and testosterone were measured. Semen was obtained for seminal fluid analysis and phenotyping assay. There is no significant change in the anthropometric indicators (height, weight, BMI); 4.2% of the infertile men were normospermic, 20.8% were azoospermic, and 75% were oligospermic. There was an increase in FSH, LH, and testosterone in all the infertile subgroups and a significant decrease ($p < 0.05$) in sperm count in infertile males. While 70% of sperm cells exhibited fast movement in the controls, sperm movement was 9.5, 5.5, and 15% normal, slow, and non-motile, respectively, among infertile men. The percentage of deletions in Azoospermia Factor a (AZFa) region using sY84 and sY86 was 66.7%, and none in the control group. It can be concluded that high plasma levels of gonadotrophins, low sperm count, and high levels of testosterone are pathognomonic of male infertility. While the deletion of AZFa region is conclusively indicative of infertility, its non-deletion does not conclusively indicate fertility; thus, factors other than hormonal abnormalities are associated with male infertility.

Keywords: Obesity**,** phenotyping, semen quality, testicle

INTRODUCTION

The inability to achieve pregnancy despite regular, adequate (3-4 times per week) unprotected sexual exposure over 2 years is a complex disorder with both genetic and environmental causes (Gunes et al. 2016). The acceptability of identifiable underlying causative factors and sharing of contributory factors between men and women has eroded the primitive African taboo and beliefs that infertility is mainly a female problem rather than male or both. These beliefs were extended to outcomes of fertility in which case the blames of having female children was placed on the woman as being a weaker partner with resultant matrimonial neglect and option of taking up new wives. While in some cases taking up another wife results in having a male child, in other cases it results in having more female children, pointing to the superior role of fathers in determining the sex of children rather than mothers.

Factors of etiological importance in male infertility include congenital abnormalities, prolonged exposure of testes to excessive heat, chronic alcoholism, drugs (cocaine, marijuana, cimetidine, spironolactone, nitrofurantoin, etc.), endocrine disorders, erectile or ejaculatory dysfunction, infection (urinary tract infection, sexually transmitted infection), lifestyle choices, such as diet and exercise, obesity, testicular failure, varicocele, poor semen quality, and idiopathic (ASRM 2015; Barak et al. 2016). Idiopathic causes represent unexplained causes of azoospermia or oligospermia and constitute majority of cases. More studies of the idiopathic group revealed that infertility can be secondary to genetic abnormalities involving the sex chromosomes such as chromosomal translocations, presence of an extra X chromosome as observed in Klinefelter syndrome (XXY), cystic fibrosis, Noonan syndrome, and partial deletions of portions of Y-chromosome primarily affecting the Azoospermia Factor (AZF) regions, resulting in abnormal spermatogenesis and male infertility (Sokol 2001; Chen 2007; Dhanoa et al. 2016; Kuroda et al. 2020). Interactions between genetic factors and environmental factors influence sensitivity to environmental stressors like exposure to Endocrine-Disrupting Chemicals (EDCs) and alter gene expression thereby impairing reproduction and fertility. The importance of the human Y-chromosome in male fertility was revealed by result from several studies indicating that one or more genes located on the long arm of the Y-chromosome are or are most probably involved in spermatogenesis. Deletions of small portions of Y-chromosome responsible for spermatogenesis are believed to be an important azoospermia factor (He et al. 2017).

Partial deletion within the male-specific region of the Y-chromosome, known as Y-chromosome microdeletions (YCMs), is present in as many as 5 and 10% of severe oligospermic and azoospermic men, respectively (Rabinowitz et al. 2021). These microdeletions are distinguished by the segment of the Y-chromosome that is absent. Four subsidiary non-overlapping sub-regions were identified as AZFa (located in the most proximal segment of Yq11, AZFb (located in the middle segment of Yq11), AZFc (located in the distal segment of Yq11), and AZFd (located between AZFb and AZFc). Patients with complete AZFa deletion present with Sertoli cell-only syndrome (Foresta et al. 2001; Ferlin et al. 2003), while those with AZFd microdeletions may have mild oligospermia or normal sperm count but abnormal sperm morphology (Ceylan et al. 2009).

The reported prevalence of YCMs within the world's populations of infertile men displays vast heterogeneity based on region and ethnicity (Rabinowitz et al. 2021). In Africa and Asia, YCMs are a common cause of male infertility, with prevalence of between 10 and 15%, but less than 5% in other populations. The most common deletions occurring in the AZFc region of the Y-chromosome (Trinh et al. 2023). A study reported that complete Y-chromosome microdeletions are rare in men with sperm count > 1 million sperm/mL (Khon et al. 2019). Routine screening for Y-chromosome microdeletions should be done only if sperm concentration is ≤ 1 million sperm/mL (Khon et al. 2019). Both Y-chromosome microdeletion and chromosomal abnormalities increase in prevalence as sperm concentrations decrease and azoospermic men have been reported to have the greatest frequency of genetic abnormalities (Liu et al. 2020).

Nigeria has many regions and ethnic groups. Thus the frequency of AZF microdeletions is expected to vary among Nigerians in different regions. Therefore, it is important to understand the frequency and pattern of Y-chromosome microdeletion, in addition to the effect of body mass index and hormonal disruption, among infertile men in southwestern Nigeria. This is important because idiopathic causes are also important to be investigated in a country with diverse ethnic groups.

MATERIALS AND METHODS

Study area

The study was carried out in Abeokuta, Ogun state, Nigeria, among male subjects attending the infertility clinic of the State Hospital, Sokenu, Abeokuta, Ogun state, Nigeria.

Procedure

Study design

The study is a case-control and cross-sectional study that included diagnosed male infertility, while control subjects were male with proven fertility.

Study population

In this study period, 48 infertile males and 12 men who have proven evidence of fatherhood and whose wives have given birth to 2 or more children were selected as cases and controls, respectively. The test subjects were randomly recruited among people that attended the Infertility Clinic of Ogun State Hospital, Ijaye, Abeokuta, for the purpose of impaired fertility. In contrast, the control subjects were recruited, in a similar manner, among male staff of the hospital. Structured questionnaires were administered to both test and control subjects to obtain their biodata such as age, social status, and dietary habits.

Inclusion and exclusion criteria

Subjects included in the study were male subjects diagnosed with infertility (primary or secondary), age range 26-55 years. Excluded from the study were male subjects less than 26 years and above 55 years in age; those having physical abnormalities (testicular atrophy, hypoplastic testes, varicocoele); those diagnosed with other chronic conditions such as coronary heart disease, diabetes mellitus, hypertension, and stroke; heavy cigarette smokers; chronic alcoholics; and drug addicts.

Medical history and clinical examination

Medical history was taken for demographic and other characteristic purposes, and clinical examination was carried out on all the tests and controls to detect physical abnormalities in their genitalia and scrotum.

Anthropometric measurement

Anthropometric measurements (height and weight) were done using standard methods (Olooto et al. 2016). Body Mass Index (BMI) was computed using the formula BMI = weight in kilograms/height in metres squared (kg/m^2). Tests and controls were categorized based on BMI as underweight (<18.5); healthy weight (18.5-24.9); overweight (25-29.9); class I obesity (30.0-34.9); class II obesity (35-39.9); and class III obesity (≥40.0) respectively (WHO 2004).

Sample collection and storage

Seminal fluid

The participants were advised to abstain from sexual intercourse (oral, anal, vaginal) for a period of 2-7 days prior to sample collection in order to improve sperm concentration. Semen was collected from the test and control subjects by masturbation, in a private room close to the laboratory in order to shorten the time intervals between collection and analysis, hence, to limit the exposure of the semen to temperature fluctuations. The collection was done in a clean, dry, wide-mouthed glass bottle that is non-toxic to spermatozoa. The collected semen was analyzed within one hour of collection. Neubauer hemocytometer chamber was used to estimate the sperm count. Sperm analysis (total sperm cell count, cellular morphology, viscosity, white blood cell count and percentage motility) was carried out according to the World Health Organization guidelines (WHO 2010). The seminal fluid was categorized as aspermia (no ejaculate), azoospermia (no sperm cell), oligospermia ($<20 \times 10^6$ sperm/mL), and severe oligospermia ($<5 \times 10^6$ sperm/mL) (WHO 2010).

Blood sample

Next, 10 mL of venous blood sample was aseptically collected from each participant's antecubital vein (tests and controls), transferred into a clean, plain, labelled bottle; allowed to clot; and then centrifuged at 6000 rpm for 5 minutes at room temperature to obtain the serum. The clear serum was separated and kept at -20°C till assayed.

Hormonal assays

The hormones (LH, FSH and testosterone) were estimated by radioimmunoassay (RIA) method using Enzyme-Linked Immunosorbent Assay (ELISA) kits supplied by Immunometrics (UK) Limited. FSH, LH and testosterone assessments were done using the methods of Fahie-Wilson (Fahie-Wilson et al. 2000) and genomic analysis was done using the method described by Wang et al. (2012).

Phenotyping assay

Aberrant sperm cells were examined after smearing of semen and staining with New Zealand methylene blue to detect abnormalities of germ cells using the Diff Quick Method laid down (Lee et al. 2002).

PCR amplification of the AZFa gene (SY84 and SY86)

DNA was extracted by a salting-out method from leukocytes of peripheral blood samples and amplified using PCR (Miller et al. 1988). The PCR reaction was performed with the Solis Biodyne 5X HOT FIREPol Blend Master mix. Thermal cycling was conducted in a Peltier thermal cycler (PTC100) (MJ Research Series) at 95°C for 15 minutes to carry out initial denaturation. This is followed by 35 amplification cycles at 95°C for 30 seconds; at 61°C for 60 seconds for annealing, and at 72°C for 90 seconds to carry out extension; and at a temperature of 72°C for a period of 600 seconds to carry out final extension. The amplification product was separated on a 1.5% agarose gel, electrophoresis was carried out at 80V for 1 h 30 mins, and DNA bands were visualised by ethidium bromide staining using 100bp DNA ladder (Solis Biodyne) as DNA molecular weight marker. Two Sequence-Tagged Sites (STS) markers on the long arm of Y-chromosome were used for the detection of interstitial microdeletions for AZFa (Krausz et al. 2014). The markers used are SY84 and SY86, with the sequences and sizes of their base pair shown in Table 1.

Data analysis

Data were analysed using SPSS version 21.0. The variables were all expressed as the mean and standard error of mean (Mean ± SEM). A bar chart was used to describe variables. An independent student t-test was performed to compare means of variables between the test and control groups. Differences amongst variables were considered significant at $p < 0.05$.

Ethical consideration

Ethical approval was achieved from the ethical committee of State Hospital, Sokenu, Abeokuta, Ogun state, Nigeria, based on the recommendations Declaration of Helsinki. The approval number is SHA/RES/VOL 2/187. After explaining the procedures involved in the research to each participant, informed consent was also obtained from them before the commencement of the study.

RESULTS AND DISCUSSION

The results of this study are presented in the following tables and figures. Table 2 shows the anthropometric measurements of both test and control subjects. There was no statistically significant difference ($p > 0.05$) between the two groups. Table 3 shows the serum hormone levels in both test and control subjects. The values of LH, FSH and testosterone were observed to be non-significantly ($p > 0.05$) higher among the test subjects than among the control subjects.

Table 2. Anthropometric measurements of both test (infertile men) and control subjects

Parameters	Test	Control	t-value	p-value
Age (Yrs)	42.89 ± 6.03	42.0 ±4.71	0.476	0.64
Weight (Kg)	64.79 ±4.76	64.33 ±3.34	0.310	0.76
Height (m)	1.60 ±0.04	1.63 ±0.04	0.233	0.82
BMI (kg/m^2)	24.35 ±1.81	24.10 ±1.62	0.439	0.66

Note: Values are mean ± SEM, level of statistical significance was considered at $p < 0.05$

Table 3. Serum hormone levels in both test (infertile men) and control subjects

Parameter	Test N=48	Control N=12	t-value	p-value
LH (miu/mL)	8.27±4.86	6.6±3.08	2.74	0.48
FSH (miu/mL)	3.60±1.73	3.25±0.78	3.00	0.21
Testosterone (ng/mL)	4.30±0.81	3.65±0.07	3.75	0.39

Note: Values are mean ± SEM, level of statistical significance was considered at $p < 0.05$

Table 1. STS markers of AZF regions with sequences and their product size

STS marker	Locus (region)	Sequence 5'-3'	Size of PCR product Base Pair (BP)
SY84	AZFa	F- AGA AGG GTC TGA AAG CAG GT R- GCC TAC TAC CTG GAG GCT TC	326
SY86	AZFa	F- GTG ACA CAC AGA CTA TGC TTC R- ACA CAC AGA GGG ACA ACC CT	320

Note: STS: Sequence Tagged Sites; F: Forward primer; R: Reverse primer

Figure 1 shows sperm count among the test group and the control group. It shows a higher sperm count among the control group (79.0 × 10^6 cells/mL) than values obtained in the test group (15.05 × 10^6 cells/mL)

Figure 2 shows sperm cell viability among the control and test subject groups. It shows that 85 and 15% of the sperm cells produced by the control group are viable sperm cells and dead cells, respectively, as compared to the 40% and 60% living and dead cells, respectively, observed in infertile test group.

Figure 3 shows morphological abnormalities among the tests group and the control group. Abnormal sperm cells were observed in 45% of the tests (infertile men) compared to 20% in the control group.

Table 4 shows the motility profile of sperm cells among the test and control subjects. Hence, 70% of the control group exhibited significant fast motility among while 11% of the tests exhibited significant fast motility. Table 4 in the Sperm Cell Motility Profile shows the same p-value (at 0.001), but the t-value varies, as in the results in the test and control columns.

Table 5 shows the proportion of the AZFa gene that had a microdeletion among the control and test groups. No microdeletion of the AZFa gene was observed in the control group (0.0%), while 33.3% of the test group had it.

Figure 4 shows the electrophoresis results of the blood cells of subjects for the analysis of microdeletions in the AZFa region using sY84 Amplifying at 326bp. Lane M consists of a 100bp DNA marker base-pair ladder as a negative control, lanes A and B represent the control group, while lanes C, D, and E represent the test group.

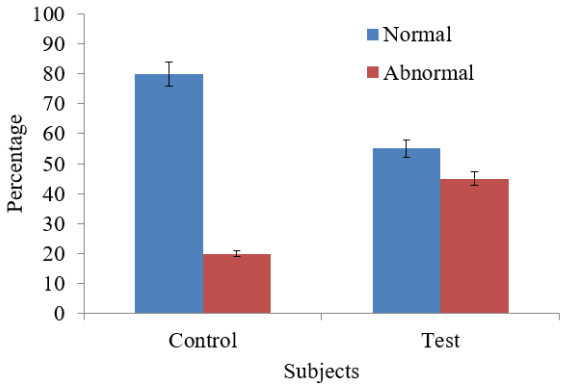

Figure 3. Bar chart showing the difference in sperm cell morphology among the test and control subject groups. Values are expressed as mean ± SEM

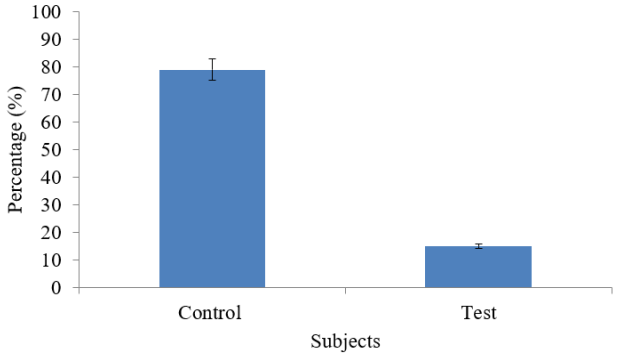

Figure 1. Bar chart showing total sperm count in the test and control subject groups. Values are expressed as mean ± SEM

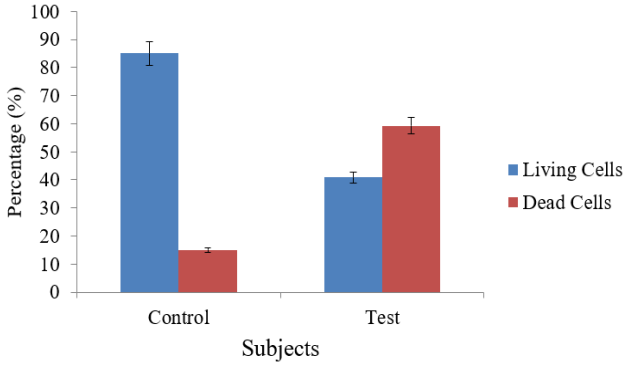

Figure 2. Bar chart showing comparative sperm cell viability among the control and the test subjects group. Values are expressed as mean ± SEM

Table 4. Motility profile of sperm cells among the control and subject groups

Motility	Test	Control	t- value	p-value
Rapidly progressively motile (%)	11.00±10.00	70.00±10.00	2.34	0.0007
Slowly progressively motile (%)	13.3±9.83	9.5±3.53	1.74	0.0010
Non-progressive motile (%)	16.7±16.02	5.50±3.54	1.26	0.0013
Non motile (%)	59.0±1.45	15.0±1.62	2.96	0.0006

Note: Values are mean ± SEM, level of statistical significance was considered at $p < 0.05$

Table 5. Proportion of micro-deletions of AZFa gene among the control and the subject groups

AZFa gene	Control				Test			
	Present		Absent		Present		Absent	
	Number (n)	Percentage (%)	Number (n)	Percentage (%)	Number (n)	Percentage (%)	Number (n)	Percentage (%)
sY84	12	100.0	0	0.0	16	33.3	32	66.7
sY86	12	100.0	0	0.0	16	33.3	32	66.7

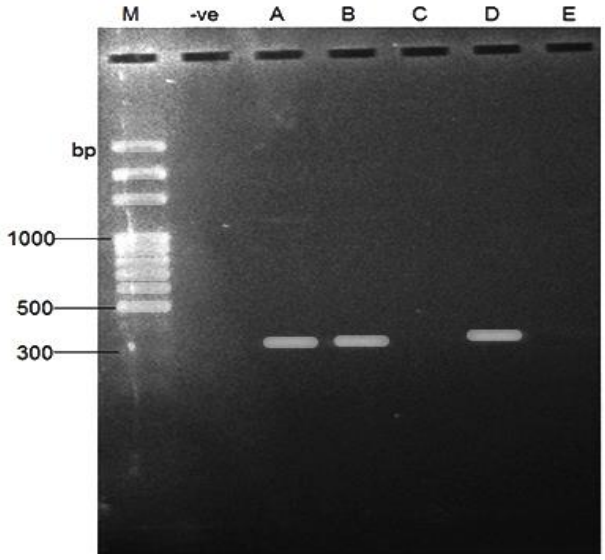

Figure 4. Electrophoresis pattern of blood cells of subjects for microdeletions in the AZFa region using sY84 amplifying at 326bp

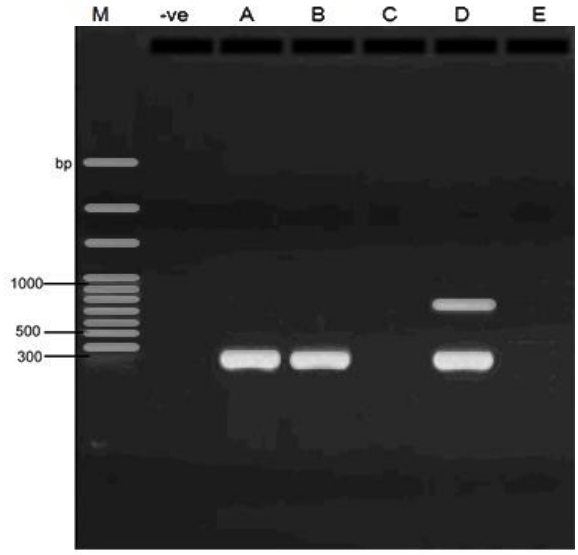

Figure 5. Electrophoresis pattern of blood cells of subjects for microdeletions on AZFa region using sY86 amplifying at 320bp

Figure 5 shows the electrophoresis results of blood cells of subjects for the analysis of microdeletions in the AZFa region using sY86 Amplifying at 320bp. Lane M consists of a 100bp DNA marker base-pair ladder as a negative control; lanes A and B represent the control group, while lanes C, D, and E represent the test group.

Discussion

Results obtained in this study revealed no significant difference in the anthropometric indices between the test and controls (Table 2), corroborating earlier reports (Oztekin et al. 2020). There are controversial reports on the impact of obesity on male infertility. Contrasting reports are being made; while some report impaired semen parameters and impaired fertility, others do not show an impact (Ameratunga et al. 2023). A study reported that obesity impacts male fertility by causing multifaceted reproductive disruptions (Chaudhuri 2022), while another study reported that body mass index has no effect on semen parameters but correlates negatively with hormones (Oztekin et al. 2020). These variations in hormones were due to fat accumulation in adipose tissues. The obtained results in this study indicate that infertility is not related to anthropometric variations in the test group but rather due to hormone and semen qualities.

The importance of hormonal evaluation in male infertility cannot be overemphasized. Some researchers had reported this in a study where male sex hormones, especially testosterone, were found to be the key players in male-related infertility (Nunes et al. 2023). Determining the levels of testosterones and gonadotropins (FSH, LH) in infertile men presenting with oligospermia and azoospermia has been emphasized (Concepción-Zavaleta et al. 2022), to provide evidence-based information on the functionality status of the hypothalamic-pituitary-testicular axis. This leads to possible need to evaluate the adrenal, thyroid, and lactotrophs in patients with central hypogonadism. Another study on the importance of hormonal evaluation in infertile men with non-obstructive azoospermia recommended that estradiol should be measured when there is an alteration in testosterone concentration (Salama and Blgozah 2020). Elevated levels of serum prolactin have a detrimental effect on male reproduction through inhibition of the pulsatile release of gonadotropins from the anterior pituitary gland (Dabbous and Atkin 2018). From this study, a non-significant ($p > 0.05$) increase in the serum levels of LH, FSH and testosterone was observed in the test group when compared to the control group (Table 3). A similar finding was reported in a previous study (Deventhiran et al. 2017). The observed increase in LH, FSH and testosterone levels indicates physiologic or compensatory responses to azoospermia and oligospermia and reflects problems at the gonadal level.

The total sperm count recorded among the control and the test groups revealed a higher count among the control group (79.0×10^6 cells/mL) than values obtained in the test group (15.05×10^6 cells/mL) (Figure 1). Also, 4.2% (2 out of 48) of the studied infertile males were observed to be normospermic, 20.8% (10 out of 48) were azoospermic, while 75% (36 out of 48) were oligospermic. This finding is supported by a previous study where sperm count was found to decline significantly in infertile men and adversely affect fertility (Levine et al. 2023).

Sperm vitality (the percentage of viable sperm cells) has also been described as an important factor in male infertility. The result obtained from this study revealed that 85% of the sperm cells produced by the control group are living and viable as compared to the 40% of living sperm cells observed in the infertile test group (Figure 2). Also, 60% of the sperm cells produced by the test group were observed to be dead, as compared to 15% of dead sperm cells observed among the control group. This corroborates a previous study, which reported a high rate of abnormal

semen quality in male partners of infertile couples (Bani et al. 2023).

A study (Agarwal et al. 2022) has emphasized the importance of sperm morphology in semen analysis for evaluating male fertility. For sperm morphology, results from this study show abnormal sperm cells in 45% of the tests (infertile men) compared to 20% observed among the control group (Figure 3). The observed morphologic abnormalities will assist in deciding the assisted reproductive treatment modalities to be adopted for the affected couples in order to achieve pregnancy in their female partner.

Semen analysis for motility assessment classifies spermatozoa as “rapidly progressive”, “slowly progressive”, “non-progressive”, and “immotile” (Sikka and Ayaz 2018). While the most common cause of male infertility is low sperm count, some men are infertile because of poor sperm motility. In this study, it was observed that 11% of infertile men exhibited rapidly progressive spermatozoa motility, 13.3% exhibited slowly progressive spermatozoa motility, 16.7% exhibited non-progressive spermatozoa motility, and 59% exhibited non-motility among the test group. In comparison, 70% exhibited rapidly progressive motility, 9.5% exhibited slowly progressive motility, 5.5% exhibited non-progressive motility, and 15% exhibited non-motility among the controls (Table 4). The observed differences in motility between the two groups were significant ($p < 0.05$) and thus constituted a major factor responsible for the observed infertility in this group of people. The significance of the mobility of sperm in semen analysis has been reported in a previous study (Dcunha et al. 2020).

Accumulating molecular studies have shown that the deletion of AZFa, AZFb, and AZFc is the most common genetic microdeletion in Y-chromosome of infertile males throughout the world (Liu et al. 2019). In this study, the percentage of Y-chromosome deletions in AZFa region using sY84 and sY86 was observed to be 33.3% (Table 5). This result corroborates that of Ilango and Poongothai (2017), who reported Y-chromosome deletion at AZFa portion in 53% of the studied infertile male subjects. This finding indicates that problems associated with male infertility are not limited to structural and hormonal abnormalities but are also due to genetic factors. Small Y-chromosome microdeletions have been reported among 2% of men with normal fertility and 7% of infertile men (16% in azoospermia or severe oligozoospermia) (Liu et al. 2019). This suggests that the presence of Y-chromosome microdeletion is not an absolute indicator or marker of infertility.

In conclusion, based on the findings from this study, it could be concluded that male infertility is not limited to hormonal and sperm quality abnormalities, but Y-chromosome abnormalities. Still, Y-chromosome deletion is a factor to be considered, especially in idiopathic male infertility. Screening for Y-chromosome microdeletions in infertile men as a routine diagnostic tool will be of immense assistance in the management options available for azoospermic and oligozoospermic patients.

ACKNOWLEDGEMENTS

This study was prompted by our quest to contribute to finding solutions to the increasing prevalence and incidence of male infertility. We want to appreciate the patients of State Hospital, Sofekun, Abeokuta, Ogun State, who volunteered to take part in this study and the hospital's staff for their cooperation.

REFERENCES

Agarwal A, Sharma R, Gupta S, Finelli R, Parekh N, Selvam MK, Henkel R, Durairajanayagam D, Pompeu C, Madani S, Belo A. 2021. Sperm morphology assessment in the era of intracytoplasmic sperm injection: Reliable results require focus on standardization, quality control, and training. World J Mens Health 40 (3): 347-360. DOI: 10.5534/wjmh.210054.

Ameratunga D, Gebeh A, Amoako A. 2023. Obesity and male infertility. Best Pract Res Clin Obstet Gynaecol 90: 102393. DOI: 10.1016/J.bpobgyn.2023.102393.

ASRM. 2015. Practice Committee of the American Society for Reproductive Medicine. Diagnostic evaluation of the infertile male: A committee opinion. Fertil Steril 103 (3): e18-25. DOI: 10.1016/j.fertnstert.2014.12.103.

Bani SB, Anachem R, Banyeh M, Dapare PPM, Adams Y, Nkansah C, Mensah K, Appiah SK, Bani F, Osumanu H, Abbam G, Daud S. 2023. Study on semen quality among men seeking infertility treatment in Tamale, Ghana. Asian J Res Rep Urol 6 (1): 27-36.

Barak S, Baker HWG. 2016. Clinical management of male infertility. In: Jameson JL, De Groot LJ (eds.). Endocrinology: adult and pediatric E-Book. Elsevier Health Sciences. DOI: 10.1016/B978-0-323-18907-1.00141-4.

Ceylan GG, Ceylan C, Elyas H. 2009. Genetic anomalies in patients with severe oligozoospermia and azoospermia in eastern Turkey: A prospective study. Genet Mol Res 8 (3): 915-922. DOI: 10.4238/vol8-3gmr616.

Chaudhuri GR, Das A, Kesh SB, Bhattacharya K, Dutta S, Sengupta P, Syamal AK. 2022. Obesity and male infertility: Multifaceted reproductive disruption. Middle East Fertil Soc J 27: 8. DOI: 10.1186/S43043-022-00099-2.

Chen CP. 2007. Chromosomal abnormalities associated with omphalocele. Taiwan J Obstet Gynecol 46 (1): 1-8. DOI: 10.1016/S1028-4559(08)60099-6.

Concepción-Zavaleta M, Paz Ibarra JL, Ramos-Yataco A, Coronado-Arroyo J, Concepción-Urteaga L, Roseboom PJ, Williams CA. 2022. Assessment of hormonal status in male infertility. An Update. Diabetes Metab Syndr 16 (3): 102447. DOI: 10.1016/J.dsx.2022.102447.

Dabbous Z, Atkin SL. 2018. Hyperprolactinaemia in male infertility: Clinical case scenarios. Arab J Urol 16 (1): 44-52. DOI: 10.1016/j.aju.2017.10.002.

Dcunha R, Hussein RS, Ananda H, Kumari S, Adiga SK, Kannan N, Zhao Y, Kalthur G. 2020. Current insights and latest updates in sperm motility and associated applications in assisted reproduction. Reprod Sci 29 (1): 7-25. DOI: 10.1007/s43032-020-00408-y.

Deventhiran R, Ramanathan K, Nandakumar N. 2017. Prevalance of male infertility in India: Studies on the effects of gonadotropin releasing hormones. Asian J Pharm Clin Res 10 (8): 208-210. DOI: 10.22159/ajpcr.2017.v10i8.18254.

Dhanoa JK, Mukhopadhyay CS, Arora JS. 2016. Y-chromosomal genes affecting male fertility: A review. Vet World 9 (7): 783-791. DOI: 10.14202/vetworld.2016.783-791.

Fahie-Wilson M. 2000. Detection of macroprolactin causing hyperprolactinemia in commercial assays for prolactin. Clin Chem 46 (12): 2022-2023. DOI: 10.1093/clinchem/46.12.2022.

Ferlin A, Moro E, Rossi A, Dallapiccola B, Foresta C. 2003. The human Y chromosome’s Azoospermia Factor b (AZFb) region: Sequence, structure, and deletion analysis in infertile men. J Med Genet 40 (1): 18-24. DOI: 10.1136/jmg.40.1.18.

Foresta C, Moro E, Ferlin A. 2001. Y chromosome microdeletions and alterations of spermatogenesis. Endocr Rev 22 (2): 226-239. DOI: 10.1210/edrv.22.2.0425.

Gunes S, Arslan MA, Hekim GNT, Asci R. 2016. The role of epigenetics in idiopathic male infertility. J Assist Reprod Genet 33 (5): 553-569. DOI: 10.1007/s10815-016-0682-8.

He T, Zhang X, Deng H, Zhou W, Zhao X, Zhao H, Lu J, Zheng Y, Zhang C, Zhang L, Yin A. 2017. A novel Y chromosome microdeletion potentially associated with defective spermatogenesis identified by custom array comparative genome hybridization. Reprod Biomed Online 34 (1): 75-81. DOI: 10.1016/j.rbmo.2016.09.010.

Ilango L, Poongothai J. 2017. Screening of Y-chromosomal microdeletions using 8 STS primers in idiopathic infertile men from Coimbatore District, Tamilnadu. Intl J Innovative Sci Res Technol 2 (10): 614-620.

Khon TP, Khon JR, Owen RC, Coward RM. 2019. The prevalence of Y-chromosome microdeletions in oligozoospermic men: A systematic review and meta-analysis of European and North American Studies. Eur Urol 76 (5): 626-636. DOI: 10.1016/J.eururo.2019.07.033.

Krausz C, Hoefsloot L, Simoni M, Tüttelmann F. 2013. EAA/EMQN best practice guidelines for molecular diagnosis of Y-chromosomal microdeletions: State-of-the-art. Andrology 2 (1): 5-19. DOI: 10.1111/j.2047-2927.2013.00173.x.

Kuroda S, Usui K, Sanjo H, Takeshima T, Kawahara T, Uemura H, Yumura Y. 2020. Genetic disorders and male infertility. Reprod Med Biol 19 (4): 314-322. DOI: 10.1002/rmb2.12336.

Lee RK, Hou JW, Ho HY, Hwu YM, Lin MH, Tsai YC, Su JT. 2002. Sperm morphology analysis using strict criteria as a prognostic factor in intrauterine insemination. Intl J Androl 25 (5): 277-280. DOI: 10.1046/j.1365-2605.2002.00355.x.

Levine H, Jørgensen N, Martino-Andrade A, Mendiola J, Weksler-Derri D, Mindlis I, Pinotti R, Swan SH. 2023. Temporal trends in sperm count: A systematic review and meta-regression analysis. Hum Reprod Update 23 (6): 646-659. DOI: 10.1093/humupd/dmx022.

Liu JL, Peña V, Fletcher SA, Kohn TP. 2020. Genetic testing in testing in male infertility – reassessing screening thresholds. Curr Opin Urol 30 (3): 317-323. DIO: 10.1097/MOU.0000000000000764.

Liu T, Song YX, Jiang YM. 2019. Early detection of Y chromosome microdeletions in infertile men is helpful to guide clinical reproductive treatments in southwest of China. Medicine (Baltimore) 98 (5): e14350. DOI: 10.1097/MD.0000000000014350.

Miller SA, Dykes DD, Polesky HF. 1988. A simple salting out procedure for extracting DNA from human nucleated cells. Nucleic Acids Res 16 (3): 1215. DOI: 10.1093/nar/16.3.1215.

Nunes DC, Ribeiro JC, Alves MG, Oliveria PF, Bernardino RL. 2023. Male sex hormones, metabolic syndrome, and aquaporins: A triad of players in male (in) fertility. Intl J Mol Sci 24 (3): 1960. DOI: 10.3390/ijms24031960.

Olooto WE, Olawale OO, Amballi AA, Ezima Nkechi E, Ogundahunsi AO. 2016. Plasma lipid profile and hepatic transaminase activities as indicator of cardiovascular disorder and hepatocellular damage in type 2 diabetes mellitus patients. Afr J Sci Nat 3: 10-16.

Oztekin U, Caniklioglu M, Sari S, Gurel A, Selmi V, Isikay L. 2020. The impact of BMI on reproductive hormones, testosterone/estradiol ratio and semen parameters. Cent Eur J Urol 73 (2): 226-230. DOI: 10.5173/ceju.2020.0020.

Rabinowitz MJ, Huffman PJ, Haney NM, Kohn TP. 2021. Y-chromosome microdeletions: A review of prevalence, screening, and clinical considerations. Appl Clin Genet 14: 51-59. DOI: 10.2147/TACG.S267421.

Salama N, Blgozah S. 2020. Serum estradiol levels in infertile men with non-obstructive azoospermia. Ther Adv Reprod Health 14:2633494120928342. DOI: 10.1177/26334941.20928342.

Sikka CS, Ayaz A. 2018. Standardized semen analysis and quality control management for multicenter male reproductive toxicology clinical trials. Bioenvironmental Issues Affecting Men's Reproductive and Sexual Health. Academy Press. DOI: 10.1016/B978-0-12-801299-4.00023-2.

Sokol RZ. 2001. Infertility in men with cystic fibrosis. Curr Opin Pulm Med 7 (6): 421-426. DOI: 10.1097/00063198-200111000-00011.

Trinh ST, Nguyen NN, Le HTT, Pham HTM, Trieu ST, Tran NTM, Ho S, Tran V, Trinh V, Nguyen HT, Pham MN, Dang TD, Dinh VH, Doan HT. 2023. Screening Y Chromosome Microdeletion in 1121 Men with Low Sperm Concentration and the Outcomes of Microdissection Testicular Sperm Extraction (mTESE) for Sperm Retrieval from Azoospermic Patients. Appl Clin Genet 16: 155-164. DOI: 10.2147/TACG.S420030.

Wang J, Fan HC, Behr B, Quake SR. 2012. Genome-wide single-cell analysis of recombination activity and de novo mutation rates in human sperm. Cell 150 (2): 402-412. DOI: 10.1016/j.cell.2012.06.030.

World Health Organization. 2004. WHO Classification of obesity by BMI.

World Health Organization. 2010. WHO laboratory manual for the examination and processing of human semen, 5th edition. Cambridge University Press, Cambridge.

ASIAN J TROP BIOTECHNOL
Volume 22, Number 1, June 2025
Pages: 23-29

ISSN: 0216-6887
E-ISSN: 2301-8658
DOI: 10.13057/biotek/c220104

Diversity, abundance, and enzyme activity of Actinomycetes recovered from tropical freshwater sediment for potential biotechnological applications

CHINYERE AUGUSTA AJUZIEOGU♥, GERALD ONYEDIKACHI ONU, ESTHER ONYINYECHI ONYEKACHI
Department of Microbiology, Faculty of Science, Federal University Otuoke. 400 University Boulevard, Yenegoa, Bayelsa State, Nigeria.
Tel.: +234-803-873-4603, ♥email: ajuzieoguca@fuotuoke.edu.ng

Manuscript received: 8 January 2025. Revision accepted: 11 May 2025.

Abstract. *Ajuzieogu CA, Onu GO, Onyekachi EO. 2025. Diversity, abundance, and enzyme activity of Actinomycetes recovered from tropical freshwater sediment for potential biotechnological applications. Asian J Trop Biotechnol 22: 23-29.* Actinomycetes are a set of Gram-positive bacteria known for their ability to produce a wide variety of secondary metabolites, including antibiotics and enzymes. This study assessed the diversity of Actinomycetes in tropical freshwater sediment and their amylase production potential. Sediment samples were obtained from four points (shore, middle, downstream, and upstream) within a tropical freshwater system. Physicochemical analysis, bacterial isolation, and enumeration were conducted following standard methods. Tentative identification of isolates was done using culture-dependent methods. Results showed that the sediment samples belonged to the loam soil textural class; upstream sediment recorded the highest pH and total organic carbon content (6.3 and 0.98%, respectively), and middle sediment recorded the highest nitrate content (9.632 mg/kg). In comparison, sediment from the shore recorded the lowest pH (5.70) and highest phosphate level (8.716 mg/kg). The highest total culturable heterotrophic counts were observed in sediment from the middle point. A total of 9 Actinomycetes species were recovered, out of which six (6) were positive for amylase activity. The isolates were tentatively identified as *Micrococcus* spp., *Streptomyces* sp., *Streptomyces coelicolor,* and *Actinomyces viscosus.* This study revealed that tropical freshwater sediments harbor a diverse and abundant bacterial community, particularly Actinomycetes, with possible potential for biotechnological exploration.

Keywords: Actinomycetes, amylase, API CORYNE, freshwater sediment, *Streptomyces coelicolor*

INTRODUCTION

Actinomycetes are Gram-positive bacterial species belonging to the Phylum Actinobacteria. Their DNA has a high Guanine-Cytosine (GC) content, up to more than 70% in *Streptomyces* and *Frankia* and as high as 51% in certain Corynebacteria. Recently, some freshwater-dwelling species with considerably low GC content have been reported (De Simeis and Serra 2021). The majority form branching mycelia and produce spores, which help them survive under diverse environmental conditions (Kontro et al. 2022).

Their ability to produce a myriad of biologically active compounds has made them impactful in medicine and biotechnology. The biotechnological significance of Actinomycetes was first discovered in the 1940s with Selman Waksman's uncovering of streptomycin. This was the first antibiotic effective against tuberculosis (Ahmad et al. 2019). This breakthrough led to more exploration of Actinomycetes for other biologically active compounds. Currently, over two-thirds of natural antibiotics are recovered from Actinomycetes, particularly from the genus *Streptomyces* (Law et al. 2019).

The use of enzymes, particularly of Actinomycetes origin, in food production and other industrial processes is fast advancing to fulfill the demands of the textile, food processing, and pharmaceutical industries. Amylase, which is one of the enzymes produced by Actinomycetes, is one of the frequently exploited enzymes in several starch industries and has several industrial applications in the manufacturing of syrup, re-sizing clothing fabrics, detergent formulations to enhance cleaning performance (i.e., the alkaliphilic Actinomycetes strains), and others. Amylase represents about 25% of the global enzyme market demand (Praveen Kumar et al. 2015; Miao et al. 2018; Shigeri et al. 2019).

Increasing concern about contamination of aquatic and soil ecosystems has led to several studies on the use of Actinobacteria for bioremediation purposes (Alvarez et al. 2017). Although there are extant techniques to remediate contaminated ecosystems, they are not completely successful, especially with respect to inorganic compounds (John et al. 2022). Oftentimes, these compounds are only partially degraded, generating metabolites (intermediates) that could be more harmful than the parent compound. Owing to the presence of Actinomycetes in soil and water and their functional capacity to maintain ecological balance (i.e., breaking down inorganic and organic compounds in their habitat), they are an excellent option for bioremediation. Jagannathan et al. (2021) reported that several *Streptomyces* strains, including *Streptomyces espinosus*, produce tyrosinase enzymes, which are important for eliminating phenols (a common ingredient in pesticides and petroleum products) that contaminate water supplies.

Compared to widely used tyrosinase, which was previously isolated from mushrooms, *Streptomyces*-derived tyrosinase was more effective (Roy et al. 2014).

According to past literature, the majority of Actinomycetes are recovered from soil, aquatic, and extreme ecosystems such as deep oceans and deserts (Ezeobiora et al. 2022), resulting in several bioactive compounds such as anticancer agents, antifungals, antibiotics, enzymes, and other therapeutically valuable compounds (Sarkar and Suthindhiran 2022). However, as interest in microbial diversity has expanded, researchers have increasingly switched focus to less explored environments, including aquatic ecosystems such as freshwater sediments (Selim et al. 2021).

Zothanpuia et al. (2018) highlighted the significance of freshwater sediments as untapped reservoirs of diverse microbial communities, including Actinomycetes. They identified a plethora of Actinomycetes species in freshwater sediments collected from various water bodies in India. Interestingly, many of the recovered strains expressed unique metabolic capabilities and potential for producing novel bioactive compounds with enzyme and antimicrobial activities. Their study unveiled the significance of exploring the unexploited diversity of Actinomycetes in aquatic ecosystems and the vast biotechnological potential awaiting discovery.

Similarly, Sarkar and Suthindhiran (2022) reviewed the diversity and biotechnological potential of Actinomycetes isolated from different marine environments. Their study revealed the presence of novel Actinomycetes species, some of which exhibited promising antimicrobial and enzyme-producing potential. Their study underscored the value of exploring indigenous microbial resources for biotechnological applications.

Despite these notable contributions, there remains a significant gap in our understanding of Actinomycetes diversity in tropical freshwater sediments, especially in regions like Niger Delta, Nigeria. Most research in this area has focused on temperate or subtropical regions, neglecting the unique environmental conditions and microbial communities present in tropical ecosystems (Olanrewaju and Babalola 2018).

Hence, this research aimed to assess the diversity of Actinomycetes in tropical freshwater sediments and their enzyme (amylase) production potential for biotechnological exploration.

MATERIALS AND METHODS

Study area

This study was conducted at the Department of Microbiology, Federal University Otuoke, Bayelsa State, Nigeria, which is situated at coordinates: Latitude 4°.47'27.91" N and 4°.47'44.37" N of the Equator and Longitude 6°19'19.4" and 6°19'52.12" E of the Greenwich Meridian.

Sample collection

Freshwater sediments were collected from Otuoke River, in Ogbia Local Government Area, Bayelsa State, Nigeria, at coordinates: Latitude 4°.57'16.83" N and 6°.18'35.87" E. The samples were collected from four different points 50 meters apart (i.e., upstream, middle, downstream, and shore) in Otuoke River, Bayelsa State. The sediment samples were collected from each point at a depth between 0-15 cm using a grab sampler, placed in sterile glass containers, and transferred into an ice pack (Song et al. 2023). These were transported to the laboratory for further analysis.

Physio-chemical analysis

The conductivity and pH were measured using a HANNA Conductivity meter (HI 9835) and a digital Oakton pH meter (model PCD 650), respectively. The pH and conductivity meters were standardized with buffer solutions (4 & 7) and conductivity standard solutions, respectively. The tip of the probe in each case was rinsed with deionized water and cleaned with a paper towel. The probe was then immersed in the sample, and the corresponding steady reading was taken in each case. Nitrate, phosphate, and total organic carbon were determined following the method adopted by APHA (2017).

Determination of nitrate

This was done following the method adopted from (APHA 4500-NO_3-B). Next, a sample cell was filled with 10 mL of the sample, and the contents of one Nitra Ver 5 Nitrate Reagent powder pillow were added (the prepared sample). A second sample cell was filled with the sample (the blank) used in zeroing the equipment. The prepared sample was then placed into the cell holder and resulting in parts per million (ppm) nitrate nitrogen (NO_3-N) being read. The equipment used was a DR 5000TM UV spectrophotometer.

Total Organic Carbon (TOC)

The TOC method was adopted from APHA 5310B (high-temperature combustion method). The sample is homogenized, and a micro portion is injected into the reaction chamber packed with heated barium chromate. The water was then vaporized, and the organic carbon was oxidized to H_2O and CO_2. The CO_2 from the oxidation of inorganic and organic carbon is taken in the carrier gas stream and measured by means of an infrared analyzer.

Phosphate determination

The method for phosphate determination was adopted from APHA 4500-P. Next, 10 mL of the sample was added to the sample cell, and the content of one Phosphate Reagent Powder Pillow was added (the prepared sample). A second sample cell was filled with the sample (the blank) used in zeroing the equipment. The prepared sample was then placed into the cell holder, and the result in ppm was read. The equipment used was a DR 5000TM UV spectrophotometer.

Isolation and enumeration of bacteria

Isolation and enumeration were done according to the method of Adeyemo et al. (2021). Freshwater sediment samples were serially diluted up to $10^{-5.}$ Then, a 0.1 mL

aliquot of each dilution (10^{-4} and 10^{-5}) was inoculated using the spread plate method on starch casein agar and nutrient agar plates in duplicates. The plates were incubated for 5 days at 37±2°C. After incubation, the morphological characteristics of the colonies were examined and recorded, and all discrete colonies were counted and expressed in colony-forming units per gram (CFU/g). Different colonies were subcultured on starch casein agar and later incubated for another 48 hours at 37°C to obtain pure cultures, which were preserved on nutrient agar slants at 4±2°C for further analyses.

Screening of Actinomycetes for amylase activity

Isolates were screened for amylolytic properties by starch hydrolysis test on starch agar plates following the procedure described by Praveen Kumar et al. (2015). The streaked isolates were incubated at 30±2°C for 7 days. After the incubation, 1% iodine solution (freshly prepared) was flooded on the starch agar plates, and a clear zone of hydrolysis was considered as amylase producers.

Biochemical characterization of the isolates

Gram staining and other biochemical tests, such as catalase, citrate, Triple Sugar Iron (TSI), motility, indole, and urease (MIU), were performed on the isolates following the standard procedures of Cheesbrough (2010).

Gram staining

A thin smear of the bacterial culture was prepared on a clean, grease-free glass slide and allowed to air dry. The smear was heat-fixed by passing the slide through the flame. The smear was flooded with crystal violet for 60 seconds before rinsing gently with distilled water. Lugol's iodine solution was added and allowed to sit for 60 seconds before rinsing gently with distilled water. The smear was decolorized with 95% ethanol for 30 seconds before rinsing with distilled water. It was then counter-stained with safranin for 60 seconds before rinsing with distilled water and air dried. Gram-stained slides were examined under a microscope with a ×100 objective lens using oil immersion.

Catalase test

A drop of aqueous hydrogen peroxide solution was placed on a grease-free slide, and a loopful of the test organism was smeared on it. The mixture on the slide was observed for the production of gas bubbles, which indicated a positive reaction result.

Citrate utilization test

This test determined the ability of bacteria to use citrate as their sole carbon source. Each isolate was inoculated on a freshly prepared Simmons' citrate agar slant and incubated at 37°C for 12-24 hours. A change of color from blue to green indicated a positive result, while no color change indicated a negative result.

Triple Sugar Iron (TSI) agar test

This test was carried out to differentiate bacteria based on their ability to ferment sugars (glucose, lactose, and sucrose) and produce hydrogen sulfide. During the test, the butt of the TSI agar slant was stabbed with an inoculating needle containing the test organism, then streaked on the surface of the slant. The slant was incubated at 37°C for 18-24 hours. After which, it was observed for color change and gas production. The result was interpreted as follows: yellow slant/yellow butt: glucose, lactose, and/or sucrose fermentation; red slant/yellow butt: glucose fermentation only; red slant/red butt: no sugar fermentation; black precipitate in the butt: hydrogen sulfide production; cracks or bubbles: gas production.

Motility-Indole-Urea (MIU) test

This test was carried out to determine bacterial motility, indole production, and urease activity in a single test. Next, using a sterile inoculating needle, the MIU medium was stabbed with the test organism. The test tube was incubated for 24-48 hours at 37°C. Next, the test tubes were observed for motility by checking for diffusion of growth away from the stab line after the incubation period. A few drops of Kovac's reagent were added to the medium to test for indole production. The tube was also observed for a color change in the medium, indicating urease activity. The results were interpreted as follows: Motility is positive if there is a diffuse growth spreading away from the stab line and negative if growth is only along the stab line.

Indole production was considered positive if a red or pink color appeared after adding Kovac's reagent, and negative if there was no color change. Urease production was considered positive if the medium turned pink, and negative if there was no color change.

Identification of the isolates using the (Analytical Profile Index (API) CORYNE, BioMerieux, France) test kit

The API CORYNE strip consists of 20 microtubes containing dehydrated substrates for the demonstration of enzymatic activity or the fermentation of carbohydrates (CHO). The addition of a dense test suspension of bacteria rehydrates the enzymatic substrates. The metabolic end products produced during incubation are detected through spontaneous colored reactions or by the addition of reagents. The fermentation tests are inoculated with an enrichment medium (containing a pH indicator), which reconstitutes the CHO substrates. Color changes in the pH indicator detect fermentation of CHO.

To carry out the fermentation tests, about 0.5 mL of bacterial suspension was transferred to an ampoule containing 2 mL of GP medium. After homogenization, this new suspension was distributed into the fermentation tubes and overlaid the cupules with mineral oil. The same was done for the urea hydrolysis tube. The strip was then incubated at 37°C for 24 hours. Blood agar was also incubated as a control.

The readings, except for the esculin, urease, and gelatin tests, were done after adding the appropriate reagents. The fermentation reactions were considered positive when they turned yellow.

The reactions are read according to the Reading Table and the identification is obtained by referring to the Analytical Profile Index or using the APIweb, API identification software.

RESULTS AND DISCUSSION

Physico-chemical characteristics

The physico-chemical properties of the sediment samples are presented in Table 1. Upstream sediment recorded the highest pH and TOC values (6.30 and 0.98%), while shore sediment recorded the lowest pH (5.70) and the highest phosphate concentration (8.716 mg/kg). Sediment from the middle recorded the highest nitrate (9.632 mg/kg) and conductivity (115 µs).

Bacterial counts from sediment samples across different microbiological media

The results revealed that middle sediment recorded the highest total culturable heterotrophic bacterial counts (TNTC) on Nutrient agar, followed by upstream sediment (1.46×10^{-7}CFU/g). At the same time, sediments from downstream and shore were too few to count (TFTC), as shown in Table 2.

Enzyme (amylase) activity of isolates

Table 3 presents the enzyme activities of the isolates. Six (6) isolates were positive for amylase production (Figure 1).

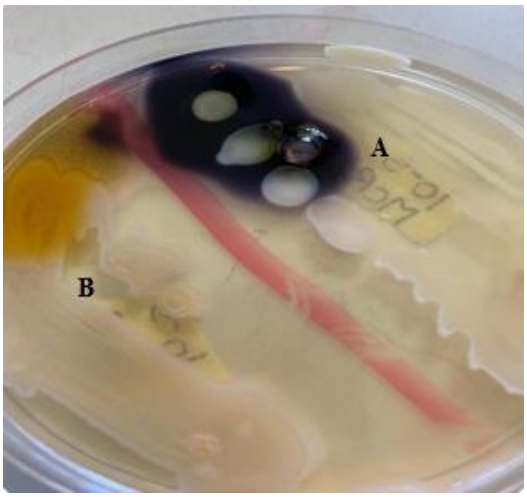

Figure 1. A. Positive Amylase activity of *Micrococcus* sp. (SMCR2); B. Negative amylase activity of *Streptomyces* sp. (SD C)

Biochemical characteristics and analytical index profile (API) identities of isolates

The biochemical characteristics and API tests tentatively identified the isolates as *Micrococcus roseus*, *Micrococcus luteus* (Schroeter, 1872) Cohn, 1872, *Micrococcus* sp., *Actinomyces* sp., *Actinomyces viscosus* (Howell et al., 1965) Georg et al., 1969, *Streptomyces coelicolor*, and *Streptomyces* sp. (Tables 4 and 5).

Table 2. Enumeration of bacterial isolates on various microbiological media

Sample code	Total culturable heterotrophic bacteria counts (CFU/g) on NA	Actinomycetes count (CFU/g) on SCA
SS	TFTC	3.4×10^{-7}
SM	TNTC	6.2×10^{-7}
SD	TFTC	1.6×10^{-7}
SU	1.46×10^{-7}	TFTC

Note: NA: Nutrient agar; SCA: Starch casein agar; TFTC: Too few to count (less than 30 colonies); TNTC: Too numerous to count (greater than 30 colonies and above); SS: sediment from shore; SM: Sediment from middle; SD: Sediment from downstream; SU: Sediment from upstream, CFU/g: Colony forming unit per gram

Table 3. Amylase activity of the isolates

Isolate code	Amylase activity
SM CR2	+
SM CR	-
SS WR	+
SD C	-
SM CI	+
SD CM	-
SM CE	+
SS W	+
SM Y	+

Note: +: positive; -ve: negative

Table 1. Physicochemical characteristics of sediment samples

Parameters	Analysis method	SU	SM	SD	SS
Phosphate (mg/kg)	APHA 4500-P	2.404	2.152	2.132	8.716
Nitrate (mg/kg)	ASTM D3867-04	6.624	9.632	3.600	2.488
pH	ASTM D1293-99	6.30	6.10	6.20	5.70
Conductivity (µs)	ASTM D 1125	107	115	95	101
TOC (%)	APHA 5310B	0.98	0.86	0.69	0.80
	PSD				
Sand (%)	Sieve	35.30	28.20	37.70	27.70
Clay (%)	Sieve	5.50	7.90	4.20	8.30
Silt (%)	Sieve	59.10	61.40	57.30	62.00

Note: SS: Sediment from shore; SM: Sediment from the middle; SD: Sediment from downstream; SU: Sediment from upstream; PSD: Particle size distribution

Table 4. Biochemical characterization of the bacterial isolates

Isolate code	Shape	Color	Citrate	Catalase	Slant	TSI Butt	Gas	H_2S	Motility	MIU Indole	Urease	Tentative identity of organism
SM CR2	Cocci	Purple	-ve	+ve	Yellow	Red	-ve	-ve	+ve	-ve	+ve	*Micrococcus* sp.
SM CR	Rods	Purple	+ve	+ve	Red	Yellow	-ve	-ve	-ve	+ve	-ve	*Streptomyces* sp.
SS WR	Rods in diploid	Purple	-ve	+ve	Yellow	Red	-ve	-ve	+ve	-ve	+ve	*Streptomyces* sp.
SD C	Filamentous rods with spores	Purple	-ve	+ve	Yellow	Yellow	-ve	-ve	-ve	-ve	+ve	*Streptomyces* sp.
SM CI	Cocci	Purple	-ve	+ve	Red	Red	-ve	-ve	-ve	-ve	+ve	*Micrococcus* sp.
SD CM	Filamentous rods	Purple	-ve	+ve	Red	Red	-ve	-ve	-ve	-ve	+ve	*Actinomyces* sp.
SM CE	Cocci	Purple	-ve	+ve	Red	Yellow	+ve	-ve	+ve	-ve	+ve	*Micrococcus* sp.
SS W	Cocci in clusters	Purple	-ve	+ve	Yellow	Yellow	-ve	-ve	+ve	-ve	+ve	*Micrococcus roseus*
SM Y	Cocci	Purple	-ve	+ve	Red	Yellow	-ve	-ve	-ve	-ve	+ve	*Micrococcus luteus*

Note: +ve: Positive; -ve: Negative; TSI: Triple Sugar Iron (Cheesbrough 2010)

Table 5. Identification of bacterial isolates using the Analytical Profile Index test

Isolate code	IND	URE	GLU	MAN	LAC	SAC	MAL	SAL	XYL	ARA	GEL	ESC	GLY	CEL	MNE	MLZ	RAF	SOR	RHA	TRE	CAT	API % SIMILARITY IDENTITY	ORGANISM TENTATIVE IDENTITY
SS WR	-	+	-	+	+	-	NT	NT	-	+	+	+	-	-	-	-	+	-	+	-	+	99.9%	*Streptomyces coelicolor*
SD CM	-	-	+	-	+	+	+	-	-	-	-	-	+	-	+	-	+	-	-	-	+	98.4%	*Actinomyces viscosus*

Note: +: Positive; -: Negative; IND: Indole; URE: Urease; GLU: Glucose; MAN: Mannitol; LAC: Lactose; SAC: Saccharose; MAL: Maltose; SAL: Salicin; XYL: Xylose; ARA: Arabinose; GEL: Gelatin; ESC: Esculin; GLY: Glycerol; CEL: Celliobiose; MNE: Mannose; MLZ: Melezitose; RAF: Raffinose; SOR: Sorbitol; RHA: Rhamnose; TRE: Trehalose; CAT: Catalase; NT: Not tested (Soto et al. 1994)

Discussion

The variations observed in phosphate, nitrate, pH, conductivity, and TOC across different sediment locations indicate diverse microenvironments that influence microbial diversity. Nitrate concentrations were notably higher in sediment from the middle, suggesting that this area may have a higher level of nutrient influx or retention compared to the shore and downstream sediments. The sediments from the shore and middle had the highest phosphate and nitrate content levels, respectively (Table 1), which are conducive for microbial growth (high bacterial population), as shown in Table 2, supporting previous studies that link higher nutrient levels with increased microbial activity (Francioli et al. 2016; Maron et al. 2018). On the other hand, the lower pH observed in shore sediment could be attributed to a higher accumulation of organic matter, such as decaying plant material and other organic debris around shore areas, which usually undergo microbial decomposition, resulting in the production of organic acids such as humic and fulvic acids, which can lower the pH of the sediment alongside other ongoing anthropogenic activities (Lalas et al. 2018; Yang et al. 2019).

The particle size distribution results showed that silt was the dominant fraction in all samples, which is consistent with findings by Xia et al. (2020), who stated that fine particles like silt provide a greater surface area for microbial colonization and are usually associated with the relative abundances of some fungi and filamentous bacteria such as Actinobacteria. The combination of these physicochemical properties possibly contributed to the microbial diversity and abundance observed in the sediments.

The diversity, abundance, and amylase activity of isolates recovered in this study emphasize the rich microbial ecosystem within these sediments, highlighting their potential as a source of novel bioactive compounds with significant biotechnological value (Praveen Kumar et al. 2015; Zothanpuia et al. 2018; Shigeri et al. 2019; Ribeiro et al. 2023).

The bacterial counts from the sediment samples revealed significant variations in microbial abundance, especially between different points and media types. The highest count was observed in the middle sediment on SCA, which aligns with the nutrient-rich nature of this location as indicated by its higher nitrate content (Table 2). This finding is particularly enlightening as it is consistent with the findings of Li et al. (2023), who reported that microbial biomass and composition in sediment were strongly influenced by nitrogen inundation (nutrient availability). The lower microbial population observed in downstream sediment suggests a less favorable environment for heterotrophic bacteria and Actinomycetes or starch-degrading bacteria, possibly due to lower organic carbon, nitrate, and phosphate content (Tables 1 and 2). Similar observations were reported by Zanane et al. (2018), where the presence of Actinomycetes recovered in their study was majorly influenced by the prevailing physicochemical properties (e.g., organic carbon, pH, moisture, and others).

The biochemical characterization and API tentative identification of the isolates further emphasize the diversity of the bacterial community within the sediment samples. The prevalence of *Micrococcus* and *Streptomyces* species is notable, as these genera are well-known for their resilience in diverse environments and their ability to produce antibiotics, enzymes, and other secondary metabolites (Barka et al. 2016). The identification of *S. coelicolor* with a 99.9% similarity identity is consistent with previous studies that recovered this species from diverse soil and sediment environments (Patin et al. 2017). *Streptomyces* species are renowned for their secondary metabolite production, including antibiotics, which highlights the potential biotechnological applications of these isolates (Alam et al. 2022). The presence of *Actinomyces viscosus*, known for its role in soil health and organic matter decomposition, further supports the rich microbial diversity observed in these sediments (Ataikiru et al. 2020). The overall identification results are consistent with those of Ribeiro et al. (2020), who reported similar bacterial diversity in tropical sediments, with a significant presence of Actinomycetes and other gram-positive bacteria.

In conclusion, this study highlights the rich bacterial diversity and abundance present in tropical freshwater sediments, especially among Actinomycetes, which were found to be abundant and diverse across the different sediment locations within the freshwater system. The variations in physicochemical properties, especially pH, nutrient content, and particle size distribution, played a significant role in shaping the bacterial community. The identification of species with known biotechnological potential (amylase activity), such as *S. coelicolor* and *M. luteus*, emphasizes the value of these sediments as sources of novel bioactive compounds. These findings provide a foundation for future research aimed at exploring the biotechnological applications of these microorganisms, particularly in the development of new antibiotics, enzymes, and other secondary metabolites, and for their molecular identification, as this gives a more accurate identification of microorganisms compared to culture-dependent identification methods used in this study.

ACKNOWLEDGEMENTS

The authors acknowledge the Department of Microbiology Laboratory, Federal University Otuoke, Bayelsa State, Nigeria, for providing laboratory equipment and workspace used during this research.

REFERENCES

Adeyemo OM, Ja'afaru MI, Adams FV. 2021. Isolation, characterization, antimicrobial and other bioactivity profiles of three *Streptomyces* strains isolated from Lake Gerio, Yola, Adamawa State, Nigeria. Bull Natl Res Cent 45: 147. DOI: 10.1186/s42269-021-00606-x.

Ahmad I, Althubiani AS, Dar MS, Samreen, Qais FA, Abulreesh HH, Bagama MA, Al-Ghamdi SB, Alshehrei F. 2019. Actinomycetes as Continued Source of New Antibacterial Leads. In: Ahmad I, Althubiani AS, Dar MS, Samreen, Qais, FA, Abulreesh HH, Bamaga MA, Al-Ghamdi SB, Alshehrei F (eds.). Antibacterial Drug

Discovery to Combat MDR. Springer, Singapore. DOI: 10.1007/978-981-13-9871-1_16.

Alam K, Mazumder A, Sikdar S, Zhao YM, Hao J, Song C, Wang Y, Sarkar R, Islam S, Zhang Y, Li A. 2022. *Streptomyces*: The biofactory of secondary metabolites. Front Microbiol 13: 968053. DOI: 10.3389/fmicb.2022.968053.

Alvarez A, Saez JM, Davila Costa JS, Colin VL, Fuentes MS, Cuozzo SA, Benimeli CS, Polti MA, Amoroso MJ. 2017. *Actinobacteria*: Current research and perspectives for bioremediation of pesticides and heavy metals. Chemosphere 166: 41-62. DOI: 10.1016/j.chemosphere.2016.09.070.

American Public Health Association (APHA). 2017. Standard Methods for the Examination of Water and Wastewater (23rd Edition). American Public Health Association, Washington DC.

Ataikiru TL, Okerentugba PO, Okpokwasili GC. 2020. Identification of carbofuran and paraquat degrading microorganisms from soil. SAJRM 7 (1): 40-52. DOI: 10.9734/sajrm/2020/v7i130164.

Barka EA, Vatsa P, Sanchez L, Gaveau-Vaillant N, Jacquard C, Klenk HP, Clément C, Ouhdouch Y, van Wezel GP. 2016. Taxonomy, physiology, and natural products of Actinobacteria. Microbiol Mol Biol Rev 80 (1): 1-43. DOI: 10.1128/mmbr.00019-15.

Cheesbrough M. 2010. District Laboratory Practice in Tropical Countries. 2nd Edition. Cambridge University Press, Cambridge, United Kingdom. DOI: 10.1017/CBO9780511581304.

De Simeis D, Serra S. 2021. Actinomycetes: A never-ending source of bioactive compounds-An overview on antibiotics production. Antibiotics (Basel) 10 (5): 483. DOI: 10.3390/antibiotics10050483.

Ezeobiora CE, Igbokwe NH, Amin DH, Enwuru NV, Okpalanwa CF, Mendie UE. 2022. Uncovering the biodiversity and biosynthetic potentials of rare Actinomycetes. Future J Pharm Sci 8: 23. DOI: 10.1186/s43094-022-00410-y.

Francioli D, Schulz E, Lentendu G, Wubet T, Buscot F, Reitz T. 2016. Mineral vs. organic amendments: Microbial community structure, activity and abundance of agriculturally relevant microbes are driven by long-term fertilization strategies. Front Microbiol 7: 1446. DOI: 10.3389/fmicb.2016.01446.

Jagannathan SV, Manemann EM, Rowe SE, Callender MC, Soto W. 2021. Marine Actinomycetes, new sources of biotechnological products. Mar Drugs 19 (7): 365. DOI: 10.3390/md19070365.

John JA, Samuel MS, Govarthanan M, Selvarajan E. 2022. A comprehensive review on strategic study of cellulase producing marine *Actinobacteria* for biofuel applications. Environ Res 214 (Pt 3): 114018. DOI: 10.1016/j.envres.2022.114018.

Kontro MH, Yaradoddi JS, Banapurmath NR, Ganachari SV, Hungund BS. 2022. Biotechnological Importance of Actinomycetes. In: Yaradoddi JS, Kontro MH, Ganachari SV (eds.). Actinobacteria. Rhizosphere Biology. Springer, Singapore. DOI: 10.1007/978-981-16-3353-9_15.

Lalas S, Athanasiadis V, Dourtoglou VG. 2018. Humic and fulvic acids as potentially toxic metal reducing agents in water. CLEAN - Soil, Air, Water 46 (2): 1700608. DOI: 10.1002/cclen.201700608.

Law JWF, Pusparajah P, Ab Mutalib NS, Wong SH, Goh BH, Lee LH. 2019. A review on mangrove actinobacterial diversity: The roles of *Streptomyces* and novel species discovery. Prog Microbes Mol Biol 2 (1): a0000024. DOI: 10.36877/pmmb.a0000024.

Li W, Xie L, Zhao C, Hu X, Yin C. 2023. Nitrogen fertilization increases soil microbial biomass and alters microbial composition especially under low soil water availability. Microb Ecol 86 (1): 536-548. DOI: 10.1007/s00248-022-02103-8.

Maron PA, Sarr A, Kaisermann A, Lévêque J, Mathieu O, Guigue J, Karimi B, Bernard L, Dequiedt S, Terrat S, Chabbi A, Ranjard L. 2018. High microbial diversity promotes soil ecosystem functioning. Appl Environ Microbiol 84 (9): e02738-17. DOI: 10.1128/AEM.02738-17.

Miao M, Jiang B, Jin Z, BeMiller JN. 2018. Microbial starch converting enzymes: Recent insights and perspectives. Compr Rev Food Sci Food Saf 17 (5): 1238-1260. DOI: 10. 1111/1541-4337.12381.

Olanrewaju OS, Babalola OO. 2018. *Streptomyces*: Implications and interactions in plant growth promotion. Appl Microbiol Biotechnol 103 (3): 1179-1188. DOI: 10.1007/s00253-018-09577-y.

Patin NV, Schorn M, Aguinaldo K, Lincecum T, Moore BS, Jensen PR. 2017. Effects of Actinomycetes secondary metabolites on sediment microbial communities. Appl Environ Microbiol 83 (4): e02676-16. DOI: 10.1128/AEM.02676-16.

Praveen Kumar P, Preetam Raj JP, Nimal Christhudas IVS, Sagaya Jansi R, Murugan N, Agastian P, Arunachalam C, Alharbi SA. 2015. Screening of Actinomycetes for enzyme and antimicrobial activities from the soil sediments of Northern Tamil Nadu. South India. J Biol Active Prod Nat 55 (1): 58-70.

Ribeiro I, Antunes JT, Alexandrino DAM, Tomasino MP, Almeida E, Hilário A, Urbatzka R, Leão PN, Mucha AP, Carvalho MF. 2023. *Actinobacteria* from Arctic and Atlantic deep-sea sediments-Biodiversity and bioactive potential. Front Microbiol 14: 1158441. DOI: 10.3389/Fmicb.2023.1158441.

Roy S, Das I, Munjal M, Karthik L, Kumar G, Kumar S, Rao KVB. 2014. Isolation and characterization of tyrosinase produced by marine *Actinobacteria* and its application in the removal of phenol from aqueous environment. Front Biol 9: 306-316. DOI: 10.1007/s11515-014-1324-0.

Sarkar G, Suthindhiran K. 2022. Diversity and biotechnological potential of marine Actinomycetes from India. Indian J Microbiol 62 (4): 475-493. DOI: 10.1007/s12088-022-01024-x.

Selim MSM, Abdelhamid SA, Mohamed SS. 2021. Secondary metabolites and biodiversity of Actinomycetes. J Genet Eng Biotechnol 19 (1): 72. DOI: 10.1186/s43141-021-00156-9.

Shigeri Y, Matsui T, Watanabe K. 2019. Decomposition of intact chicken feathers by a thermophile in combination with an acidulocomposting garbage treatment process. Biosci Biotechnol Biochem 73 (11): 2519-2521. DOI: 10.1271/bbb.90398.

Song P, Zhang X, Wang, S, Xu W, Wang F, Fu R, Wei F. 2023. Microbial proteases and their applications. Front Microbiol 14: 1236368. DOI: 10. 3389/fmicb.2023.1236368.

Soto A, Zapardiel J, Soriano F. 1994. Evaluation of API Coryne system for identifying coryneform bacteria. J Clin Pathol 47 (8): 756-759. DOI: 10.1136/jcp.47.8.756.

Xia Q, Rufty T, Shi W. 2020. Soil microbial diversity and composition: Links to soil texture and associated properties. Soil Biol Biochem 149: 107953. DOI: 10.1016/j.soilbio.2020.107953.

Yang F, Zhang S, Cheng K, Antonietti M. 2019. A hydrothermal process to turn waste biomass into artificial fulvic and humic acids for soil remediation. Sci Total Environ 686: 1140-1151. DOI: 10.1016/j.apenergy.2019.05.033.

Zanane C, Latrache H, Elfazazi K, Zahir H, Ellouali M. 2018. Isolation of Actinomycetes from different soils of Beni Amir Morocco. J Mater Environ Sci 9 (10): 2994-3000.

Zothanpuia, Passari AK, Leo VV, Chandra P, Kumar B, Nayak C, Hashem A, Abd Allah EF, Alqarawi AA, Singh BP. 2018. Bioprospection of *Actinobacteria* derived from freshwater sediments for their potential to produce antimicrobial compounds. Microb Cell Fact 17 (1): 68. DOI: 10.1186/s12934-018-0912-0.

ASIAN J TROP BIOTECHNOL
Volume 22, Number 1, June 2025
Pages: 30-40

ISSN: 0216-6887
E-ISSN: 2301-8658
DOI: 10.13057/biotek/c220105

Molecular docking studies of phytochemicals from *Triumfetta cordifolia* and *Spondias mombin* against COX-1 and COX-2 enzymes

BAMIDELE MARTIN AMOS-TAUTUA[1,♥], IMOMOTIMI TIMIPA AJOKO[1], SAMUEL JACOB BUNU[2,3]

[1]Department of Chemical Sciences, Faculty of Science, Niger Delta University. Wilberforce Island 560103, Bayelsa, Nigeria.
Tel.: +234-703-9871566, ♥email: bmamos64@gmail.com

[2]Department of Pharmaceutical and Medicinal Chemistry Sciences, Faculty of Pharmacy, Niger Delta University. Wilberforce Island 560103, Bayelsa, Nigeria

[3]Drug Analysis and Research Center, Ebisamdex Global Ventures Ltd. Yenagoa, Bayelsa, Nigeria

Manuscript received: 8 January 2025. Revision accepted: 27 May 2025.

Abstract. *Amos-Tautua BM, Ajoko IT, Bunu SJ. 2025. Molecular docking studies of phytochemicals from* Triumfetta cordifolia *and* Spondias mombin *against COX-1 and COX-2 enzymes. Asian J Trop Biotechnol 22: 30-40. Triumfetta cordifolia* A.Rich. and *Spondias mombin* Jacq. are plants with a long history of traditional use as anti-inflammatory agents are the subjects of this study. The study employs molecular docking to evaluate the inhibitory potential of phytochemicals identified by GC-MS from the leaf extracts of *T. cordifolia* and *S. mombin* against aspirin-acetylated cyclooxygenase-1 (PDB ID: 3N8Y) and celecoxib-bound COX-2 (PDB ID: 3LN1) using the Schrodinger suite. About six major phytochemical compounds including apigenin, catechin, quercetin, luteolin, kaempferol, and myricetin, were analyzed for their drug likeliness based on Lipinski's rule. All studied phytochemicals complied with Lipinski's Rule of Five, indicating favorable drug-likeness and potential oral bioavailability. Molecular docking results revealed strong binding affinities, with apigenin (-8.66 kcal/mol) and catechin (-8.64 kcal/mol) exhibiting the highest binding scores for COX-1, surpassing diclofenac (-7.20 kcal/mol). Similarly, quercetin (-8.06 kcal/mol) and luteolin (-8.14 kcal/mol) demonstrated strong interactions with COX-2, outperforming aspirin (-6.47 kcal/mol). Ligand-protein interaction analysis confirmed the presence of key hydrogen bonds and hydrophobic interactions, reinforcing the stability of these compounds within the active sites of COX enzymes. These findings underscore the strong inhibitory potential of the phytochemicals from *T. cordifolia* and *S. mombin* possess strong inhibitory potential against COX-1 and COX-2, highlighting their promise as natural anti-inflammatory agents.

Keywords: Anti-inflammatory, cyclooxygenase, *in silico* analysis, phytochemicals bindings, *Spondias mombin*, *Triumfetta cordifolia*

Abbreviations: cLogP: calculated LogP, HAC: Heavy Atom Count, HBA: Hydrogen Bond Acceptors, HBD: Hydrogen Bond Donors, LE: Ligand Efficiency, MW: Molecular Weight, STD: standard compounds

INTRODUCTION

Inflammation is a fundamental biological response to infection, injury, and harmful stimuli, involving complex biochemical and cellular processes. It is also a defense response of the body characterized by pain, redness, heat, swelling, and loss of function (Bandaru et al. 2021). Inflammation is orchestrated by immune cells, cytokines, and lipid mediators, particularly prostaglandins, which play a crucial role in pain and fever regulation (Maddipati 2020). Two forms of COX enzymes have recently been identified (Bandaru et al. 2021). In addition, the cyclooxygenase enzymes (COX-1 and COX-2) are central to prostaglandin synthesis, with COX-1 involved in physiological homeostasis and COX-2 predominantly expressed during inflammation (Ali et al. 2023). Overexpression of COX-2 has been implicated in various chronic diseases, including arthritis, cancer, and cardiovascular disorders (Chen et al. 2021).

The most common Non-Steroidal Anti-Inflammatory Drugs (NSAIDs) used to inhibit COX enzymes and alleviate inflammation are ibuprofen, naproxen, diclofenac, indomethacin, and ketoprofen (Ghosh et al. 2015). These drugs inhibit the expression of cyclooxygenase 2 (COX-2) enzymes responsible for the biosynthesis of prostaglandin E2 (PGE2) (Jemal 2019). However, their long-term use is associated with significant risks, including gastrointestinal ulceration and renal toxicity. These adverse effects are primarily due to the non-selective inhibition of cyclooxygenase-1 (COX-1) and cyclooxygenase-2 (COX-2) enzymes, leading to a decrease in protective prostaglandins in the gastrointestinal tract and kidneys (Tai and McAlindon 2021). In addition, these drugs are very expensive. This has driven interest in plant-derived bioactive compounds as safer alternatives with selective COX-2 inhibition, potentially reducing adverse effects. Plant-derived bioactive compounds have emerged as a promising avenue in this regard, offering the potential for selective COX-2 inhibition with fewer adverse effects (Nwankwo et al. 2021; Bunu et al. 2023). Many natural compounds, such as flavonoids, alkaloids, and polyphenols, have demonstrated anti-inflammatory properties by selectively targeting COX-2 while sparing COX-1 (Nasim et al. 2022).

Molecular docking is a widely used computational approach that predicts the binding interactions between small molecules and target proteins, aiding in drug discovery and lead optimization (Agu et al. 2023). The primary objective of ligand-protein docking is to identify

the most probable binding conformation between a ligand and a target protein (Saravanan et al. 2022). These predictions play a crucial role in aiding researchers to design potent drugs capable of effectively interacting with the target protein. Moreover, molecular docking can be used to optimize lead compounds by guiding the rational design of chemical modifications that enhance binding affinity, selectivity, and pharmacokinetic properties (Pinzi and Rastelli 2019; Baba and Bunu 2025). In-silico approaches facilitate the rapid screening of numerous therapeutic candidates within a virtual framework, thereby reducing the need for extensive animal experimentation and addressing associated ethical considerations. Additionally, these computational insights enable the identification of high-potential lead molecules for further confirmation through laboratory-based *in vitro* and *in vivo* investigations (Puspa et al. 2024).

Triumfetta cordifolia A.Rich. and *Spondias mombin* Jacq. are medicinal plants known for together diverse pharmacological properties, including antidiabetic, antioxidant, and anti-inflammatory (Ajaegbu et al. 2022; Ajoko et al. 2023). Phytochemical analysis of these plants has revealed the presence of flavonoids, alkaloids, tannins, phenolic compounds, and terpenoids (Ikponmwosa-Eweka and Omoregie 2024; Ajoko et al. 2020). Previous reports have indicated the possibility of anti-inflammatory properties in *T. cordifolia* and *S. mombin* (Ajoko et al. 2023; Amos-Tautua et al. 2025). However, until now, no detailed molecular docking analysis has been carried out to investigate the therapeutic potential of these plants.

Therefore, this study aims to address this gap by conducting a molecular docking analysis on *T. cordifolia* and *S. mombin* against cox-1 and cox-2 enzymes. To the best of our knowledge, this report represents the first attempt to conduct a molecular docking analysis of these plants with cox-1 and cox-2. The findings will provide valuable insights into their potential as lead compounds for drug development.

MATERIALS AND METHODS

Collection of plant materials

Spondias mombin and *T. cordifolia* leaves were collected from Yenagoa (4°55'36.30" N, 6°16'3.50" E) and Amassoma (4°58'13.15" N, 6°06'32.94" E), respectively, in Bayelsa State, Nigeria (Figure 1). Prof. K.K. Ajibesin identified both plants from the Department of Pharmacognosy and Herbal Medicine, Niger Delta University, Nigeria.

Molecular docking

Six major bioactive compounds (Figure 2) identified by HPLC analysis from *T. cordifolia* and *S. mombin* leaf extracts as earlier reported in our studies (Ajoko et al. 2023; Amos-Tautua et al. 2025) were selected and subjected to molecular docking (*in-silico*) analysis with the X-ray crystal structures of aspirin-acetylated COX-1 (PDB ID: 3N8Y) and celecoxib-bound COX-2 active site (PDB ID: 3LN1) enzymes (Sidhu et al. 2010; Wang et al. 2010), retrieved from the Protein Data Bank (PDB) (https://www.rcsb.org/). Aspirin and diclofenac (anti-inflammatory) were used as standard controls. The ligands and the target protein were prepared using the Maestro Molecular Modeling Suite 2020. The canonical smiles of the bioactive compounds were retrieved from the PubChem database and were converted to a 3-D structure using the LigPrep wizard of Schrödinger's Maestro.

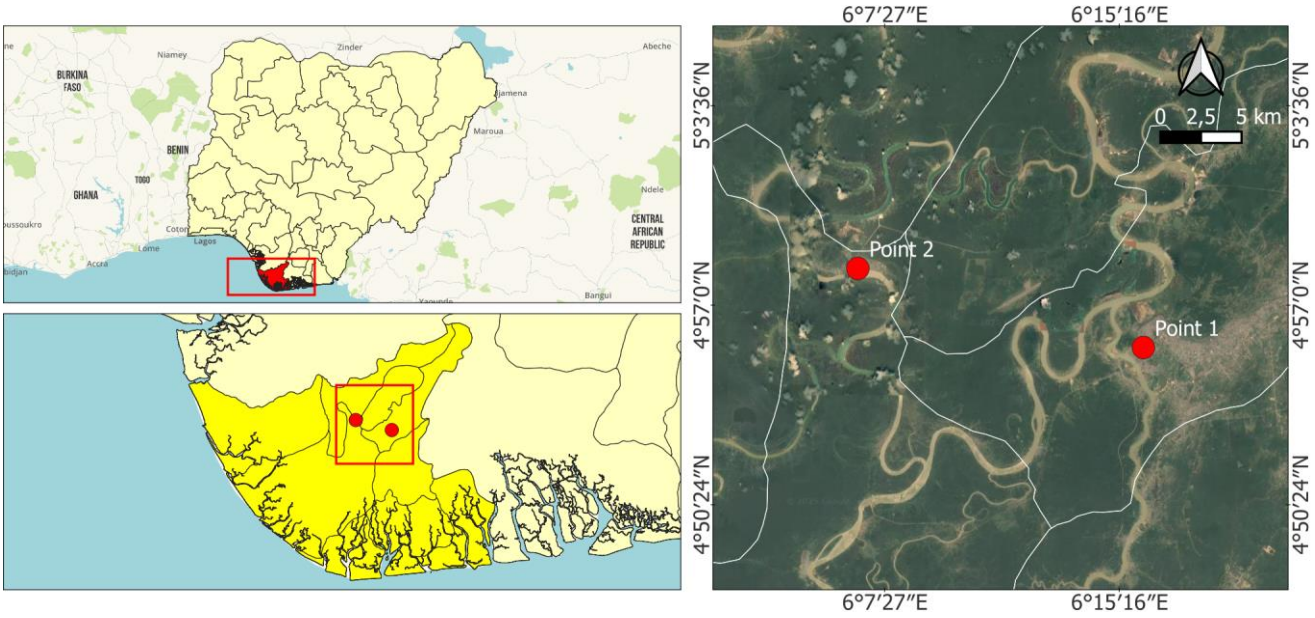

Figure 1. Location of study area in Bayelsa State, Nigeria, i.e., Yenagoa (point 1) indicating the collection site of *Spondias mombin*, and Amassoma (point 2) indicating the collection site of *Triumfetta cordifolia*

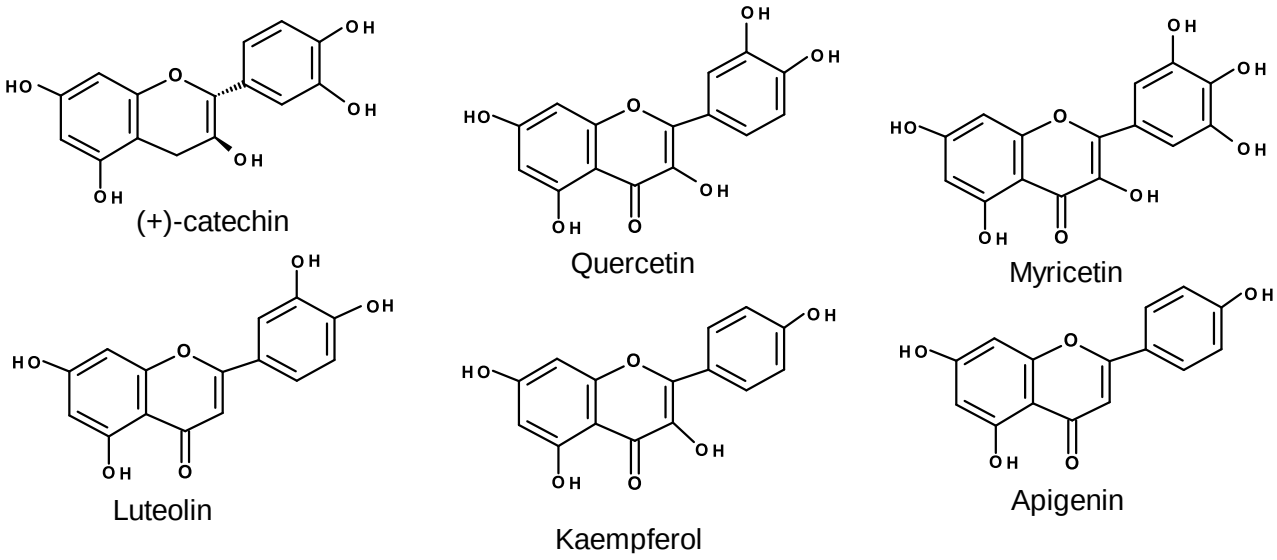

Figure 2. Bioactive compounds identified by HPLC analysis from *Triumfetta cordifolia* and *Spondias mombin* leaf extracts

Preparation of the proteins' crystallographic structures was accomplished using the protein preparation module of Schrödinger's Maestro molecular modeling suite. In this management, bond orders were assigned, water molecules were deleted beyond 5 Å from het groups, and het state was left in default pH (7.0 ± 2.0) using Epik. Lastly, grid generation was done, and the bounding box was set, which can cover the whole target site for docking simulation. After the completion of the pre-requisite steps, the docking simulations were carried out in the SP glide of Schrödinger's Maestro Suite (Maestro 2020). The phytocompounds were selected based on Lipinski's rule of five parameters, such as molecular weight, LogP, number of hydrogen bond donors, number of hydrogen bond acceptors, and HAC (Table 1).

RESULTS AND DISCUSSION

Drug-likeness analysis of compounds

Drug-likeness characteristics play a crucial role in assessing the quality of emerging anti-inflammatory compounds. Lipinski's Rule of Five is a widely accepted criterion used to assess the drug-likeness of compounds. It evaluates Molecular Weight (MW), Hydrogen Bond Acceptors (HBA), Hydrogen Bond Donors (HBD), and calculated LogP (cLogP) to predict oral bioavailability (Haritha 2024). According to Lipinski's 5 rules (Lipinski 2004), an oral drug should have a Molecular Weight (MW) not exceeding 500 mg/mol, hydrogen bond acceptors not exceeding 10, hydrogen bond donors not exceeding 5, and a LogP value less than 5. Generally, a molecule is considered non-oral active if two or more of these rules are broken (Afroz Shoily et al. 2025). Interestingly, in our study, all six compounds from *T. cordifolia and S. mombin* have good drug-likeness parameters since they follow Lipinski's RO5 as indicated in Table 1. This compliance suggests that these compounds possess good pharmacokinetic properties, which is promising for their development as orally active anti-inflammatory agents.

Binding affinity analysis

The binding affinity of phytochemicals to COX-1 (3N8Y) and COX-2 (3LN1) was evaluated using molecular docking scores. The docking results were represented in the form of e-negative values (Table 2). In the docking studies, higher negative e-values represent high binding affinity between the receptor and ligand molecules, indicating the higher efficiency of the bioactive compounds (Jemal 2019). As shown in Table 2, all the phytochemicals except myricetin displayed stronger binding than the standards diclofenac (-7.20 kcal/mol) and aspirin (-5.71 kcal/mol for COX-1 enzyme. Similarly, for 3LN1, all the phytochemicals, including myricetin, outperformed aspirin (-6.47 kcal/mol).

These results suggest that certain phytochemicals could act as potential COX inhibitors, potentially outperforming conventional NSAIDs. These results highlight that phytochemicals, particularly apigenin, catechin, quercetin, and luteolin, exhibit superior binding affinity, suggesting their potential use as natural anti-inflammatory agents. The interaction with COX-2, a preferred target for selective inhibition to reduce gastrointestinal side effects, also suggests that luteolin and quercetin may have favorable pharmacological properties (Rouzer and Marnett 2020). The high binding affinity of these compounds suggests that they may interfere with the enzymatic activity of COX-1 and COX-2, thereby reducing inflammation through prostaglandin inhibition (Verma et al. 2020). Furthermore, the interaction profiles of these phytochemicals indicate their potential to serve as selective COX-2 inhibitors, minimizing the adverse effects commonly associated with non-selective NSAIDs. The docking results of bioactive compounds are shown in Figures 3, 5, 7, and 9.

Table 1. Lipinski's properties of the selected phytocompounds from extracts of *Triumfetta cordifolia* and *Spondias mombin*

Ligand	PubChem ID	MW	HBA	HBD	cLogP	HAC
Aspirin	2244	286.2	4	1	0.52	13
Diclofenac	3033	296.10	3	2	3.67	19
Apigenin	5280443	270.24	5	3	3.07	20
Catechin	9064	290.27	6	5	1.92	21
Kaempferol	5280863	286.20	6	4	2.80	21
Luteolin	5280445	286.20	6	4	2.80	21
Myricetin	5281672	318.20	8	6	2.26	23
Quercetin	5280343	302.20	7	5	2.53	22

Table 2. Docking scores and ligand efficiency of selected phytochemicals and standards on COX-1 and COX-2

Ligand	COX-1(3N8Y)		COX-2 (3LN1)	
	Docking Score (kcal/mol)	Ligand Efficiency	Docking Score (kcal/mol)	Ligand Efficiency
Aspirin	-5.71	-0.44	-6.47	-0.50
Diclofenac	-7.20	-0.38	-8.20	-0.43
Apigenin	-8.66	-0.43	-7.40	-0.37
Catechin	-8.64	-0.41	-7.75	-0.37
Kaempferol	-8.24	-0.39	-7.38	-0.35
Luteolin	-7.33	-0.35	-8.14	-0.39
Myricetin	-6.28	-0.27	-6.54	-0.28
Quercetin	-7.63	-0.35	-8.06	-0.37

Ligand efficiency of standards and phytochemicals

Ligand efficiency is a measurement of the binding energy per atom of a ligand to its binding partner, such as a receptor or enzyme (Hopkins et al. 2014). A "good" ligand efficiency is normally counted to be about -0.3 kcal/mol per heavy atom. This underscores that a molecule with a higher LE value achieves a substantial level of binding affinity relative to its molecular size, making it a more needed lead compound in drug discovery. The ligand efficiency values for the studied phytochemicals and standard drugs are presented in Table 3. The LE values were calculated using the Equation 1:

$$\text{LE - Ligand Efficiency (kcal/atom)} = \frac{\text{Docking Score (kcal/mol)}}{\text{HAC}}$$

The docking scores and ligand efficiency values that reveal important trends in the binding interactions between selected phytochemicals and standard drugs (aspirin and diclofenac) with COX-1 (3N8Y) and COX-2 (3LN1) enzymes are presented in Table 2. Aspirin demonstrates moderate binding affinity (-5.71 for COX-1 and -6.47 for COX-2), which aligns with its established mechanism of reversible COX-1 inhibition and irreversible COX-2 acetylation. In contrast, diclofenac shows significantly stronger binding (-7.20 for COX-1 and -8.20 for COX-2), consistent with its well-documented potency as a COX-2-preferential anti-inflammatory agent (Na'imah 2019; Bunu et al. 2023). Among the phytochemicals, apigenin and catechin exhibit particularly high docking scores for COX-1 (-8.66 and -8.64, respectively), indicating robust binding interactions. These computational findings are supported by experimental studies demonstrating the COX-1 inhibitory activity of such flavonoids (Ribeiro et al. 2015). Similarly, luteolin and quercetin display notable binding affinity for COX-2 (-8.14 and -8.06, respectively), reinforcing their potential as COX-2 inhibitors, as evidenced by previous research on their anti-inflammatory properties (Li et al. 2016).

The ligand efficiency metric, which accounts for molecular size, offers valuable insights into drug-like characteristics. While diclofenac shows stronger absolute binding, its ligand efficiency (-0.38 for COX-1, -0.43 for COX-2) is lower than that of aspirin (-0.44, -0.50), reflecting its larger molecular structure. Apigenin demonstrates well-balanced ligand efficiency (-0.43 for COX-1, -0.37 for COX-2), suggesting it as a promising lead compound. In contrast, myricetin's relatively low ligand efficiency (-0.27 to -0.28) may be attributed to its higher molecular weight and polarity, factors known to limit bioavailability potentially. The data reveal distinct selectivity patterns: most phytochemicals, including apigenin and catechin, preferentially bind COX-1, while luteolin and quercetin show greater affinity for COX-2. This variability in selectivity among flavonoids has been previously documented (Yang et al. 2023) and mirrors the COX-2 preference observed with diclofenac, a clinically used COX-2 preferential NSAID. Additional support comes from studies linking apigenin COX-1 inhibition to antiplatelet effects (Zaragozá et al. 2022) and quercetin's COX-2 binding to macrophage suppression (Xiao et al. 2011), both validating the current docking results.

On the other hand, kaempferol and luteolin displayed moderate ligand efficiency, suggesting they could serve as promising drug candidates with further structural optimization. Higher ligand efficiency values indicate that a compound binds strongly with minimal structural complexity, making it a preferable candidate for further drug development. Apigenin and catechin, which showed relatively high ligand efficiency, could be explored for structural modifications to enhance their specificity and potency against COX-2, reducing off-target effects typically associated with NSAIDs (Listyani et al. 2024).

Ligand-protein amino acid interactions with 3N8Y and 3LN1

The affinity between proteins and ligands is fundamental to many biological processes, as it dictates molecular recognition through specific physical and chemical interactions (Akhtar et al. 2024). The results of the molecular interactions of ligands (*T. cordifolia* and *S. mombin* leaf extract compounds) with COX-1 and COX-2 are presented in Tables 3 and 4. The binding interactions include hydrogen bonding, hydrophobic interactions, polar contacts, and π-π stacking, all of which contribute to ligand stability within these enzymes' active sites.

Table 3 shows the ligand-protein amino acid interactions with COX-1. The 2D structures of Figures 3 and 5 show all forms of interactions, while the 3D interactions (Figures 4 and 6) show the H-bonding interactions with respective receptor (protein) residues. This can be compared with the standard, along with binding affinity (docking scores). The COX-1 standard NSAIDs, aspirin and diclofenac, did not

exhibit hydrogen bonding interactions but relied predominantly on hydrophobic interactions, particularly with residues such as VAL-116, LEU-352, and ALA-537. The strong hydrophobic interactions observed with the phytochemicals, especially apigenin and catechin, indicate their ability to fit into the COX-1 active site and possibly act as competitive inhibitors (Shahwan et al. 2023). Furthermore, π–π stacking interactions were observed in catechin and luteolin with TYR-385 and TYR-355. Catechin, luteolin, and myricetin exhibit hydrogen bond, hydrophobic bond, polar, and π-π stacking interactions, whereas apigenin, kaempferol, and quercetin exhibit only hydrogen bond, hydrophobic bond, and polar interactions. Apigenin and kaempferol formed hydrogen bonds with MET-522 and TYR-385, both of which are crucial for the catalytic function of COX-1. Similarly, myricetin exhibited the highest number of hydrogen bonds, interacting with TYR-385, TYR-355, and ARG-120, suggesting enhanced stability within the enzyme's active site. Catechin formed a hydrogen bond with MET-522, and quercetin also formed hydrogen bonds with MET-522, TYR-355, reinforcing their potential to disrupt the enzyme's activity.

Table 3. Ligand-protein amino acid interactions with COX-1 (3N8Y)

Ligand	Type of interaction & protein residues			
	H-bonding	Hydrophobic	Polar	π–π stacking
Aspirin	-	VAL-116, LEU-352, LEU-359, ALA-537, LEU534, TRP-387	SER-353, SER-530	-
Diclofenac	-	VAL-116, LEU-534, ALA-527, MET-522, LEU-531, TYR-355	SER-353, SER-530	-
Apigenin	MET-522, TYR-385	ILE-523, LEU-359, VAL-116, ALA-527	SER-353, SER-530	-
Catechin	MET-522	MET-113, LEU-531, ALA-527, TYR-355	SER-353, SER-530	TYR-385
Kaempferol	TYR-385, MET-522	ALA-527, ILE-532, VAL-116, LEU-531	SER-353, SER-530	-
Luteolin	TYR-385	LEU-359, VAL-349, VAL-116, PHE-516	SER-353, SER-530	TYR-355
Myricetin	TYR-385, TYR-355, ARG-120	LEU-352, VAL-349, LEU-534, PHE-205, ALA-527, ILE-523	SER-353, SER-530	TYR-355
Quercetin	TYR-385, MET-522	VAL-116, LEU-531, ALA-527, PHE-518	SER-353, SER-530	-

Table 4. Ligand-protein amino acid interactions with COX-2 (3LN1)

Ligand	Type of interaction and protein residues				
	H-bonding	Hydrophobic	Polar	π–π Stacking	π– Cation
Aspirin	-	LEU-338, VAL-335, MET-508, VAL-509, ALA-513, LEU-517	SER-339, SER-516	-	-
Diclofenac	TYR-371	PHE-504, MET-508, VAL-509, ALA-513, LEU-517, VAL-335	SER-339, SER-516	TRP-373	-
Apigenin	ARG-106	LEU-517, ALA-513, VAL-335, ALA-502	SER-339, SER-516, HIE-75, GLN-178	-	-
Catechin	LEU-338	TYR-341, VAL-102, LEU-345, VAL-335	SER-339, SER-516, HIE-75, GLN-178	-	ARG-106
Kaempferol	-	VAL-509, ALA-502, LEU-517, VAL-335	SER-339, SER-516, HIE-75, GLN-178	-	ARG-106
Myricetin	LEU-338	TYR-341, VAL-335, ALA-513, LEU-517	SER-516, GLN-178, SER-339, -HIE-75	-	-
Luteolin	LEU-338	TYR-341, VAL-335, ALA-513, LEU-517	SER-339, SER-516, HIE-75, GLN-178	-	ARG-106
Quercetin	LEU-338	TYR-341, ILE-503, VAL-335, LEU-517	SER-339, SER-516, HIE-75, GLN-178	-	ARG-106

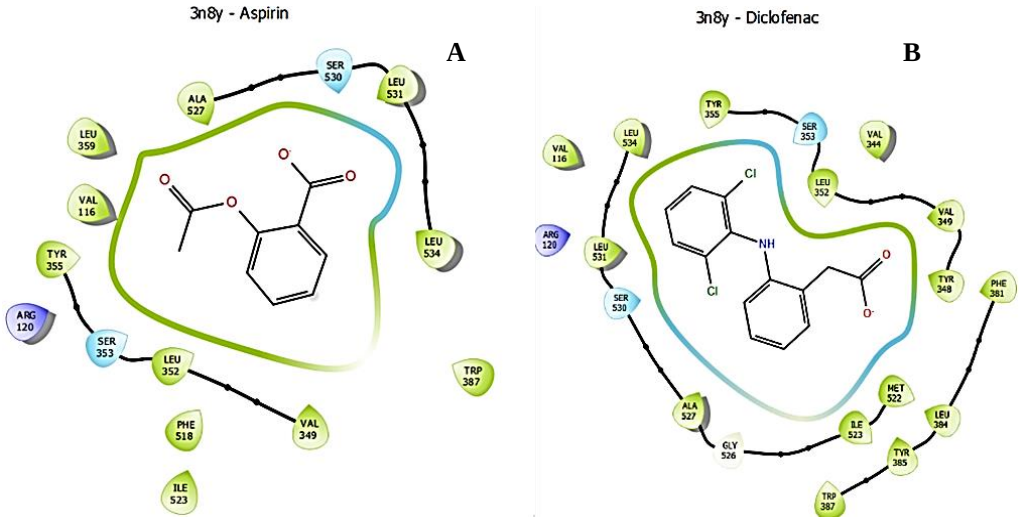

Figure 3. 2D interactions of standard compounds with 3N8Y. A. Aspirin, B. Diclofenac

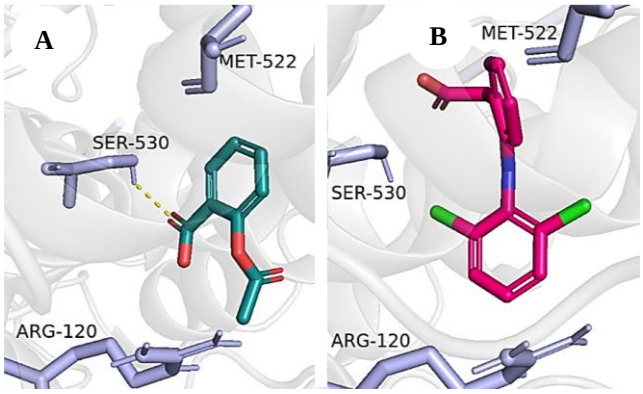

Figure 4. 3D interactions with COX-1(3N8Y). Standard compounds: A. Aspirin; B. Diclofenac

Table 4 shows the ligand-protein amino acid interactions with COX-2 (3LN1). The 2D structures of Figures 7 and 9 show all forms of interactions, while the 3D interactions (Figures 8 and 10) show the H-bonding interactions with respective receptor (protein) residues. Aspirin exhibited strong hydrophobic interactions with amino residues such as LEU-338, VAL-335 and MET-508 but lacked hydrogen bonding, which may explain its relatively weaker binding affinity. Diclofenac, in contrast, formed a hydrogen bonding with TYR-371 and a π-π stacking interaction with TRP-373, contributing to its enhanced stability within the active site. Among the phytochemicals, apigenin interacted with ARG-106 via hydrogen bonding, as well as hydrophobic interactions with LEU-517, ALA-513, and VAL-335. Similarly, catechin engaged in multiple hydrophobic interactions with TYR-341, VAL-102, and LEU-345, alongside a unique π-cation interaction with ARG-106, enhancing its binding stability.

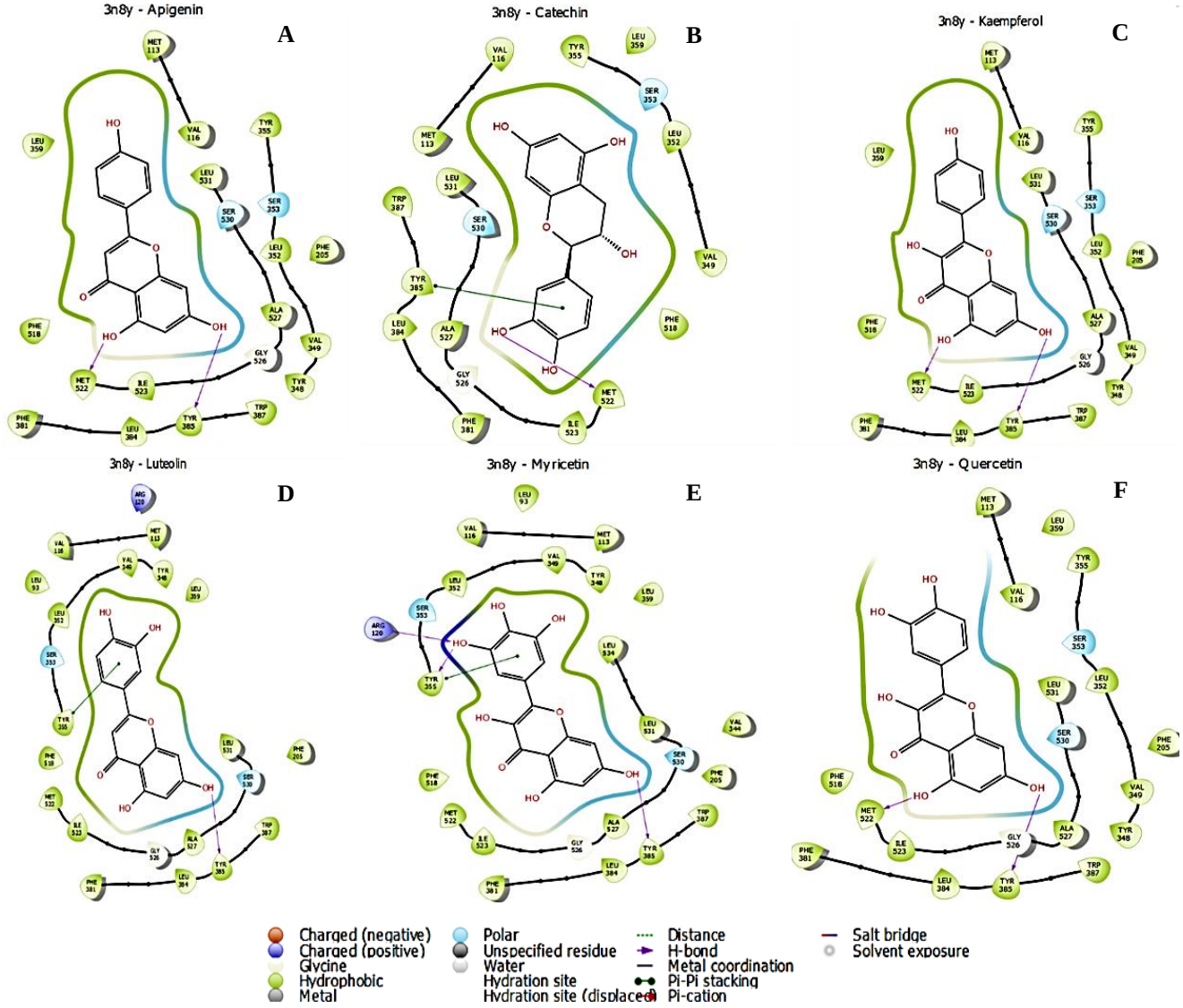

Figure 5. 2D interactions of phytochemicals present in both plants with COX-1(3N8Y). A. (apigenin, catechin, kaempferol, luteolin, myricetin, quercetin)

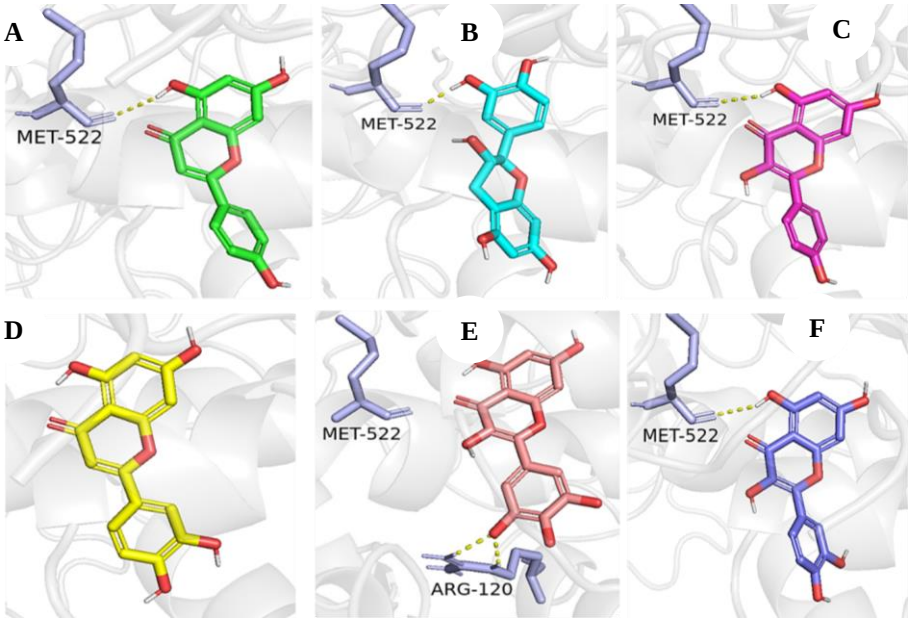

Figure 6. 3D interactions of phytochemicals present in both plants with COX-1 (3N8Y). A. Apigenin; B. Catechin; C. Kaempferol; D. Luteolin; E. Myricetin; F. Quercetin

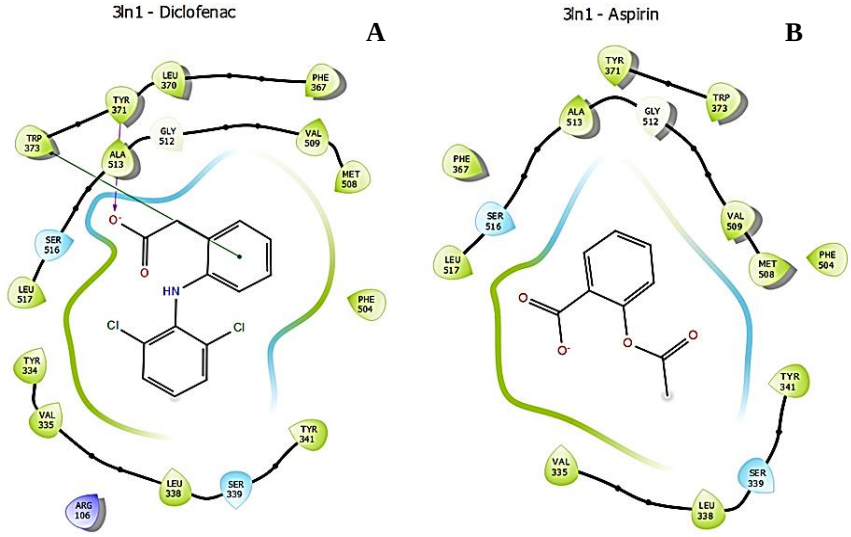

Figure 7. 2D interactions of standard compounds with COX-2 (3LN1)

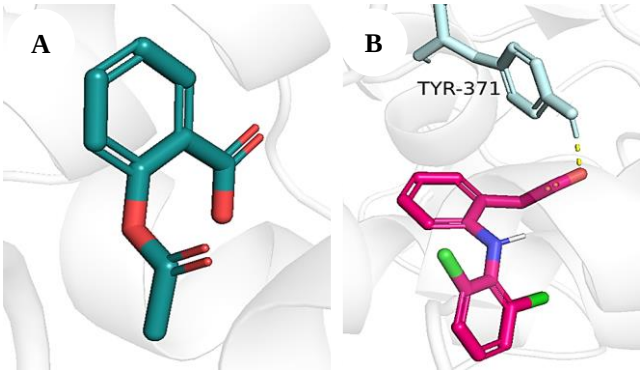

Figure 8. 3D interactions with COX-2 (3LN1). Standard compounds: A. Aspirin; B. Diclofenac

Hydrophobic synergy is the main aspect of the firmness of proteins. Hydrogen bonding further maintains protein firmness, yet to a minimized degree than hydrophobic synergy (Bandaru et al. 2021). The presence of strong hydrophobic interactions and hydrogen bonding in both COX-1 and COX-2 binding studies suggests that these phytochemicals have high affinity for their target enzymes. In addition, analysis of the binding interactions of these phytochemicals and standard NSAIDs suggests that myricetin demonstrates the highest potential for COX inhibition due to its extensive hydrogen bonding and hydrophobic interactions. Apigenin and catechin also exhibited strong interactions with key COX-1 and COX-2 residues, suggesting their dual-inhibition potential. The ability of these compounds to engage in multiple interaction types, including π–π stacking, hydrophobic contacts, and hydrogen bonding, reinforces their suitability as alternative anti-inflammatory agents (Deogratias et al. 2022; Prohens et al. 2025).

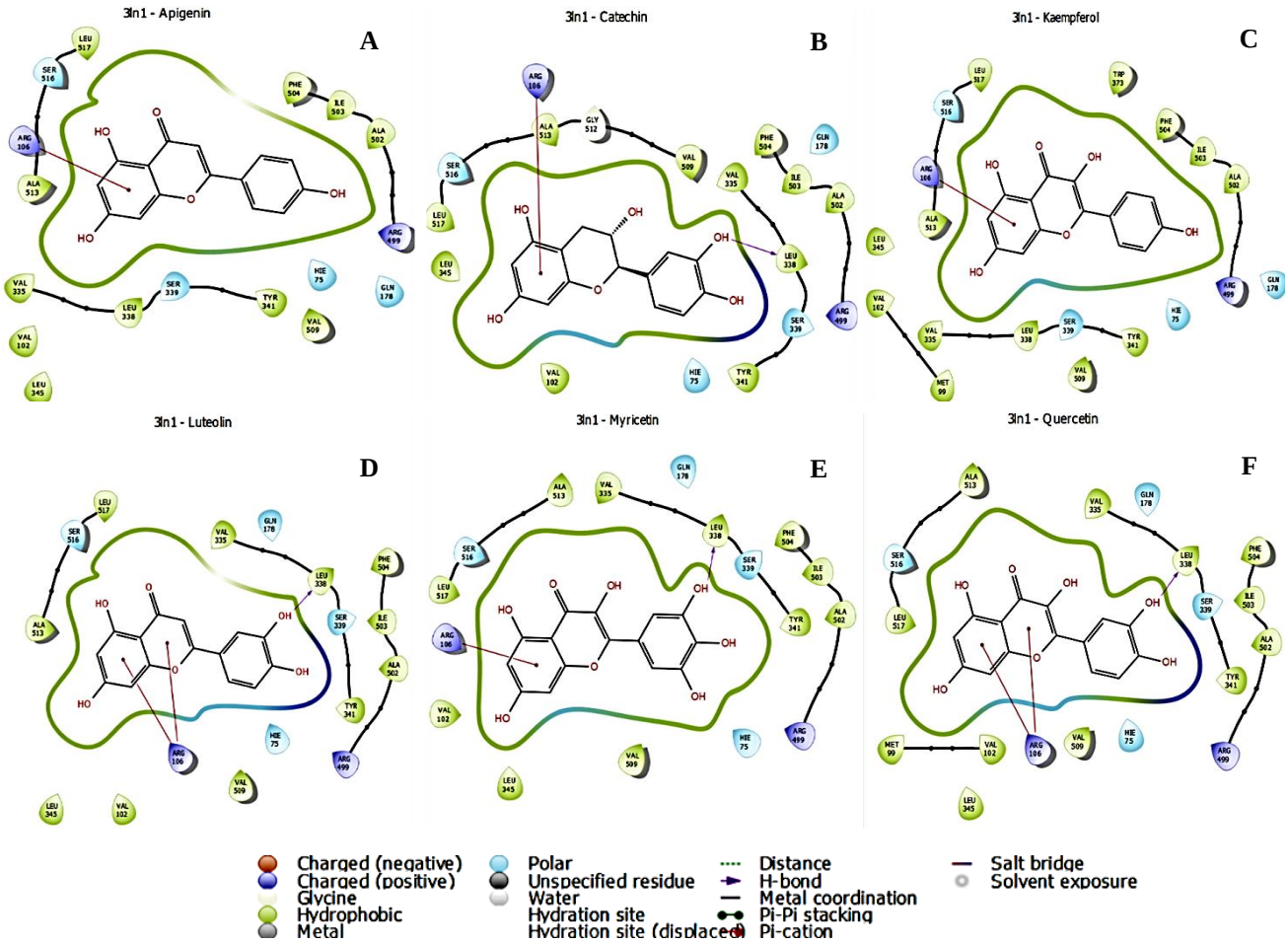

Figure 9. 2D interactions of phytochemicals present in both plants with COX-2 (3LN1). A. Apigenin, B. Catechin, C. Kaempferol, D. Luteolin, E. Myricetin, F. Quercetin

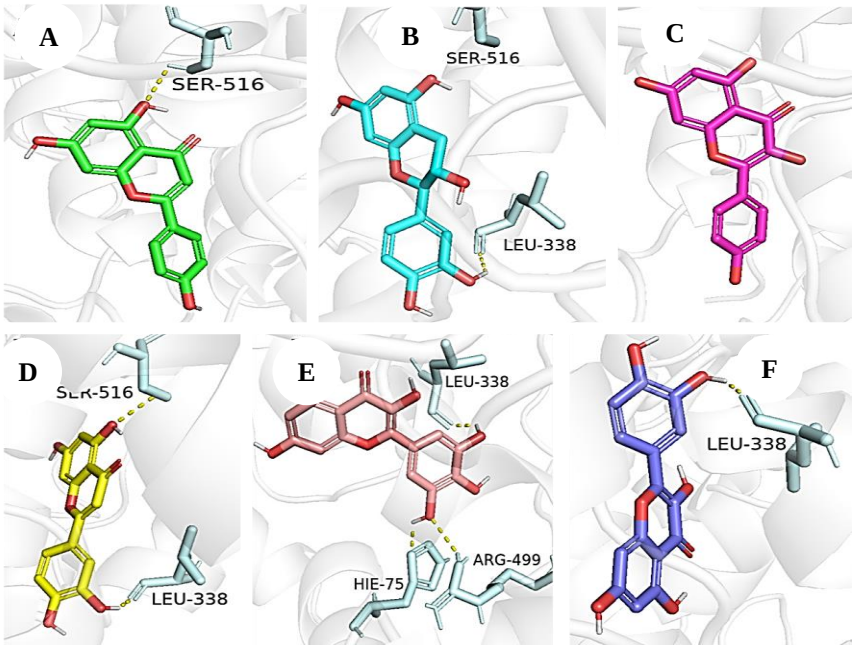

Figure 10. 3D interactions of phytochemicals present in both plants with COX-2 (3LN1). A. Apigenin; B. Catechin; C. Kaempferol; D. Luteolin; E. Myricetin; F. Quercetin

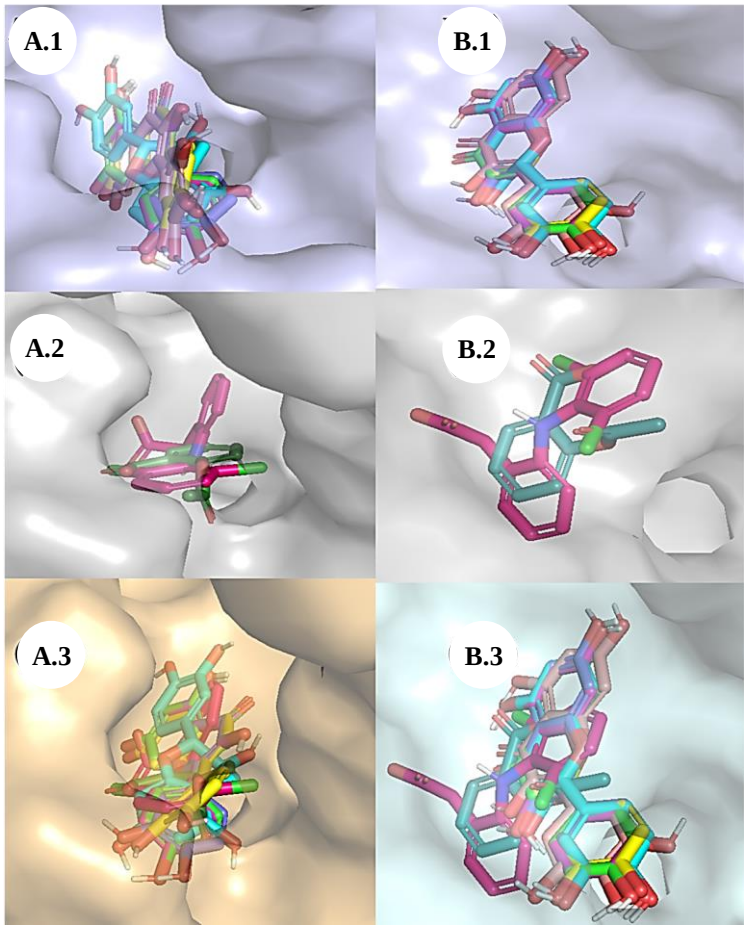

Figure 11. Binding modes with COX-1 (3N8Y). A.1. Phytochemicals: apigenin, catechin, kaempferol, luteolin, myricetin, quercetin; A.2. Standard compounds (aspirin, and diclofenac); A.3. Combined binding pose. Binding modes with COX-2 (3LN1), B.1. Phytochemicals; apigenin, catechin, kaempferol, luteolin, myricetin, quercetin; B.2. Standard compounds: aspirin and diclofenac; B.3. Combined binding poses

Figure 11 illustrates the interaction patterns of selected phytochemicals and reference compounds with the two COX enzyme structures (3N8Y and 3LN1). For COX-1 (3N8Y), phytochemicals such as apigenin, catechin, kaempferol, luteolin, myricetin, and quercetin are predicted to bind at the enzyme's active site, forming hydrogen bonds with key residues (Arg120, Tyr355, Ser530) essential for COX-1 inhibition. Notably, quercetin and myricetin interact with the catalytic Tyr385, interfering with arachidonic acid metabolism (Bai and Zhu 2010). Meanwhile, apigenin and kaempferol bind near the hydrophobic region (Val523, Leu352), resembling the mechanism of selective COX-1 inhibitors like celecoxib (Mandery et al. 2010). Research supports that these flavonoids act as competitive inhibitors, with quercetin exhibiting stronger binding due to its additional hydroxyl groups (Wang et al. 2020). In contrast, aspirin inhibits COX-1 irreversibly by acetylating Ser530, targeting the enzyme's channel entrance (Roth et al. 2020), while diclofenac binds to Arg120/Tyr355, mimicking arachidonic acid (Giménez-Bastida et al. 2019), with its carboxylate group playing a key role in ionic interactions. The combined binding pose suggests a potential synergistic effect, where phytochemicals like quercetin and diclofenac may simultaneously block catalytic and allosteric sites, enhancing inhibition.

For COX-2 (3LN1), a mutated form of the enzyme, binding affinities may vary. For example, luteolin exhibits stronger interactions due to increased conformational flexibility (Song et al. 2022), while catechin (being less polar than myricetin) favors hydrophobic subsites like Leu384. Aspirin shows reduced efficacy in 3LN1 because of Ser530 mutations (Giménez-Bastida et al. 2019), and diclofenac maintains binding but with diminished affinity due to disrupted salt bridges in the altered active site (Sharma et al. 2012). The combined binding strategy suggests that pairing kaempferol with aspirin could help overcome mutation-induced resistance. This analysis highlights the distinct binding mechanisms of phytochemicals and standard drugs, emphasizing their potential for synergistic COX-2 inhibition and drug resistance mitigation.

Interactions of flavonoids with COX-1 and COX-2

Flavonoids are a diverse class of polyphenolic compounds present in fruits, vegetables, and medicinal plants, and have gained considerable attention for their anti-inflammatory properties. Their effects are primarily attributed to interactions with cyclooxygenase enzymes, COX-1 and COX-2, which play a crucial role in

prostaglandin synthesis and the regulation of inflammation. Studies have demonstrated that specific flavonoids inhibit both COX-1 and COX-2 enzymes, leading to a decrease in pro-inflammatory prostaglandin production. For instance, Ribeiro et al. (2015) reported that flavonoids possessing a catechol moiety effectively inhibit COX enzymes and modulate cytokine production in human whole blood. Their findings indicated that flavonoids containing a catechol group in the B ring were particularly effective in simultaneously inhibiting the production of inflammatory prostaglandin E_2 (PGE_2) and pro-inflammatory cytokines, emphasizing the importance of specific structural features in their anti-inflammatory efficacy. This suggests that specific structural features, such as the catechol moiety, are critical determinants of their anti-inflammatory efficacy. Further studies have highlighted that the presence of a 4-oxo group in the C-ring, along with a 3′,4′-dihydroxy (catechol) structure in the B-ring, enhances the suppression of COX-2 transcriptional activity. These structural attributes contribute to the flavonoids' ability to modulate inflammatory responses effectively (Shamsudin et al. 2022). Beyond direct enzymatic inhibition, flavonoids such as nobiletin, amentoflavone, and apigenin have been observed to modulate COX-2 gene expression in various cellular systems. This dual ability to suppress COX-2 expression and inhibit its enzymatic activity underscores the multifaceted role of flavonoids in modulating inflammatory responses. The modulation of cyclooxygenase-2 (COX-2) expression by flavonoids is indeed context-dependent, varying with experimental conditions. A study by Chagas et al. (2022) investigated the effects of nine flavonoids on COX-2 expression in intestinal epithelial cells (IEC18). Under basal conditions, certain flavonoids increased COX-2 expression and activated NF-κB-dependent gene transcription. However, upon lipopolysaccharide (LPS) stimulation, the impact of flavonoids on COX-2 levels varied: some increased, others decreased, and some had no effect. This variability underscores the complex interactions between flavonoids and inflammatory pathways, influenced by the specific flavonoid structure and the cellular environment (Chagas et al. 2022). The structural characteristics of flavonoids significantly influence their interaction with cyclooxygenase (COX) enzymes, particularly in their anti-inflammatory activities. However, it's important to note that not all flavonoids uniformly inhibit COX enzymes. Some, such as myricetin and quercetin, have been reported to stimulate COX activity under certain conditions, indicating that the interaction between flavonoids and COX enzymes can be complex and context-dependent (D'Ambrosio et al. 2021). Hence, flavonoids' anti-inflammatory efficacy is closely linked to their structural characteristics, particularly the presence of catechol groups and other functional moieties that influence their interaction with COX enzymes.

In conclusion, the findings from this study highlight the potential of phytochemicals from *T. cordifolia* and *S. mombin* as promising COX-1 and COX-2 inhibitors. All tested compounds complied with Lipinski's Rule of Five, indicating their suitability for oral administration with favorable pharmacokinetic properties. Molecular docking results revealed that apigenin, catechin, quercetin, and luteolin exhibited strong binding affinities to COX-1 and COX-2, in some cases outperforming the standard NSAIDs, as aspirin and diclofenac. The ligand efficiency analysis further suggested that apigenin and catechin could serve as lead compounds due to their optimal balance between molecular size and binding affinity. These phytochemicals interacted with key residues via hydrogen bonding, hydrophobic forces, and π-π stacking, enhancing their stability within the enzyme active sites. These findings suggest that phytochemicals from *T. cordifolia* and *S. mombin* possess strong inhibitory potential against COX-1 and COX-2, highlighting their promise as natural anti-inflammatory agents. The need for further *in vitro* and *in vivo* studies is recommended to confirm their pharmacological efficacy and therapeutic potential.

While docking scores provide valuable insights into molecular interactions, they cannot fully predict in vivo effectiveness because they do not account for critical factors such as metabolic stability and cellular uptake. To verify these computational results, further experimental studies, such as enzymatic inhibition assays, are essential. These findings indicate that phytochemicals, particularly apigenin and quercetin, exhibit strong potential as COX inhibitors, with binding efficiencies rivaling conventional drugs. Further research into their selectivity could pave the way for more precise anti-inflammatory treatments.

REFERENCES

Afroz Shoily MS, Islam ME, Rasel NM, Parvin S, Barmon J, Hasan Aqib A, Nath Roy D, Parvin MS. 2025. Unveiling the biological activities of *Heliotropium indicum* L. plant extracts: Anti-inflammatory activities, GC-MS analysis, and *in-silico* molecular docking. Sci Rep 15 (1): 3285. DOI: 10.1038/s41598-024-79559-w.

Agu PC, Afiukwa CA, Orji OU, Ezeh EM, Ofoke IH, Ogbu CO, Ugwuja EI, Aja PM. 2023. Molecular docking as a tool for the discovery of molecular targets of nutraceuticals in diseases management. Sci Rep 13: 13398. DOI: 10.1038/s41598-023-40160-2.

Ajaegbu EE, Uzochukwu IC, Okoye FBC. 2022. Antioxidant and anti-inflammatory activities of extract and fractions of *Spondias mombin* leaf and isolation of its active principles. Trop J Nat Prod Res 6 (1): 80-86. DOI: 10.26538/tjnpr/v6i1.15.

Ajoko IT, Amos-Tautua BMW, Bamgbade EO. 2023. HPLC analysis and anti-inflammatory effect of methanol extract of the leaves of *Triumfetta cordifolia* A. Rich. (Malvaceae) available in Bayelsa State, Nigeria. Sch Intl J Chem Mater Sci 6 (6): 115-125. DOI: 10.36348/sijcms.2023.v06i06.001.

Ajoko IT, Amos-Tautua BMW, Songca SP. 2020. Ethnomedicinal and economical profile of *Triumfetta cordifolia*: A mini review. J Med Plants Stud 8 (5): 208-212.

Akhtar R, Dharumadurai D, Kumar TS. 2024. Novel antifungal compound from *Prunella vulgaris*: An *in-silico* approach towards the discovery of potent inhibitor to combat phytopathogenic fungi. Biocatal Agric Biotechnol 58: 103187. DOI: 10.1016/j.bcab.2024.103187.

Ali KA, Maity A, Roy SD, Pramanik SD, Das PP, Shaharyar MA. 2023. Insight into the mechanism of steroidal and non-steroidal anti-inflammatory drugs. In How Synthetic Drugs Work (pp. 61-94). Academic Press. DOI: 10.1016/B978-0-323-99855-0.00004-X.

Amos-Tautua BM, Ajoko IT, Ebong CU. 2025. Phytocompounds profiling and assessment of the antioxidant and anti-inflammatory efficacies of *Spondias mombin* (Linn) leaf extracts. South Asian Res J Nat Prod 8 (1): 1-20. DOI: 10.9734/sarjnp/2025/v8i1159.

Baba H, Bunu SJ. 2025. Spectroscopic, and molecular docking analysis of phytoconstituent isolated from *Solenostemon monostachyus* as potential cyclooxygenase enzymes inhibitor. Intl J Chem Res 9 (1): 1-6. DOI: 10.22159/ijcr.2025v9i1.241.

Bai HW, Zhu BT. 2010. Myricetin and quercetin are naturally occurring co-substrates of cyclooxygenases *in vivo*. Prostaglandins Leukot Essent Fatty Acids 82 (1): 45-50. DOI: 10.1016/j.plefa.2009.10.006.

Bandaru N, Prasanth DSNBK, Reddy AR, Rao GSNK, Nemmani KVS, Rao AN. 2021. *In-silico* molecular docking studies of some isolated phytochemicals from *Biophytum veldkampii* against cyclooxygenase-ii enzyme and *in vivo* anti-inflammatory activity. Pharmacogn Res 13 (4): 192-198. DOI: 10.5530/pres.13.4.11.

Bunu SJ, Okei JO, Miediegha O, Ebeshi BU, Chukwuemerie OL 2023. Assessment of secondary metabolites and thin-layer chromatographic analysis of *Carica papaya* (Caricaceae) leaves ethanolic extract. J Pharm Res Intl 35 (36): 21-28. DOI: 10.9734/jpri/2023/v35i367489.

Chagas MdSS, Behrens MD, Moragas-Tellis CJ, Penedo GXM, Silva AR, Gonçalves-de-Albuquerque CF. 2022. Flavonols and flavones as potential anti-inflammatory, antioxidant, and antibacterial compounds. Oxid Med Cell Longev 2022 (1): 9966750. DOI: 10.1155/2022/9966750.

Chen W, Zhong Y, Feng N, Guo Z, Wang S, Xing D. 2021. New horizons in the roles and associations of COX-2 and novel natural inhibitors in cardiovascular diseases. Mol Med 27 (1): 123. DOI: 10.1186/s10020-021-00358-4.

D'Ambrosio M, Bigagli E, Cinci L, Gori A, Brunetti C, Ferrini F, Luceri C. 2021. Ethyl acetate extract from *Cistus x incanus* L. leaves enriched in myricetin and quercetin derivatives, inhibits inflammatory mediators and activates Nrf2/HO-1 pathway in LPS-stimulated RAW 264.7 macrophages. Z Naturforsch C J Biosci 76 (1-2): 79-86. DOI: 10.1515/znc-2020-0053.

Deogratias G, Shadrack DM, Munissi JJE, Kinunda GA, Jacob FR, Mtei RP, Masalu RJ, Mwakyula I, Kiruri LW, Nyandoro SS. 2022. Hydrophobic π-π stacking interactions and hydrogen bonds drive self-aggregation of luteolin in water. J Mol Graph Model 116: 108243. DOI: 10.1016/j.jmgm.2022.108243.

Giménez-Bastida JA, Boeglin WE, Boutaud O, Malkowski MG, Schneider C. 2019. Residual cyclooxygenase activity of aspirin-acetylated COX-2 forms 15R-prostaglandins that inhibit platelet aggregation. FASEB J 33 (1): 1033-1041. DOI: 10.1096/fj.201801018R.

Haritha M, Sreerag M, Suresh CH. 2024. Quantifying the hydrogen-bond propensity of drugs and its relationship with Lipinski's rule of five. New J Chem 48 (11): 4896-4908. DOI: 10.1039/d3nj05476d.

Hopkins AL, Keserü GM, Leeson PD, Rees DC, Reynolds CH. 2014. The role of ligand efficiency metrics in drug discovery. Nat Rev Drug Discov 13 (2): 105-121. DOI: 10.1038/nrd4163.

Ikponmwosa-Eweka O, Omoregie ES. 2024. Characterization of the phytochemical constituents of methanol extract of *Spondias mombin* stem bark using high performance-liquid chromatography and gas chromatography mass spectroscopy. Scientia Africana 23 (3): 47-58. DOI: 10.4314/sa.v23i3.5.

Jemal K. 2019. Molecular docking studies of phytochemicals of *Allophylus serratus* against cyclooxygenas2enzyme. BioRxiv 866152. DOI: 10.1101/866152.

Li Y, Yao J, Han C, Yang J, Chaudhry MT, Wang S, Liu H, Yin Y. 2016. Quercetin, inflammation and immunity. Nutrients 8 (3): 167. DOI: 10.3390/nu8030167.

Lipinski CA. 2004. Lead-and drug-like compounds: The rule-of-five revolution. Drug Discov Today Technol 1 (4): 337-341. DOI: 10.1016/j.ddtec.2004.11.007.

Listyani TA, Addawiyyah M, Raharjo D, Chyang PJ. 2024. Docking and structural modification of flavonoid derivative compounds as cycloxygenas-2 enzyme inhibitors. Indones J Glob Health Res 7 (1): 311-322. DOI: 10.37287/ijghr.v7i1.4041.

Maddipati KR. 2020. Non-inflammatory physiology of "inflammatory" mediators–Unalamation, a new paradigm. Front Immunol 11: 580117. DOI: 10.3389/fimmu.2020.580117.

Maestro release 2020-3. Schrödinger. LLC, New York, NY, USA, 2020.

Mandery K, Bujok K, Schmidt I, Keiser M, Siegmund W, Balk B, König J, Fromm MF, Glaeser H. 2010. Influence of the flavonoids apigenin, kaempferol, and quercetin on the function of organic anion transporting polypeptides 1A2 and 2B1. Biochem Pharmacol 80 (11): 1746-1753. DOI: 10.1016/j.bcp.2010.08.008.

Na'imah J. 2019. In silico study of COX-2 on indomethacin and diclofenac as nonsteroidal anti-inflammatory drugs (NSAIDs). Farmasains: Jurnal Farmasi dan Ilmu Kesehatan 4 (1): 31-36. DOI: 10.22219/farmasains.v4i1.7767.

Nasim N, Sandeep IS, Mohanty S. 2022. Plant-derived natural products for drug discovery: Current approaches and prospects. Nucleus (Calcutta) 65 (3): 399-411. DOI: 10.1007/s13237-022-00405-3.

Nwankwo OL, Chukwuebuka OC, Collins OO, Samuel BJ, Obasi JC, Iloh ES, Nwankwo EO. 2021. Quantitative phytochemical analysis of the fungus endophytic extracts isolated from *Azadirachta indica* using gas chromatography flame ionization detector. J Drug Deliv Ther 11 (5): 80-83. DOI: 10.22270/jddt.v11i5.4999.

Pinzi L, Rastelli G. 2019. Molecular docking: Shifting paradigms in drug discovery. Intl J Mol Sci 20 (18): 4331. DOI: 10.3390/ijms20184331.

Prohens R, Barbas R, Abrego G, Frontera A. 2025. Interplay of hydrogen bonding and π-stacking interactions in the solid-state architecture of pranoprofen: Insights from X-ray crystallography and computational analyses. CrystEngComm 27: 1742-1748. DOI: 10.1039/d4ce01279h.

Puspa VR, Zumaidar, Nurdin N, Fitmawati. 2024. Phytochemical, antioxidant, and *in-silico* studies of *Erigeron sumatrensis* from Gayo Highlands as a potential inhibitor of type-2 diabetes mellitus. Biodiversitas 25 (7): 3179-3192. DOI: 10.13057/biodiv/d250739.

Ribeiro D, Freitas M, Tomé SM, Silva AM, Laufer S, Lima JL, Fernandes E. 2015. Flavonoids inhibit COX-1 and COX-2 enzymes and cytokine/chemokine production in human whole blood. Inflammation 38 (2): 858-870. DOI: 10.1007/s10753-014-9995-x.

Rouzer CA, Marnett LJ. 2020. Structural and chemical biology of the interaction of cyclooxygenase with substrates and non-steroidal anti-inflammatory drugs. Chem Rev 120 (15): 7592-7641. DOI: 10.1021/acs.chemrev.0c00215.

Saravanan KM, Zhang H, Senthil R, Vijayakumar KK, Sounderrajan V, Wei Y, Shakila H. 2020. Structural basis for the inhibition of SARS-CoV_2 main protease by Indian medicinal plant-derived antiviral compounds. J Biomol Struct Dyn 40 (5): 1970-1978. DOI: 10.1080/07391102.2020.1834457.

Shahwan M, Anwar S, Yadav DK, Khan MS, Shamsi A. 2023. Experimental and computational insights into the molecular interactions between human transferrin and apigenin: Implications of natural compounds in targeting neuroinflammation. ACS Omega 8 (49): 46967-46976. DOI: 10.1021/acsomega.3c06799.

Shamsudin NF, Ahmed QU, Mahmood S, Shah SAA, Sarian MN, Khattak MMAK, Khatib A, Sabere ASM, Yusoff YM, Latip J. 2022. Flavonoids as antidiabetic and anti-inflammatory agents: A review on structural activity relationship-based studies and meta-analysis. Intl J Mol Sci 23 (20): 12605. DOI: 10.3390/ijms232012605.

Sharma R, Choudhary S, Kishore N. 2012. Insights into the binding of the drugs diclofenac sodium and cefotaxime sodium to serum albumin: Calorimetry and spectroscopy. Eur J Pharm Sci 46 (5): 435-445. DOI: 10.1016/j.ejps.2012.03.007.

Sidhu RS, Lee JY, Yuan C, Smith WL. 2010. Comparison of cyclooxygenase-1 crystal structures: Cross-talk between monomers comprising cyclooxygenase-1 homodimers. Biochemistry 49 (33): 7069-7079. DOI: 10.1021/bi1003298.

Song MT, Wang WZ, Lu Y, Han RM, Skibsted LH, Zhang JP. 2022. Double-site binding and anti-/pro-oxidation of luteolin on bovine serum albumin mediated by copper (II) coordination. ACS Omega 7 (23): 19521-19534. DOI: 10.1021/acsomega.2c01226.

Tai FWD, McAlindon ME. 2021. Non-steroidal anti-inflammatory drugs and the gastrointestinal tract. Clin Med (Lond) 21 (2): 131-134. DOI: 10.7861/clinmed.2021-0039.

Verma U. 2020. The cellular and molecular targets of cox-2 induced PGE2 during different stages of embryonic development of chick of domestic hen. [Doctoral Dissertation]. Maharaja Sayajirao University, Baroda, India.

Wang JL, Limburg D, Graneto MJ, Springer J, Hamper JR, Liao S, Pawlitz JL, Kurumbail RG, Maziasz T, Talley JJ, Kiefer JR, Carter J. 2010. The novel benzopyran class of selective cyclooxygenase-2 inhibitors. Part 2: The second clinical candidate having a shorter and favorable human half-life. Bioorg Med Chem Lett 20 (23): 7159-7163. DOI: 10.1016/j.bmcl.2010.07.054.

Xiao X, Shi D, Liu L, Wang J, Xie X, Kang T, Deng W. 2011. Quercetin suppresses cyclooxygenase-2 expression and angiogenesis through inactivation of P300 signaling. PloS One 6 (8): e22934. DOI: 10.1371/journal.pone.0022934.

Yang R, Dong Y, Gao F, Li J, Stevanovic ZD, Li H, Shi L. 2023. Comprehensive analysis of secondary metabolites of four medicinal thyme species used in folk medicine and their antioxidant activities *in vitro*. Molecules 28 (6): 2582. DOI: 10.3390/molecules28062582.

Zaragozá C, Álvarez-Mon MÁ, Zaragozá F, Villaescusa L. 2022. Flavonoids: Antiplatelet effect as inhibitors of COX-1. Molecules 27 (3): 1146. DOI: 10.3390/molecules27031146.

ASIAN J TROP BIOTECHNOL
Volume 22, Number 1, June 2025
Pages: 41-47

ISSN: 0216-6887
E-ISSN: 2301-8658
DOI: 10.13057/biotek/c220106

High macronutrient dietary composition modifies biophysical and biochemical indices in male Wistar rats

ADEBAYO ADETOLA AMBALLI[1,♥], WASIU ENIOLA OLOOTO[1], MARIA OLUWABUNMI ALADESUSI[1], IBRAHIM ABIDEMI OGUNFOLU[2], ADEDEJI AGBOOLA ONAYEMI[1]

[1]Department of Chemical Pathology and Immunology, Faculty of Basic Medical Sciences, Olabisi Onabanjo University. Sagamu, Ogun State, Nigeria. Tel.: +234-803-3534252, ♥email: Amballi.adebayo@oouagoiwoye.edu.ng

[2]Department of Medical Laboratory Science, School of Specialised Health and Medical Technician, Ogun State College of Health Technology. PMB 2081, Ijebu-Ode, Ogun State, Nigeria

Manuscript received: 16 February 2025. Revision accepted: 7 June 2025.

Abstract. *Amballi AA, Olooto WE, Aladesusi MO, Ogunfolu IA, Onayemi AA. 2025. High macronutrient dietary composition modifies biophysical and biochemical indices in male Wistar rats. Asian J Trop Biotechnol 22: 41-47.* Nutrition is one of the most important factors to achieve and maintain a healthy status. This requires a balanced diet in terms of both the macronutrients and micronutrients. In Nigeria, there is a gradual transition from the traditional diet to Western diet. This is increasing the burden of non-communicable diseases and macronutrients play a major role. This study was designed to evaluate the effects of macronutrient composition on biophysical and biochemical indices using Wistar rat (*Rattus norvegicus* (Berkenhout, 1769)) as a pilot study. Twenty-five male Wistar rats weighing 26-46 g were randomly divided into 5 groups. Dietary composition was done, the rats were given feed and water *ad libitum*, weighing was done weekly for 8 weeks, and fasting blood samples were collected. Fasting blood glucose, lipid profile, liver and kidney function tests were conducted. In this study, the macronutrient caused increased body weight across all the groups with highest increase in the High Fat Diet (HFD) group, a tendency to cause increased body weight or obesity. Fasting Blood Sugar (FBS) was observed to increase significantly only in the HFD group, a tendency to cause Diabetes mellitus. A non-significant increase across the test groups was observed in the liver enzymes and total protein while a significant increase in albumin level was observed. However, no change was observed in the bilirubin levels across the test groups. A significant increase occurred in urea and creatinine in the HFD rats. Lipid profile in this study showed significant increase in triglycerides, cholesterol and low-density lipoprotein and a significant decrease in high-density lipoprotein among HFD-fed rats. The atherogenic and coronary risk indices were also significantly increased in HFD fed rats. No significant difference in the electrolytes. This study showed that HFD can predispose to risk factors of non-communicable diseases. Liver and kidney functions are not significantly disrupted.

Keywords: Health status, lipid profile, nutrition, obesity, Western diet

INTRODUCTION

Nutrition is one of the most important factors to achieve and maintain a healthy state. This requires the habitual intake of an adequate and balanced diet, which includes both the macronutrients and micronutrients. The macronutrients are needed in large amount in our body while the micronutrients are needed in little amounts, however they both have specific functions to maintain a good health status. The macronutrients (carbohydrates, proteins and lipids) majorly supply energy (calories) to the body and each has other specific functions while micronutrients are vitamins and minerals with their specific functions. Furthermore, the importance of hyperlipidaemia in health status must be emphasized because it plays a major role in the pathogenesis of cardiovascular disease. For clinical evaluation of cardiovascular disease it is important to estimate plasma lipid profile as well as the artherogenic and coronary risk indices (AI and CRI).

The principal energy source for normal cellular activities is derived from three major calorigenic nutrients (carbohydrates, proteins, and lipids), food fibers, and other organic compounds (Carreiro et al. 2016; Savarino et al. 2021). Lipids give about 9 kcal per gram; proteins and carbohydrates each give 4 kcal per gram; while fibers give less calories due to their low digestibility and absorption in the gastrointestinal tract (GIT) (Carreiro et al. 2016; El-Zayat et al. 2019; Morris and Mohiuddin 2023).

Changes in body weight over time are a measure of an imbalance between the energy content of ingested foods and energy expended on life maintenance and physical activities. The rate of calories released from foods for cellular and physical activities is a function of the rate of glucose, amino acids, and fatty acid production, which are combustible metabolic fuels needed for energy generation. The availability of these units of metabolic fuel is dependent on factors like the glycemic index of ingested macronutrients, GIT motility and transition period, absorptive state of GIT epithelial surfaces, presence of anti-nutrients in ingested foods, availability of micronutrients that serve as cofactors for metabolically active enzymes, the rate of gastric emptying, and health status of individuals. The changes in body weight over time causes underweight, overweight or obesity, which are results of either undernutrition or overnutrition. The indicators of nutritional status (underweight, overweight and obesity) are changing in

Low-to-Middle-Income-Countries (LMICs) (Ahmed et al. 2020). Both undernutrition and overnutrition appear to be a growing burden on LMICs (Abdullah 2015). This growing burden is due to transition from traditional diet (high-fiber diets) to western-style diet (fast foods rich in sugar and fat). Unhealthy dietary habit is a major contributor to the burden of non-communicable diseases. Non-communicable diseases such as chronic respiratory diseases, cardiovascular disease, cancer, and diabetes mellitus are the primary causes of death in African countries with lower incomes, such as Nigeria (Gowshall and Taylor-Robinson 2018; Mapis 2020). Obesity among children is a growing concern, and children in LMICs are exposed to an unhealthy diet high in sugar and fat (Jaacks et al. 2017). These children face the danger of developing chronic diseases later in life.

Excessive intake of protein, carbohydrate, or fat in the form of energy-dense, highly processed foods and a lack of physical activity contribute to obesity-related diseases and obesity (e.g., insulin resistance, hyperlipidemias, cardiovascular disease, and cancer) (Seidelmann et al. 2018). In this circumstance, changes in energy balance, and biochemical entities are expected. A study in a Nigerian community has reported that dietary indiscretion (Western-style fast foods), poor health care funding, endemic poverty and lack of quality care to those with Non-Communicable Diseases (NCDs) are factors causing the increasing prevalence of NCDs in Nigeria (Oso 2023). Other studies have highlighted the level of financial hardship experienced by households with NCDs in Nigeria due to out-of-pocket expenses and lost productivity (Odunyemi et al. 2023).

The prevalences of hypertension, diabetes and dyslipidaemia vary amongst rural, semi-urban, and urban settings and were reported as 35.3%, 4.6% and 41.3% respectively in a community in Lagos State (Nigeria) (Idris et al. 2020). This highlights the need for researchers to tackle NCD burden. Non-Communicable Diseases (NCDs) cause about 71% of all deaths globally (equivalent to 41 million) each year and represent the leading cause of death worldwide (GBD 2016), and the four top killers are cardiovascular disease, cancer, respiratory diseases, and diabetes mellitus (GBD 2016; Bigna and Noubiap 2019). The threatening burden of NCDs in Sub-Saharan Africa has also been emphasized by some researchers (Gouda et al. 2019). The incidence of NCDs in Sub-Saharan Africa has been on an alarming increase in the past decades. It has been ascribed to the deliberate adoption of a Western diet pattern instead of a traditional diet (high-fiber diets), rich dietary pattern by Africans in general. Hence, adopting a healthy dietary pattern may aid in lowering the development of non-communicable disease (Ruthsatz and Candeias 2020). Important efforts are therefore needed to curb the burden of NCDs (Bigna and Noubiap 2019) and improve the well-being of people living with NCDs in the region. However, in the environment of this study which is a typical Nigerian community, there is no comprehensive study done to assess the effects of macronutrient dietary composition on biophysical and biochemical indices, which could be useful in guiding health policy makers and healthcare givers to improve the well-being of people living with NCDs and the public. This is the purpose of this study, although Wistar rats were used in this study because of the limiting factors in making use of humans.

MATERIALS AND METHODS

Procedures

Procurement and care of animals

Twenty-five healthy three-week-old male Wistar rats (*Rattus norvegicus* (Berkenhout, 1769)) weighing 26-46 g were procured from animal house at the Federal University of Agriculture Abeokuta. They housed (5 rats per cage) in the animal house of the Department of Anatomy, Olabisi Onabanjo University, under controlled lighting (12 h light/dark cycle, lights on 6:00). Each cage was floored with wood-shaven to accommodate animal urine and feces. All rats were provided with water and standard rat chow ad libitum for a week of acclimatization prior to the dietary manipulation. Handling of the rats conformed to the National Research Ethics Committee Guidelines (NREC 2019).

Experimental design

The study is a longitudinal study involving a total of 25 male Wistar albino rats. The rats were then randomly divided into five groups after a week of acclimatization namely: controls, High Carbohydrate Diet (HCD), High Protein Diet (HPD), High Fat Diet (HFD) and an equal proportion of carbohydrate, protein, and fat (MN) groups. Each group contains 5 male Wistar rats as described: Group 1: Fed on standard rat chow and water *ad libitum*, Group 2: Fed on a high carbohydrate diet (powder form) consisting of 75% carbohydrate, Group 3: Fed on a high protein diet (powder form) consisting of 75% protein, Group 4: Fed on a high fat diet (semi-solid oily form) consisting of 75% fat, Group 5: Fed on a diet (powder form) consisting of 25% each of fat, protein, and carbohydrate.

The rats were allowed access to water ad libitum and the compounded feeds as indicated in group 2-5 for 8 weeks.

DIETS' composition and feeding

The composition of the diets was based on the guidelines for nutrient requirements of laboratory animals (Chukwudike et al. 2017). The feeds for the control and test groups were prepared from ingredients purchased from Forlard feed mills in Sagamu, Ogun State, Nigeria, according to the composition shown in Table 1.

Food and energy intake

Hence, 24 hours of total food intake were recorded daily, and body weight of rats in each group was measured weekly. Food intake (FI) values were calculated as the difference between the total food given (initial diet, Di) and the amount of food remaining per day (final diet, Df) divided by the number of rats in the cages: (FI (g) = (Di - Df) * 0.2) (Malta et al. 2014). Energy intake was calculated based on weekly food intake (g/100g body weight) and diet density (kcal/g).

Table 1. Nutrient requirement of laboratory rats

Ingredients (dry matter)	Control (g/kg)	HCD group (g/kg)	HPD group (g/kg)	HFD group (g/kg)	MN group (g/kg)
Maize	654.0 g	750.0 g	100.0 g	100.0 g	250.0 g
Soyabean meal	50.0 g	20.0 g	400.0 g	20.0 g	150.0 g
Fish meal 72%	20.0 g	10.0 g	200.0 g	10.0 g	20.0 g
FF soya	40.0 g	10.0 g	50.0 g	10.0 g	30.0 g
GNC	60.0 g	20.0 g	100.0 g	10.0 g	50.0 g
Soya oil	70.0 g	70.0 g	50.0 g	750.0 g	250.0 g
Corn bran	10.0 g	20.0 g	24.0 g	24.0 g	70.05 g
PKC	30.0 g	34.0 g	10.0 g	10.0 g	100.5 g
Bone meal	25.0 g	25.0 g	25.0 g	25.0 g	30.0 g
Limestone	5.0 g	5.0 g	5.0 g	5.0 g	10.0 g
Lysine	7.0 g	7.0 g	7.0 g	7.0 g	10.0 g
Methionine	4.5 g	4.5 g	4.5 g	4.5 g	5.0 g
Toxin binding	1.0 g	1.0 g	1.0 g	1.0 g	1.0 g
Enzyme binding	1.0 g	1.0 g	1.0 g	1.0 g	1.0 g
Salt	2.5 g	2.5 g	2.5 g	2.5 g	2.5 g
Vitamin premix	20 g	20 g	20 g	20 g	20 g
Metabolizable energy (Kcal/kg)	3484.05	3490.95	2962.15	7589.15	4253.79
Crude protein (%)	16.69	10.47	40.69	3.80	16.58

Specimen collection, preparation, and storage

At the expiration of 8 weeks, the rats were fasted overnight. Blood samples were collected through periorbital /orbital venous plexus bleeding into heparinized and plain bottles, centrifuged at 10,000 rpm for five minutes to obtain the plasma and serum respectively which were stored at -20°C until assayed.

Biochemical parameters

The collected specimens were analyzed for the biochemical parameters notably FPG, triglycerides, total cholesterol, HDLC, aspartate transaminase (AST), alanine transaminase (ALT), alkaline phosphatase (ALP), total protein, albumin, bilirubin, urea, and creatinine according to standard procedures (Jendrassik and Grof 1938; Kadish and Sternberg 1969; Anon 1970; Wybenga et al. 1971; Friedewald et al. 1972; Schettler and Nussel 1975; Nägele et al. 1984). The LDLC, and globulin were computed for all samples.

Data analysis

The statistical analysis on descriptive statistics and bar charts was done using SPSS software version 25 to describe and represent the variables studied. The obtained data showed normal distribution ($p = 0.764$), and thus an independent t-test was considered to compare the differences in mean between two groups while one-way ANOVA was used to compare differences in mean between more than two groups. The level of statistical difference was set at $p < 0.05$.

RESULTS AND DISCUSSION

Effects of dietary composition on weight

The result of the effects of dietary composition on weight among control and treatment groups, using the differences between initial weight as at week 0 and the final weight as at the end of week 8 across groups I-V, showed a weight increase (Table 2). The percentage increment in the weight in each group was observed to be 280% in the group fed on normal rat chow, 300% in the HCD-fed group, 250% in the HPD-fed group, 350% in the HFD-fed group, and 250% in the equal proportion diet fed group (Figure 1).

Effects of dietary composition on plasma hepatorenal markers

The result of plasma glucose showed an increase in FPG among HFD-fed rats and a decrease in FPG among HPD-fed rats. The result of hepatic function markers showed a non-significant ($p > 0.05$) increase in plasma AST, ALT, ALP and total protein, while a significant increase in albumin level was observed among all text groups when compared to the group fed on normal rat chow (Table 3). Also, a little or no change was observed in plasma total and conjugated bilirubin concentration among the test groups (Table 3). However, a significant increase ($p < 0.05$) in plasma urea ($p = 0.000$) and creatinine ($p = 0.030$) concentrations was observed among HPD- and HFD-fed rats when compared to rats fed on normal chow (Table 3), indicating a possible impairment in chronic fat diet.

Effects of dietary composition on plasma lipid and lipoproteins

The result of lipid profile showed a significant increase ($p < 0.05$) in plasma cholesterol (p = 0.000), triglycerides ($p = 0.000$), LDLC ($p = 0.000$), and a significant decrease ($p < 0.05$) in plasma HDLC ($p = 0.000$) among HFD-fed rats (Table 4). A significant ($p < 0.05$) decrease in plasma cholesterol ($p = 0.000$), triglycerides ($p = 0.000$), and LDLC ($p = 0.000$) was also observed among HPD and HCD-fed rats (Table 4). Atherogenic and coronary risk indices were observed to be significantly increased ($p = 0.000$; $p < 0.05$) among HFD-fed rats when compared to other groups (Table 4).

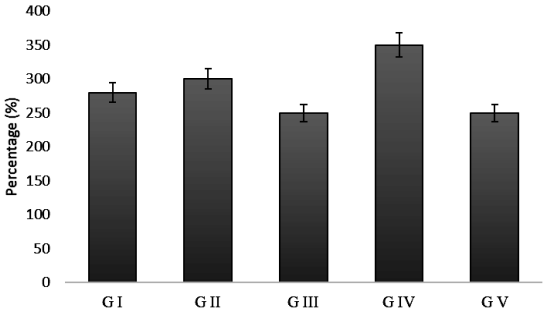

Figure 1. Percentage weight changes among the different groups. Group I = Normal rat chow, Group II = High carbohydrate diet (75%), Group III = High protein diet (75%), Group IV = High fat diet (75%), Group V = Equal proportion of carbohydrate, protein, and fat diet (25% each). Values are expressed as mean ± standard deviation (mean) and are statistically significant at $p < 0.05$

Table 2. The effects of dietary composition on weight among control and treatment groups

Weight	G I	G II	G III	G IV	G V	F	P value
Week 0	42.2±5.97	43.2±6.91	43.2±14.72	41.6±10.01	43.4±4.16	1.39	0.253
Week 1	57.6±14.60	58.0±8.51	65.2±11.61	66.2±16.02	55.0±9.08	5.58	0.001*
Week 2	73.0±25.18	72.6±9.40	68.0±35.33	77.2±16.99	66.2±12.70	7.69	0.000*
Week 3	95.2±30.79	91.6±11.44	96.8±10.03	89.4±20.88	84.0±16.63	15.29	0.000*
Week 4	112.2±34.45	116.2±10.76	116.0±7.97	106.2±23.97	100.0±14.99	24.45	0.000*
Week 5	126.4±18.22	135.8±14.18	130.2±10.03	141.8±36.40	123.8±31.67	29.64	0.000*
Week 6	141.4±20.39	147.0±20.62	138.2±6.98	158.2±37.52	136.2±32.09	32.76	0.000*
Week 7	156.8±24.99	160.4±23.27	146.0±7.38	173.2±37.84	151.6±38.66	37.50	0.000*
Week 8	161.6±25.43	174.2±24.85	149.4±9.04	185.4±41.69	154.0±43.30	37.67	0.000*

Note: Group I = Normal rat chow, Group II = High carbohydrate diet (75%), Group III = High protein diet (75%), Group IV = High fat diet (75%), Group V = Equal proportion of carbohydrate, protein, and fat diet (25% each). Values are expressed as mean ± standard deviation (mean) and are statistically significant at $p < 0.05$. Weights of the rats were taken using a digital precision scale

Table 3. The effects of dietary composition on plasma hepatorenal markers among the control and treatment

Parameters	G I	G II	G III	G IV	G V	F	P value
FPG (mg/dl)	85.60±11.70	82.00±14.77	77.13±22.84	127.25±28.04	80.78±7.29	5.63	0.000
AST (IU/L)	37.00±12.12	34.00±6.48	33.80±3.77	34.00±1.15	34.20±8.32	1.86	0.140
ALT (IU/L)	19.20±7.53	17.00±4.08	18.80±2.59	19.36±7.53	17.40±4.67	0.25	0.910
ALP (IU/L)	15.20±3.63	14.00±3.65	17.40±2.97	24.67±5.77	17.60±4.72	2.18	0.090
TP (mg/dL)	7.98±1.75	8.08±1.09	8.66±1.00	10.10±0.95	8.48±2.10	0.85	0.510
Alb (mg/dL)	3.92±0.38	4.00±0.89	4.30±0.51	5.10±0.26	4.46±0.44	3.67	0.010
TB (mg/dL)	0.04±0.01	0.04±0.01	0.05±0.01	0.05±0.15	0.04±0.01	2.10	0.100
CB (mg/dL)	0.02±0.01	0.03±0.01	0.03±0.01	0.03±0.01	0.03±0.01	0.78	0.540
Urea (mg/dL)	39.4±5.28	35.0±6.27	42.2±15.71	46.00±13.53	34.40±6.43	5.40	0.000
Creat (mg/dL)	0.9±0.03	0.7±0.04	1.3±0.05	1.6±0.06	0.7±0.02	3.18	0.030

Note: Group I = Normal rat chow, Group II = High carbohydrate diet (75%), Group III = High protein diet (75%), Group IV = High fat diet (75%), Group V = Equal proportion of carbohydrate, protein, and fat diet (25% each). Values are expressed as mean ± standard deviation (mean) and are statistically significant at $p < 0.05$

Table 4. The effects of dietary composition on plasma lipid and lipoproteins among the control and treatment groups

Parameters	G I	G II	G III	G IV	G V	F	P value
Chol (mg/dL)	146.2±64.4	120.0±16.2	87.8±21.1	244.0±14.0	92.60±23.51	14.79	0.000
Trig (mg/dL)	89.6±62.3	71.3±21.1	72.5±20.1	126.0±16.9	38.20±9.31	8.06	0.000
HDL (mg/dL)	48.8±21.6	45.5±6.1	44.3±7.8	43.3±4.6	29.6±4.33	12.70	0.000
LDL (mg/dL)	79.48±32.5	60.24±3.4	75.7±33.3	100.0±2.5	55.60±12.93	11.10	0.000
AI	1.63±0.12	1.32±0.01	1.71±0.03	4.05±0.06	1.89	74.27	0.000
CRI	2.99±0.05	2.64±0.04	3.04±1.63	5.64±0.14	3.32	10.03	0.000

Note: Group I = Normal rat chow, Group II = High carbohydrate diet (75%), Group III = High protein diet (75%), Group IV = High fat diet (75%), Group V = Equal proportion of carbohydrate, protein, and fat diet (25% each). Values are expressed as mean ± standard deviation (mean) and are statistically significant at $p < 0.05$

Table 5. The effects of dietary composition on plasma electrolytes among the control and treatment groups

Parameters	G I	G II	G III	G IV	G V	F	P value
Potas (mEq/L)	5.0±0.80	5.2±0.25	4.9±0.94	4.6±0.10	4.7±0.42	0.64	0.640
Sodiu (mEq/L)	143.4±7.64	142.8±6.40	147.0±7.97	140.0±5.13	146.4±5.73	2.43	0.070
Chlori (mEq/L)	100.0±6.89	100.8±7.45	98.4±10.06	102.0±2.65	101.0±7.18	0.75	0.570
Bicar (mg/dL)	20.5±1.42	21.28±3.92	19.0±1.02	26.0±5.51	21.9±3.85	0.60	0.670
Ph	7.18±0.85	7.68±0.32	7.02±0.84	8.20±0.10	7.46±0.56	0.19	0.940

Note: Group I = Normal rat chow, Group II = High carbohydrate diet (75%), Group III = High protein diet (75%), Group IV = High fat diet (75%), Group V = Equal proportion of carbohydrate, protein, and fat diet (25% each). Values are expressed as mean ± standard deviation (mean) and are statistically significant at $p < 0.05$

Effects of dietary composition on plasma electrolytes

The plasma electrolyte result revealed a non-significant decrease ($p > 0.05$) in potassium ($p = 0.064$) and sodium ($p = 0.070$) and a non-significant increase ($p > 0.05$) in plasma chloride ($p = 0.057$), bicarbonate ($p = 0.067$), and pH ($p = 0.094$) among HFD-fed rats compared to rats in other groups. However, the values are within normal ranges (Table 5).

Discussion

In human, the ideal carbohydrate intake is 40-70% of total energy intake, protein is 0.80 g/kg body weight, and total fat is 20-35% of total calories (Liu Ann et al. 2017; Shafiee 2019). Chronic administration of HFD has been reported to result in increased body weight, obesity and increased blood glucose (Putri et al. 2021). In this study, an increase in body weights was observed across all the groups but was most obvious in the HFD-fed group (Table 2). The percentage increment in body weight was 280% in normal rat chow, 300% in HCD, 250% in HPD, 350% in HFD and 250% in the equal proportion diet group (Figure 1). The observed increase in body weight among HFD-fed rats confirms the existence of obesity in this group as facilitated by the development of a positive energy balance leading to an increase in peripheral and visceral fat deposition and ultimately obesity. This finding corroborates reports from similar studies (Abi et al. 2020). The observed relatively low weight among HPD-fed group reflects a reduction in food and calorie intake due to increased satiety as determined by a marginal increase in satiety hormones secretion (GIP, and glucagon-like peptide-1) and reduction in ghrelin secretion, an anorexigenic hormone (Anyakudo and Adeniji 2020). The sustained satiety induces a negative energy balance, thereby promoting weight loss.

The macronutrient components of diet determine the digestibility and availability of end-products for oxidative generation of energy for cellular activities. Results from this study revealed an increase in FPG among HFD-fed rats and a decrease among HPD-fed rats when compared to other groups (Table 3). This corroborates a report from a previous study (Lozano et al. 2016). The observed increase in FPG among HFD-fed rats reflects existing visceral adiposity, some degree of insulin resistance, hyperinsulinemia, reduced fatty acid synthesis, increased basal lipolysis and consequent increase in fatty acid delivery to the liver. The observed little or no change in glucose concentration among HPD-fed rats reflects compensatory metabolic changes through glycogenolysis and gluconeogenesis involving lactate, glycerol, glucogenic amino acids, and odd-chain fatty acids to maintain glucose homeostasis. However, excess amino acids from HPD are oxidatively converted to glucose.

Excessive dietary components are absorbed through the intestinal mucosa to reach the liver through the portal vein, hence making the hepatocytes vulnerable to lesions. The presence of liver lesions or damage involving hepatocyte destruction with plasma membrane disruption is confirmed using plasma ALT, AST, and ALP activities, with ALT being more liver-specific and related to hepatic fat deposition and insulin resistance (Liu et al. 2021). Result from this study revealed a non-significant ($p > 0.05$) increase in plasma AST, ALT and ALP activities among rats fed on HCD, HPD, HFD and equal proportions of the macronutrients when compared with the control group, with highest activities among the HFD-fed group (Table 3). The increase in plasma ALT, AST and ALP among HFD-fed rats corroborates results from similar studies in rats (dos Santos Lacerda et al. 2018; Lasker et al. 2019). The observed increase in plasma ALT, AST and ALP among HFD-fed rats maybe due to an associated development of non-alcoholic fatty liver disease with disruption of liver functions and loss of hepatocellular integrity. Also, an increase in plasma total protein and albumin concentrations was observed among all test groups when compared to the group fed on normal rat chow (Table 3). A similar increase in plasma total protein and albumin concentrations has been reportedly found among HPD-fed rats (El-Deen et al. 2018).

Bilirubin is a product of the degradation of red blood cells in the liver, spleen, and bone marrow. The removal of this degradation product (bilirubin) from the body is done by bilirubin metabolism and its excretion by the liver. Hyperbilirubinemia results when there is a disease affecting liver function. In this study, no obvious changes in plasma total and conjugated bilirubin concentration were observed among the test groups when compared to normal rat chow-fed group (Table 3).

As a measure of the excretory function of the kidney, plasma urea and creatinine are widely used markers of adequate glomerular filtration. High plasma concentration of creatinine indicates a falling glomerular filtration rate and consequent decreased capability of the kidneys to excrete waste products. Result from this study, revealed a non-significant decrease ($p > 0.05$) in plasma urea and creatinine concentrations among HCD-fed rats and a significant increase ($p < 0.05$) in plasma urea and creatinine concentrations among HPD and HFD-fed rats when compared to rats fed on normal chow (Table 3). These findings agree with earlier reported findings by researchers (dos Santos Lacerda et al. 2018; El-Deen et al. 2018). This suggests that chronic exposure to HPD and HFD may predispose to renal dysfunction and exposure to HCD is safer.

Poor diet as indicated by hypertriglyceridemia, hypercholesterolemia and increase LDLC has been reported to be a major risk factor for some chronic diseases such as Cardiovascular Disease (CVD) (Hedayatnia et al. 2020). Results from this study showed a significant increase ($p < 0.05$) in plasma cholesterol, triglycerides, LDLC and a significant decrease ($p < 0.05$) in plasma HDLC among HFD-fed rats (Table 4). This finding corroborates reports from similar studies (Lasker et al. 2019). This may be due to high monounsaturated and saturated fat content of the HFD, increased de novo fatty acid synthesis, increased uptake and esterification of dietary fatty acids and a decrease in fatty acid oxidation. A significant ($p < 0.05$) decrease in plasma cholesterol, triglycerides, and LDLC was also observed among HPD-fed rats (Table 4). This finding is in contrast to a previous study (Tischmann et al. 2019). This observation reflects increased amino acid

contribution to energy generation, and compensatory increase in lipolysis as an alternative calorie generation due to decreased supply from dietary glucose.

Considering the impact of HCD on lipid profile, a decrease was observed in cholesterol, triglycerides, and LDLC concentrations among HCD-fed rats when compared with the rats fed on normal chow (Table 4). In contrast, an increase in plasma total cholesterol and triglyceride concentrations was reported by researchers in a previous study (Semiane et al. 2017). In determining the atherogenic effect of the administered feed, a significant increase ($p < 0.05$) in atherogenic ($p = 0.000$) and coronary risk indices ($p = 0.000$) was observed among HFD-fed rats when compared to other groups (Table 4). This indicates an increased chance of developing cardiovascular complications following ingestion of HFD by the rats.

Plasma electrolyte level reflects the hydration status, and its measurements are useful in investigating conditions that cause electrolyte imbalances, such as dehydration, kidney disease, lung diseases, endocrine (glandular) or heart conditions where high or low levels can be observed. Results from this study revealed a non-significant decrease ($p > 0.05$) in plasma potassium and sodium; and a non-significant increase ($p > 0.05$) in plasma chloride, bicarbonate, and pH among HFD-fed rats when compared to rats in other groups; however, the values are within normal ranges (Table 5). The observed changes in plasma electrolytes may be due to alterations in plasma tonicity and urinary excretion of electrolytes. This study has the support of a previous study on humans which reported the deleterious effects of excessive intake of carbohydrate on human health (Clemente-Suárez et al. 2022). Similarly diet low in fat had been reported to lower deaths from breast cancer and has a beneficial effect on human health (Billingsley et al. 2018). However, the place of protein in NCDs appears to be beneficial too (Azzini et al. 2022).

In conclusion, this study showed that HFD can predispose to obesity and Diabetes mellitus. Also the HFD fed rats developed disruption of lipid profile causing dyslipidemia and a significant increase in both Atherogenic and coronary risk indices. All these are risk factors for non-communicable diseases. The liver and kidney function markers did not show significant deleterious effects on the rats and electrolytes were not significantly affected, this study has shown that macronutrient with high fat composition can predispose to many risk factors of non-communicable disease. The findings in this pilot study highlight the need for further studies using humans in a large population.

ACKNOWLEDGEMENTS

The immense emergence of a high prevalence of non-communicable diseases seems to be of major concern to healthcare givers. The authors conceived the idea of looking at the role of diet in this epidemic. Our appreciation goes to the members of staff of the Anatomy Department of Olabisi Onabanjo University for supporting us throughout the course of the study and caring for the rats.

REFERENCES

Abdullah A. 2015. The double burden of undernutrition and overnutrition in developing countries: An update. Curr Obes Rep 4 (3): 337-349. DOI: 10.1007/s13679-015-0170-y.

Abi I, Adeniyi O, Abi E, Imam MU. 2020. Chronic high fat diet induced weight gain, hyperglycaemia and cognitive impairment in albino mice. J Biomed Res Clin Pract 3 (3): 382-388. DOI: 10.46912/jbrcp.193.

Ahmed KY, Rwabilimbo AG, Abrha S, Page A, Arora A, Tadese F, Beyene TY, Seiko A, Endris AA, Agho KE, Ogbo FA. 2020. Factors associated with underweight, overweight, and obesity in reproductive age Tanzanian women. PLoS One 15 (8): e0237720. DOI: 10.1371/journal.pone.0237720.

Anon. 1970. Optimized standard method for quantitative determination of alkaline phosphatase. Z Klin Chem Klin Biochem 8: 658.

Anyakudo MMC, Adeniji DO. 2020. Effects of proportional high-protein/low-carbohydrate formulated diet consumption in diabetic rats: Beneficial impact on glycemic and weight control. Afr J Food Agric Nutr Dev 20 (7): 16993-17005. DOI: 10.18697/ajfand.95.19950.

Azzini E, Peluso I, Intorre F, Barnaba L, Venneria E, Foddai MS, Ciarapica D, Maiani F, Raguzzini A, Polito A. 2022. Total and plant protein consumption: The role of inflammation and risk of non-communicable disease. Intl J Mol Sci 23 (14): 8008. DOI: 10.3390/ijms23148008.

Bigna JJ, Noubiap JJ. 2019. The rising burden of non-communicable diseases in Sub-Sahara Africa. Lancet Glob Health 7 (10): e1295-e1296. DOI: 101016/S2214-109X(19)30370-5.

Billingsley HE, Carbone S, Lavie CJ. 2018. Dietary fats and chronic noncommunicable diseases. Nutrients 10 (10): 1385. DOI: 10.3390/nu10101385.

Carreiro AL, Dhillon J, Gordon S, Higgins KA, Jacobs AG, McArthur BM, Redan BW, Rivera RL, Schmidt LR, Mattes RD. 2016. The macronutrients, appetite, and energy intake. Annu Rev Nutr 36: 73-103. DOI: 10.1146/annurev-nutr-121415-112624.

Chukwudike AMM, Ademidun O, Onuwabhagbe OF. 2017. High dietary protein intake potentiates metabolic and renovascular risks in diabetic rats. EC Nutr 6 (6): 198-206.

Clemente-Suárez VJ, Mielgo-Ayuso J, Martín-Rodríguez A, Ramos-Campo DJ, Redondo-Flórez L, Tornero-Aguilera JF. 2022. The burden of carbohydrates in health and disease. Nutrients 14 (18): 3809. DOI: 10.3390/nu14183809.

dos Santos Lacerda D, Garbin de Almeida M, Teixeira C, De Jesus A, da Silva Pereira Júnior É, Martins Bock P, Pegas Henriques JA, Gomez R, Dani C, Funchal C. 2018. Biochemical and physiological parameters in rats fed with high-fat diet: The protective effect of chronic treatment with purple grape juice (Bordo variety). Beverages 4 (4): 100. DOI: 10.3390/beverages4040100.

El-Deen AE, Mansour AE, Taha A. 2018. High protein diet that cause weight loss and lower blood glucose level have a serious impact on the kidney functions of male diabetic obese albino rats. Food Nutr Sci 9: 1174-1191. DOI: 10.4236/fns.2018.910085.

El-Zayat SR, Sibaii H, El-Shamy KA. 2019. Physiological process of fat loss. Bull Natl Res Cent 43: 208. DOI: 10.1186/s42269-019-0238-z.

Friedewald WT, Levy RI, Fredrickson DS. 1972. Estimation of the concentration of low-density lipoprotein cholesterol in plasma, without use of the preparative ultracentrifuge. Clin Chem 18 (6): 499-502. DOI: 10.1093/clinchem/18.6.499.

GBD 2015 Risk Factor Collaborators. 2016. Global, regional, and national comparative risk assessment of behavioral, environmental and occupational, and metabolic risk or clusters of risks 1990-2015: A systematic analysis for the global burden of disease study. Lancet 388 (10053): 1659-1724. DOI: 10.1016/S0140-6736(16)31679-8.

Gouda HN, Charlson F, Sorsdahl K, Ahmadzada S, Ferrari AJ, Erskine H, Leung J, Santamauro D, Lund C, Aminde LN, Mayosi BM, Kengne AP, Harris M, Achoki T, Wiysonge CS, Stein DJ, Whiteford H. 2019. Burden of non-communicable diseases in sub-Saharan Africa, 1990-2017: Results from the Global Burden of Disease Study 2017. Lancet Glob Health 7 (10): e375-e387. DOI: 10.1016/S2214-109X(19)30374-2.

Gowshall M, Taylor-Robinson SD. 2018. The increasing prevalence of non-communicable diseases in low-middle income countries: The view from Malawi. Intl J Gen Med 11: 255-264. DOI: 10.2147/IJGM.S157987.

Hedayatnia M, Asadi Z, Zare-Feyzabadi R, Yaghooti-Khorasani M, Ghazizadeh H, Ghaffarian-Zirak R, Nosrati-Tirkani A, Mohammadi-Bajgiran M, Rohban M, Sadabadi F, Rahimi HR, Ghalandari M,

Ghaffari MS, Yousefi A, Pouresmaeili E, Besharatlou MR, Moohebati M, Ferns GA, Esmaily H, Ghayour-Mobarhan M. 2020. Dyslipidemia and cardiovascular disease risk among the MASHAD study population. Lipids Health Dis 19 (1): 42. DOI: 10.1186/s12944-020-01204-y.

Idris IO, Oguntade AS, Mensah EA, Kitamura N. 2020. Prevalence of non-communicable diseases and its risk factors among Ijegun –Isheri Osun residents in Lagos state, Nigeria: A community based cross-sectional study. BMC Public Health 20 (1): 1258. DOI: 10.1186/5/2889-020-09349-2.

Jaacks LM, Kavle J, Perry A, Nyaku A. 2017. Programming maternal and child overweight and obesity in the context of undernutrition: Current evidence and key considerations for low- and middle-income countries. Public Health Nutr 20 (7): 1286-1296. DOI: 10.1017/S1368980016003323.

Jendrassik L, Grof P. 1938. Estimation of total serum bilirubin level by spectrophotometrically in serum and plasma. Biochem J 297: 81-89.

Kadish AH, Sternberg JC. 1969. Determination of urine glucose by measurement of rate of oxygen consumption. Diabetes 18 (7): 467-470. DOI: 10.2337/diab.18.7.467.

Lasker S, Rahman MM, Parvez F, Zamila M, Miah P, Nahar K, Kabir F, Sharmin SB, Subhan N, Ahsan GU, Alam MA. 2019. High-fat diet-induced metabolic syndrome and oxidative stress in obese rats are ameliorated by yogurt supplementation. Sci Rep 9 (1): 20026. DOI: 10.1038/s41598-019-56538-0.

Liu AG, Ford NA, Hu FB, Zelman KM, Mozaffarian D, Kris-Etherton PM. 2017. A healthy approach to dietary fats: Understanding the science and taking action to reduce consumer confusion. Nutr J 16 (1): 53. DOI: 10.1186/s12937-017-0271-4.

Liu C, Shao M, Lu L, Zhao C, Qiu L, Liu Z. 2021. Obesity, insulin resistance and their interaction on liver enzymes. PLoS ONE 16 (4): e0249299. DOI: 10.1371/journal.pone.0249299.

Lozano I, Van der Werf R, Bietiger W, Seyfritz E, Peronet C, Pinget M, Jeandidier N, Maillard E, Marchioni E, Sigrist S, Dal S. 2016. High-fructose and high-fat diet-induced disorders in rats: Impact on diabetes risk, hepatic and vascular complications. Nutr Metab (Lond) 13: 15. DOI: 10.1186/s12986-016-0074-1.

Malta A, de Oliveira JC, Ribeiro TA, Tófolo LP, Barella LF, Prates KV, Miranda RA, Elmhiri G, Franco CC, Agostinho AR, Trombini AB, Pavanello A, Gravena C, Abdennebi-Najar L, Mathias PC. 2014. Low-protein diet in adult male rats has long-term effects on metabolism. J Endocrinol 221 (2): 293-303. DOI: 10.1530/JOE-13-0473.

Mapis GJ. 2020. The Dietary Decision-Making Process of Women in Nigeria. Walden Dissertations and Doctoral Studies 7696. https://scholarworks.waldenu.edu/dissertations/7696.

Morris AL, Mohiuddin SS. 2023. Biochemistry, Nutrients. [Updated 2021 May 12]. In: StatPearls [Internet].Treasure Island (FL): StatPearls Publishing. Available from: https://www.ncbi.nlm.nih.gov/books/NBK554545/.

Nägele U, Hägele EO, Sauer G, Wiedemann E, Lehmann P, Wahlefeld AW, Gruber W. 1984. Reagent for the enzymatic determination of serum total triglycerides with improved lipolytic efficiency. J Clin Chem Clin Biochem 22 (2): 165-174. DOI: 10.1515/cclm.1984.22.2.165.

NREC (National Research Ethics Committees). 2019. Ethical Guidelines for the Use of Animals in Research. ISBN: 978-82-7682-085-0 (Printed Edition), 978-82-7682-086-7 (Digital Edition).

Odunyemi A, Ratiman T, Alam K. 2023. Economic burden of non-communicable diseases on households in Nigeria: Evidence from Nigeria living standard survey 2018-2019. BMC Public Health 23 (1): 1563. DOI: 10.1186/s12889-023-16498-7.

Oso A. 2023 Non communicable diseases: An emerging epidemic in Nigeria. Trop J Nephrol 18 (1 & 2): 31-37.

Ruthsatz M, Candeias V. 2020. Non-communicable disease prevention, nutrition, and aging. Acta Biomed 91 (2): 379-388. DOI: 10.23750/abm.v91i2.9721.

Putri RR, Casswall T, Hagman E. 2021. Prevalence of increased transaminases and its association with sex, age, and metabolic parameters in children and adolescents with obesity – a nationwide cross-sectional cohort study. BMC Pediatr 21: 271. DOI: 10.1186/s12887-021-02747-4.

Savarino G, Corsello A, Corsello G. 2021. Macronutrient balance and micronutrient amounts through growth and development. Ital J Pediatr 47 (1): 109. DOI: 10.1186/s13052-021-01061-0.

Schettler G, Nussel E. 1975. Colorimetric determineation of choleterol. Arh Med Soz Med Prav Med 10: 55.

Seidelmann SB, Claggett B, Cheng S, Henglin M, Shah A, Steffen LM, Folsom AR, Rimm EB, Willett WC, Solomon SD. 2018. Dietary carbohydrate intake and mortality: A prospective cohort study and meta-analysis. Lancet Public Health 3 (9): e419-e428. DOI: 10.1016/S2468-2667(18)30135-X.

Semiane N, Foufelle F, Ferré P, Hainault I, Ameddah S, Mallek A, Khalkhal A, Dahmani Y. 2017. High carbohydrate diet induces nonalcoholic steato-hepatitis (NASH) in a desert gerbil. C R Biol 340 (1): 25-36. DOI: 10.1016/j.crvi.2016.09.002.

Shafiee MN. 2019. Dietary fats: Health and consumers. Intl J Health Sci Res 9 (1): 270-274.

Tischmann L, Drummen M, Gatta-Cherifi B, Raben A, Fogelholm M, Hartmann B, Holst JJ, Matias I, Cota D, Mensink RP, Joris PJ, Westerterp-Plantenga MS, Adam TC. 2019. Effects of a high-protein/moderate-carbohydrate diet on appetite, gut peptides, and endocannabinoids-a preview study. Nutrients 11 (10): 2269. DOI: 10.3390/nu11102269.

Wybenga DR, Di Giorgio J, Pileggi VJ. 1971. Manual and automated methods for urea nitrogen measurement in whole serum. Clin Chem 17 (9): 891-895. DOI: 10.1093/clinchem/17.9.891.